A MODEL OF CONNECTIVE TISSUE MICROFIBRILS:
Structural Studies of Fibrillin Fragments

by

Bobbe Kerry Maddox

A DISSERTATION

Presented to
the Department of Biochemistry and Molecular Biology
and the Oregon Health Sciences University
School of Medicine
in partial fulfillment of
the requirements for the degree of

Doctor of Philosophy

May 1990

APPROVED:

[redacted]

(Professor in Charge of Thesis)

[redacted]

(Chairman, Graduate Council)

TABLE OF CONTENTS

ACKNOWLEDGEMENTS

A special thanks goes to Robert Glanville, who offered me a position in his lab long before thoughts of graduate school. It was because of this creative and rewarding experience that I considered a career as a scientist. I would also like to express my appreciation for the generous support provided to me by the entire scientific and administrative staff of the Research Department at Shriners Hospital. In particular, I thank Lynn Sakai, for sharing this fascinating fibrillin project; more importantly I thank her for encouraging me to pursue graduate school in the first place. Others in the lab I would like to acknowledge include Hans Peter Bächinger who taught me that biophysical chemistry is actually fun, Nick Morris for just being there, ready to listen, and Cynthia Bohan for constant humor and faithful dogsitting. For the friendship they provided through it all, I thank Michael Greenstreet and Barbara Nagle, neither of whom I could have lived without.

The experimentation presented in this thesis was carried out by Kerry Maddox, with the following exceptions: the electron micrographs of immunolocalization and rotary shadowing by Doug Keene, ultracentrifugation by Hans Peter Bächinger, circular dichroism by Larry Compton in the laboratory of Hans Peter Bächinger, preparation of monoclonal antibodies and fibrillin-containing cell culture medium by Lynn Sakai, isolation of fibrillin clones by Cheryl Maslen in the laboratory of Lynn Sakai, amino acid analysis performed by Kenine Comstock and Cynthia Bohan, and tissue preparation by Bob Poljak and Bruce Donaldson. The dissertation was critically reviewed by Robert Glanville prior to submission.

ABSTRACT

Extracellular matrix microfibrils present in various connective tissues have been shown to contain fibrillin. Pepsin was used to digest human amnion and solubilize microfibrillar components present in the tissue. Two fragments, PF1 and PF1B, were identified as fibrillin using a previously characterized antibody (Sakai et al., 1986). Two other fragments, PF2 and PF3, were isolated and shown to be domains of fibrillin. A monospecific antiserum prepared to PF2 and a monoclonal antibody to PF3 both immunoblotted intact fibrillin. Tissue labeling with the new antibodies by indirect immunofluorescence and immuno-electron microscopy produced a microfibrillar pattern and periodicity of the microfibril characteristic of a fibrillin specific antibody. Partial amino acid sequences were determined for all four fragments towards a goal of primary structure determination at the cDNA level. Oligonucleotide probes derived from PF2 peptide sequences have identified cDNA fibrillin clones. These are being used to investigate a link between Marfan syndrome and microfibrillar abnormalities.

Rotary shadowed images of PF1, PF1B, and PF2 demonstrate flexible linear fragments, while PF3 is a complex crab-like structure with a dense central globular region and extended arms. The similarity of PF3 to recently isolated chains of beaded units (see Appendix II) has led to speculation that these beaded chains correspond to the macromolecular form of fibrillin present in tissues. In support of this, mAb69 which was made to PF3, demonstrated immunoreactivity with the beaded structure. A model is proposed that describes pepsin digestion of the microfibrils and release of the fibrillin fragments characterized in this thesis. A second model suggests major events thought to occur in fibrillogenesis, from secretion of a fibrillin molecule, to formation of an intermediary oligomer, to final assembly into the microfibril.

INTRODUCTION

THE EXTRACELLULAR MATRIX

The extracellular matrix is a milieu of structural elements that together with specialized cells compose the connective tissues. The macromolecules that form the matrix are synthesized by local connective tissue cells, such as fibroblasts and chondrocytes. Following cellular secretion of molecular components, the matrix is assembled into an organized network. Thick banded fibers are a predominant structural element found in connective tissues such as bone and ligament. More delicate filamentous networks are also present in a wide variety of tissues, notably in skin and in specialized regions of the eye.

Skin is an example of a complex and dynamic connective tissue that includes the outer cellular surface of the epidermis, and the basement membrane, a unique structure found at the interface of the cell surface and the underlying dermal stroma. The epithelium forms an exterior armor to protect internal organs from invasion and trauma. The basement membrane is a specialized tissue that functions as a selective filtration barrier not only at dermal-epidermal junctions, but also in other organs such as the kidney, blood-brain barrier, and placenta. It is composed of type IV collagen molecules that are organized into an open chicken-wire network. Also present in basement membranes are the structural glycoproteins, laminin and entactin, and heparin sulfate proteoglycan. Anchoring fibrils span the region from immediately below the basement membrane, the lamina densa, to the dermis proper. These are composed of type VII collagen molecules that are laterally aligned and thought to function like an ultrastructural suture (Keene et al., 1987).

The upper surface of the dermis is called the papillary layer and contains finer and more delicate fibrillar structures than the reticular dermis below. Oxytalan fibers are thin bundles of microfibrils that are seen intersecting the basement membrane and extend into the papillary dermis (Cotta-Pereira et al., 1976). Elaunin fibers are slightly thicker bundles and are found deeper in the papillary dermis or in the upper section of the reticular dermis. A small amount of elastin is associated with elaunin fibers. Thick elastic and collagen fibers are primarily located in the reticular layer.

Specialized extracellular matrices also compose several regions of the eye. The cornea is the protective outer surface composed primarily of collagen fibers that forms a transparent lattice. Behind the cornea is the lens, a metabolically and structurally independent tissue. The outer layer of the lens is bounded by the lens capsule, another type of basement membrane which maintains the isolation of the lens cells and the protein components. The lens is held in place by fine filaments that connect the ciliary body to the lens, thus holding the lens in place. These fibrils are called the ciliary zonule or suspensory ligament, and are of particular interest because they are the only tissue that is composed entirely of microfibrils. The ciliary muscle controls the tension on the lens through the zonule, allowing it to focus light on the retina, the photoreactive tissue of the eye.

The functional requirements of a specific tissue determine the kinds and amounts of particular elements that are present. Macromolecules of extracellular matrices form collagen fibers, elastic fibers and small filamentous networks. Collagen is the predominant component of connective tissues and represents a family of molecules that are characterized by a triple helical domain. The structures vary from thin, 3 to 20 nm fibrils, to thick,

50 to 100 nm striated fibers, depending on the specific tissue and type of collagen. Individual collagen molecules align in a parallel staggered array so that overlap and gap regions give the fibers a striated appearance.

Elastic fibers compose a second major fibrous structure. They are found in elastic tissues that require recoil, such as skin, aorta, and lung. Unlike the fibers that are formed from collagens, the elastic fiber is composed of two different structural elements. A mantle of small microfibrils surrounds the amorphous core of the fiber. Elastin composes the interior which is distinguished by lysine-derived crosslinks that form during maturation. These crosslinks are responsible for its total insolubility. Due to the resistence of elastin to most extraction methods, it has been impossible to isolate. The precursor of elastin is tropoelastin, a 76,000 dalton protein. The isolation of this soluble form of elastin enabled primary structural analysis and sites of crosslinking to be determined (Sandberg et al., 1969; Sandberg et al., 1971).

Small filamentous strands are composed of collagens as well as noncollagenous material and are found in a variety of tissues. For example, type VI collagen forms a delicate microfilamentous network often seen intertwined around large type I collagen fibers in skin. Another class of fine filaments includes the microfibrils that surround the amorphous center of the elastic fiber. Fragments isolated from the molecules that compose these extracellular microfibrils are the subject of this thesis.

MICROFIBRILS

Small filamentous strands in connective tissues, including those mentioned previously in skin, ciliary zonules, and elastic tissue, have been observed by electron microscopy for decades. In the early 1960's, Frederick Low (1962) specified a particular subgroup of fibrils with a diameter of 4 to 12 nm, and without the 67-nm banding pattern characteristic of interstitial collagen fibers. He termed this structure the microfibril. A population of small diameter fibrils, 3 to 5 nm, were shown recently to be composed of type VI collagen (Furthmayr et al., 1983; Bruns, 1986; Keene et al., 1988). A group of microfibrils with a larger diameter are morphologically distinct. These microfibrils have an average diameter of 10 nm, a somewhat beaded appearance, and a cross-section that sometimes appears to have a hollow center.

Elastin biochemists considered the microfibrils associated with the elastic fiber to be a specialized subclass of Low's microfibrillar structures. This was based on localization rather than any morphological distinction (see Cleary and Gibson for review, 1983). The elastic fiber was postulated to be a two component system based on enzyme treatment of bovine nuchal ligament, a tissue particularly rich in elastic fiber. Early researchers observed that a fine fibrous mantle remained following elastase digestion (Hall, 1957; Dempsey & Lansing, 1954). Ultrastructural analysis using the anionic stain phosphotungstate revealed a filamentous network surrounding an amorphous central core. (Karrer, 1958). Karrer hypothesized that collagen and elastic fibers shared a basic common filament, although he noted distinct morphological differences. The fine fibrils intermingled around the collagen fibers were described as being mostly beaded while the microfibrils associated with elastic fibers look more tubular. The cationic stains, uranyl acetate and lead

citrate, were applied to developing elastic tissue and were noted to have different effects on the two structural elements. The surrounding microfibrils were stained with cationic compounds, while the elastin core was stained with anionic phosphotungstate (Greenlee et al., 1966). In addition to the different sensitivities of the microfibrils and the amorphous core to enzyme digestion, here was indication that the chemical composition was different, at least that the surface charges were different. This was significant in supporting the theory that there were two structural elements in elastic fibers.

The next period of study focused on elastinogenesis, the development of elastic tissue. Using calf tissue from up to 180-day-old fetuses, the nuchal ligament was sectioned, fixed and stained with potassium permanganate and lead citrate to reveal microfibrillar and amorphous components. The first ultrastructural indication of elastogenesis was the accumulation of small extracellular fibrils, called pre-elastin filaments. These preceded fibrils that were in association with a small amount of elastin (Fahrenbach, 1966). Elastogenesis appeared to begin with secretion of the microfibrillar component followed by elastin secretion and the formation of elastic fibers. Investigations of elastogenesis have been repeated more recently (Kewley et al., 1978; Jaques and Serafini-Fracassini, 1985), confirming original work. It has been postulated that the microfibrils are required for assembly of the elastic fiber, possibly serving as nucleation sites for elastin crosslinking. There has also been speculation that the elastin precursor and the microfibrillar element form a complex with lysyl oxidase, the enzyme that initiates the formation of lysine derived crosslinks (Mecham, 1981).

Ultrastructural analysis of human fetal aortic tissue demonstrated a similar pattern of events in elastogenesis. At 14-weeks-old, the only prominent structure of the elastic fiber was the microfibrils. Elastin was not visible as an element. At 23-weeks, elastin was detectable by electron microscopy in typical, although small, amorphous regions. However, elastin antibodies immunolocalized to regions adjacent to the microfibril in 14-week-old cultures (Jaques and Serafini-Fracassini, 1985). This suggested that although elastin was not detectable, it was indeed synthesized, secreted, and associated with the microfibril. The exact nature of the interaction between the microfibrils and elastin precursor is still unclear, as are the events involved in elastogenesis. This continues to be an area of active investigation.

ATTEMPTS TO EXTRACT MICROFIBRILLAR COMPONENTS

It was concluded that the elastic fibers were composed of two structural elements based on morphology, different staining and enzyme sensitivities. The core was known to be elastin by original characterization based on harsh chemical extraction methods. The protein components of the microfibrils were unknown. Ross and Bornstein (1969) designed extraction procedures in hopes of separating elastin from microfibrils and characterizing the microfibrillar protein components. Their protocol combined tissue digestion and chemical extraction with ultrastructural analysis to determine effects of various treatments. Elastic tissue was treated with collagenase to remove collagens, leaving intact elastic fibers. The amorphous component was susceptable to elastase digest, as previously shown. The microfibrillar components were removed by digestion with trypsin and chymotrypsin, unlike the elastin core.

Extraction of the elastic fiber with guanidine-HCl did not affect the integrity of the microfibrils. However, in the presence of dithiothreitol and guanidine-HCl, the microfibrils disappeared. This was assumed to represent the solubilization of the microfibrillar proteins. The observation that the fibrils were sensitive to extraction only in the presence of DTE suggested that the microfibrils were held in the tissue through disulfide bonds. An amino acid composition was also performed on the soluble extract and showed an unusually high content of glutamic acid, aspartic acid and cysteine compared to elastin. No desmosine or isodesmosine, the crosslinked amino acids characteristic of elastin were present.

Ross and Bornstein's extraction procedure became the standard method in attempts to isolate microfibrillar proteins. Antisera that have been developed against such preparations and used as markers of elastic microfibrils have identified several components ranging in molecular weight from 30,000 to 340,000 (Sear, 1981; Gibson et al., 1986; Jacques & Sera-Fracassini, 1986; Streeten & Gibson, 1988; Gibson et al., 1989). Kewley developed the first antiserum to a guanidine-DTE extract of bovine nuchal ligament (1977). Immunofluorescence demonstrated a microfibrillar-like pattern in a ligament tissue section. Grant, Jackson and coworkers attempted to isolate these immunoreactive components from nuchal ligament using the antisera and found that the extract was excessively heterogeneous (Muir et al., 1976; Sear et al., 1978). Later they established that cultured bovine nuchal ligament fibroblasts synthesized immature elastic fibers and attempted to isolate protein components from the medium. (Sear et al., 1978). Two glycoproteins MFP I and MFP II were identified with molecular weights of 150,000 and 300,000, respectively (Sear et al., 1981). In characterizing these proteins, it was demonstrated that MFP I

was collagenase sensitive and contained significant amounts of 4-hydroxyproline. It was determined from this that MFP I probably represented a new type of collagen, and it was speculated that the microfibrils were composed of a fine network of these collagen molecules (Sear et al., 1981). MFP II was not collagenous and was thought to be possibly a microfibril-associated protein involved in aggregation or stabilization of the bundles of microfibrils.

Cleary and Gibson developed an antiserum similar to Kewley's and isolated a glycoprotein with features in common with MFP I. The molecular weight was 140,000, and amino acid composition indicated a significant hydroxyproline content and collagenase sensitivity (Gibson and Cleary, 1982). Antisera produced to this isolated component of aorta and nuclae ligament extracts demonstrated a distribution different than elastin-associated microfibrils (Gibson and Cleary, 1983). The antibodies localized to fine filaments running between collagen fibers in nonelastic tissues such as tendon, kidney, and lung rather than to the microfibrils on the surface of the elastic fibers. Later this protein, and presumably MFP I, was determined to be type VI collagen (Gibson and Cleary, 1985).

Not to be deterred, Cleary and his coworkers continued to extract proteins from bovine nuchal ligament with the intention of isolating a microfibrillar component. Their original antiserum did recognize a microfibrillar pattern, in addition to the type VI collagen distribution. The result was the isolation of a 31kD polypeptide named microfibril-associated glycoprotein, or MAGP (Gibson et al., 1986). Antisera raised against MAGP immunolocalized to the "elastin-associated microfibrils" in elastic tissues, and to microfibrils found in other tissues such as muscle, kidney, tendon, and ciliary zonules. This demonstrated that all of the morphologically similar microfibrils described by Low, also carried the same antigenic determinants.

FIBRILLIN

A major advance in determining the makeup of microfibrils was made when a monoclonal antibody was characterized identifying a unique, single-chain glycoprotein component. This new protein was named fibrillin (Sakai et al, 1986). Using a crude fraction from human amnion as an immunogen, a monoclonal antibody to a discrete network of fibers was produced. Tissue immunofluorescence using the monoclonal antibody demonstrated the presence of antigen in skin from the basement membrane where the fibers were arranged perpendicular to the dermal-epidermal junction, to deep into the dermis. The antigen was present in many other tissues: kidney, lung, muscle, tendon, placenta, and ciliary zonule. Again, the fluorescence pattern was indicative of a fibrillar network. As the staining pattern in aorta was similar to anti-elastin staining, the tissue was digested with elastase. This reduced significantly the immunofluorescence of antielastin antibodies but did not affect the intensity of the staining with the new antibody. Elastase and collagenase digestion indicated that the antigen was neither elastin nor collagen. From tissue distribution studies and enzymatic treatment it was thought that the antibody recognized a new connective tissue component.

By immunoelectron microscopy, the antibody recognized a periodic epitope along the microfibrils found in connective tissue (Sakai et al., 1986). This included microfibrils existing as bundles, unassociated with any other visible structure, and those surrounding an elastic fiber. In the latter case, the antibody bound only to the microfibrils, not to the central region of the fiber or at the interface between the core and mantle. The periodicity of the bound antibody was approximately 67 nm, coincidentally the same as the interstitial collagen band periodicity.

The protein antigen was isolated from fibroblast cell culture medium. Fibroblasts grown in the presence of [^{35}S] cysteine produced a protein that migrated to an approximate molecular weight of 300,000 by SDS-PAGE followed by autoradiography. The electrophoretic behavior was different under reducing conditions, showing a size of 350,000. This suggested that the molecule was held in a compact conformation by disulfide bonds. Further characterization revealed a glycoprotein nature indicated by staining with a periodic acid-Schiff reagent, and incorporation of [^{3}H] glucosamine added to cell culture medium into the same band by SDS-gel electrophoresis. [^{35}S] sulfate did not label the protein. Western blot analysis indicated that an antigen at the same position was responsible for the immunoreactivity and this was named fibrillin.

The biosynthesis of fibrillin molecules was studied in chick organ cultures (Sakai, 1990). They appear to be synthesized as a slightly larger molecule, 375,000 daltons, and processed extracellularly to 350,000. Attempts to extract significant amounts of monomer were difficult. Pulse-chase studies indicate that shortly after secretion of the molecules, they were removed from the medium, and assembled into a high molecular weight form. By SDS-PAGE in the presence of reducing agents, the aggregate migrated to the position of a fibrillin monomer (Sakai, 1989). This suggests that fibrillin is secreted from the cell as a monomer which very rapidly aggregates into an insoluble complex that is held together by disulfide bonds.

About the protein, we know an approximate molecular weight, that it contains a carbohydrate component that is not sulfated, and we know that its monomeric and aggregated structure is maintained by disulfide bonds.

THESIS OBJECTIVES

A molecular component of the microfibrillar element found in many extracellular matrices has been isolated and identified as fibrillin. Attempts toward further characterization of the protein have been plagued by insufficient quantity of the intact monomer. Problems in isolating the cell culture product include rapid formation of an insoluble network containing fibrillin, and the protease sensitivity of the monomer. Purification of the 350,000 dalton molecule has resulted in too little protein to analyze the amino acid composition and determine amino-terminal or internal sequences of fibrillin.

The initial aim of the work carried out and described in this thesis was to isolate portions of fibrillin from human tissue in adequate quantities to perform structural studies. Previously described antibodies were available to detect fibrillin. The amniotic membrane of human placenta was an available tissue source and one rich in fibrillin-containing microfibrils. Attempts to extract intact fibrillin with salt buffers and chaotropic agents were not successful. Application of Ross and Bornstein's methods using reducing agents in the presence of guanidine-HCl, may have extracted intact monomers successfully. However, the available fibrillin antibodies do not recognize reduced material so this would not be a useful extraction procedure. Preliminary investigations showed that proteolytic agents were successful in solubilizing material that was recognized by fibrillin antibodies.

Ciliary zonules are a microfibrillar-rich tissue of the eye that have been speculated to be defective in Marfan syndrome, a heritable connective tissue disease. A prominent clinical feature of the disorder is dislocated lenses. Because the fibrillin antibodies recognized the microfibrils of

ciliary zonule, skin sections and cultured cells from patients and families of Marfan syndrome were studied. The microfibrillar network composed of fibrillin appeared to be abnormal (Godfrey et al., 1990). These preliminary results were encouraging and it became clear that the next step was to apply molecular biology tools in an attempt to establish a link between a defect in fibrillin and Marfan syndrome. Amino acid sequence data would be required to isolate cDNA clones of fibrillin. This would be a step towards genetic linkage analysis using RFLPs to map the Marfan locus to the fibrillin gene.

The structural studies of fibrillin fragments were undertaken with the aim of not only providing primary structural information, but also to answer some questions about a higher level of structure, the macromolecular form found in tissues. A relationship between fibrillin and the microfibrils had been established by immunolocalization of antibodies along the microfibril. However there was no information on the tissue form of fibrillin, its macromolecular organization or physiological function.

SPECIFIC AIMS:

1) Isolation and characterization of native fragments from protease digest.
2) Sequence small peptides and look for regions suitable for probes.
3) Elucidate the structure of the microfibrils.

METHODS

PART I. PREPARATION AND CHARACTERIZATION OF PEPSIN FRAGMENTS

The microfibrillar network, recently shown to contain fibrillin (Sakai et al., 1986) is notoriously insoluble. Ross and Bornstein (1969) extracted microfibrillar components using chaotrophic agents and dithiothreitol, a reducing agent. The fibrillin antibody that was available only recognized antigen in a native unreduced conformation, so that the reductive GuHCl extraction procedure could not be applied. Therefore a different approach was pursued. To isolate fibrillin and/or portions of the molecule of interest, a protocol based upon a collagen extraction procedure was developed. Human amnion was digested with pepsin followed by differential salt fractionation of solubilized materials, water dialysis and a number of chromatographic steps. Initially one fragment was identified as being related to fibrillin based on immunoreactivity with a previously characterized monoclonal antibody to intact fibrillin (mAb201). Antibodies to two other fragments were produced, one a polyclonal antiserum, and the other a monoclonal antibody, both of which recognized intact fibrillin provided by Dr. Lynn Sakai. The new antibodies demonstrated a microfibrillar pattern by immunolocalization, characteristic of fibrillin containing microfibrils.

1. Isolation of pepsin fragments

Amniotic membrane was separated from normal human placenta and homogenized thoroughly with a Polytron homogenizer in cold distilled water. The suspension was centrifuged at 9600 g (4500 rpm Sorvall GSA) for 20 minutes, the pellet was resuspended in cold 1 M NaCl, and stirred at 4^{o}C until completely dispersed and

centrifuged once more. This washing procedure was repeated twice more with 1 M NaCl, once with water and the final pellet resuspended in 0.5 M acetic acid. The stirred suspension was digested with pepsin (0.8 mg pepsin/100 g wet weight) for 16 hours at 4°C. The solubilized material was collected following centrifugation at 27,500 g (13,000 rpm Sorvall GSA rotor) for 20 minutes. Sodium chloride (10% w/v) was added to the supernate and after stirring for 20 minutes, the precipitate formed was collected by centrifugation at 27,500 g for 30 minutes. The pellet was resuspended in 0.1 M Tris-HCl pH 8.1 and stirred at 4°C for at least 72 hours to inactivate the pepsin. Proteins were separated using fractional salt precipitations at 2.7 M and 4 M NaCl. The final 4 M NaCl supernatant was dialyzed against cold water. A precipitate was formed and was removed by centrifugation at 21,000 g. This fraction contained two of the fragments, PF1B and PF3. The supernatant which contained the other two fragments, PF1 and PF2, was lyophilized.

2. Chromatrographic purification of pepsin fragments

Two pepsin fragments from the water supernatant were separated using gel filtration chromatography on two Bio-Sil TSK-250 columns (21.5 mm x 60 cm, BioRad), connected in tandem, equilibrated with 40 mM Tris-HCl pH 6.8 containing 100 mM $NaSO_4$ and 6 M urea, at a flow rate of 0.6 ml/min at room temperature. Fractions from the dominant peaks were collected, further purified and desalted on a C18 reverse-phase column (Vydac TP201, The Separations Group) using an isopropanol gradient in 0.1% TFA at 50°C. The resulting fractions corresponding to PF1 and PF2, were collected and lyophilized.

The water precipitate was fractionated on two Bio-Sil TSK-400 columns connected in tandem and equilibrated in the same buffer and flow as described above. The chromatographic profile was very complex. Fractions were screened by ELISA for immunoreactivity with mAb201 and only the third peak in the chromatogram reacted. Later it was shown to have the same amino terminus as PF1, and was called PF1B. Peaks 1 and 2 were analyzed by rotary shadowing (see below, rotary shadowing). Peak 1 was an aggregated form of peak 2, which displayed a very unusual structure. A monoclonal antibody (mAb69) was produced to material that was present in peak 2, and shown to crossreact with fibrillin (see below). An antibody affinity column was prepared with mAb69 and used as a preparative purification step: 29 mg of mAb69 were coupled to cyanogen bromide (CNBr)-activated Sepharose in phosphate buffered saline, pH 7.4 (PBS). Peak 2 was dialyzed against PBS, and applied to the column. Following an extensive wash with 50 ml PBS containing 0.05% Tween20, the bound material was eluted with 0.1 M glycine-HCl pH 2.5 and fractions collected into 3 M Tris to immediately neutralize the eluant. Absorbance was monitored at 220 nm and fractions containing protein were pooled and dialyzed against 0.2 M ammonium bicarbonate. Affinity purified material from peak 2 was called PF3. Because peak 3 (PF1B) reacted with mAb201, it was further purified on a C18 reverse-phase column (PLRP-S 1512-3802, Polymer Laboratories LTD) in 0.25% TFA. The eluting buffer was 70% acetonitrile containing 0.18% TFA.

PART II. IMMUNOCHEMICAL CHARACTERIZATION

1. Preparation of antibodies.

Three antibodies were used to identify PF1, PF2, and PF3 as fibrillin. A previously characterized monoclonal antibody (mAb201) to intact fibrillin

(Sakai et al., 1986), was used initially to screen column fractions and identified a fragment which was called PF1.

Pepsin fragment PF2, isolated and purified as described above, was used to prepare a polyclonal antibody (pAb7075). The antiserum was raised in rabbits following a primary injection of 0.5 mg immunogen in PBS and complete Freund's adjuvant, followed by two secondary injections, at two week intervals, of 0.5 mg antigen in PBS and incomplete Freund's adjuvant. The collected antisera was affinity purified using PF2 coupled to CNBr-activated Sepharose 4B in PBS. Bound antibodies were eluted with 0.1 M glycine buffer, pH 2.5.

A monoclonal antibody (mAb69) was prepared to a fraction containing the PF3 fragment. Hybridomas were produced according to the method of Kohler and Milstein (Kohler and Milstein 1976) with modifications (Sakai et al, 1982). A BALB/C mouse was immunized by injecting 100 µg immunogen in PBS into the intraperitoneal cavity. The antigen was homogenized with an equal volume of Freund's complete adjuvant to act as an immune system irritant. Following this primary immunization, the mouse was reinjected or "boosted" with immunogen only. For three consecutive days, two weeks after the second injection, the mouse was injected with immunogen. On the fourth day the animal was sacrificed and the spleen was removed. The spleen cells were released by mincing the spleen aseptically in culture medium. The cell solution was centrifuged to pellet the cells. In the meantime NS-1 myeloma cells (P3-NS1/1-AG4-1) were prepared by washing in serum-free medium (Dulbecco's modified Eagle's medium) three times: centrifugation, followed by removal of the medium, and resuspension in a small amount of fresh medium. The NS-1 cells were mixed with spleen lymphocytes at an approximate ratio of 1:5 and centrifuged at 210 g (100 rpms Sorvall H-1000B) for five minutes. The cells were fused with polyethylene

glycol (PEG) 1500: 2 mls 38% PEG was added to pelleted cells, and gradually the solution was diluted to 16 mls total over 8 minutes, while the cell solution and PEG was kept at 37°C. Agitation was kept to a minimum. The mixture was centrifuged at 210 g (1000 rpms Sorvall H-1000B) for 10 minutes and the cell pellet was resuspended in HAT medium (DMEM supplemented with 10% fetal calf serum, 10^{-4} M hypoxanthine, 4 X 10^{-7} M aminopterin, and 1.6 X 10^{-5} M thymidine), for plating at a density of approximately 360 wells/mouse spleen. HAT medium selects for a hydrid cell type, the fused product between the lymphocytes and myeloma cells by effectively blocking endogeneously produced purines and pyrimidines while supplying the salvage pathway components. Myeloma cells lack enzymes required by this alternative system, and cannot survive while hybridomas are able to thrive. Spleen cells do not thrive and usually die within the first week in culture conditions.

The resulting hybridomas were screened for immunoreactivity with the immunogen and by indirect immunofluorescence of skin sections. mAb69 was a hybridoma clone that reacted with the immunogen and produced a fibrillin-type staining pattern by immunofluorescence.

2. Immunoblotting

Pepsin fragments were separated by polyacrylamide gel electrophoresis and electrotransferred to nitrocellulose for immunoblotting (Towbin et al., 1979). Hybridoma medium was diluted 1:3 with PBS; affinity purified pAb7075 was diluted 1:50. Reactivity of the new antibodies with the fibrillin molecule was established by immunoblotting fibrillin-containing culture medium with all antibodies. Fibrillin was isolated from fibroblast culture medium by precipitating with ammonium sulfate at 30% saturation. The precipitate was

resuspended in 50 mM Tris, 2 M urea pH 7.8, containing 2.6 mM phenylmethylsulfonyl fluoride (PMSF) and 1.4 mM EDTA. Additionally the sample was treated with diisopropyl fluorophosphate (DFP) to inhibit proteolytic enzyme degradation of fibrillin. This was then dialyzed overnight at 4°C in 50 mM Tris pH 7.8. Insoluble material was removed by centrifugation at 21,000 g (14,000 rpm, Sorvall SS-34) for 30 minutes, and the supernatant applied to a Waters DEAE HPLC column equilibrated in the above Tris buffer and the bound material eluted with a 1 M NaCl gradient. The fractions containing fibrillin were pooled and again treated with DFP, and dialyzed against Tris buffer containing 1 M urea. The sample was applied to a gelatin sepharose column to remove fibronectin. The unbound fraction was then applied to a Pharmacia MonoQ ion exchange column in Tris buffer containing 2M urea, with a 0 to 1 M NaCl gradient. The eluting fibrillin fraction was used as a control to characterize the new antibodies in Western blot analysis. Normal non-immune rabbit serum was used as a control for the antiserum raised against PF2.

3. Immunofluorescence

Various tissues were screened for presence of immunoreactive material with the antibodies produced. The immunofluorescent patterns were compared to those produced by a previously characterized fibrillin antibody. Tissues were deep frozen in hexane at -80°C and sections cut to 9 µm. After air-drying, the sections were fixed with acetone for 10 minutes and allowed to air-dry again. The tissue sections were incubated with primary antibodies (monoclonal culture medium undiluted; affinity-purified antiserum diluted 1:250 in PBS) for 3 hours following removal of excess antibody by washing with PBS. Antibody bound to tissue was detected by fluorescein-labeled goat anti-mouse or anti-rabbit IgG,

acting as a secondary antibody in 1:50 dilution with PBS. The sections were examined in an Olympus inverted microscope with a fluorescent filter.

4. Immunoelectronmicroscopy

Antibodies were further characterized by enbloc immunolabeling of skin, using gold conjugated secondary antibodies (Keene et al., 1988; Sakai et al., 1986). Freshly obtained human neonatal foreskin was sliced into 1 X 0.5 mm tissue pieces, including epithelium to allow orientation in the electron microscope. Unfixed tissues were washed in PBS at 4°C for 2 hours and then incubated in primary antibody (monoclonal culture medium undiluted; affinity-purified antiserum diluted 1:5 in PBS) overnight at 4°C. Following a 6 hour wash in PBS at 4°C, samples were incubated in goat anti-mouse (GAM) or anti-rabbit (GAR) 5-nm gold conjugate (Janssen Life Science Products) diluted 1:3 in bovine serum albumin (BSA) buffer (20 mM Tris-HCl, 0.9% NaCl, 1 mg/ml BSA, 20 mM NaN_3), pH 8.0 overnight at 4°C, followed by an extensive rinse in PBS as above. The samples were then rinsed briefly in 0.1 M sodium cacodylate buffer, pH 7.4, fixed in cacodylate-buffered 3% formaldehyde/3% gluteraldehyde, rinsed again in cacodylate buffer, and postfixed in buffered 1.0% OsO_4. The samples were then rinsed in buffer, dehydrated in a stepwise series of ethanol dilutions to 100% ethanol, washed in propylene oxide, infiltrated in Spurr's epoxy (hard formula, Electron Microscopy Sciences) and embedded to obtain cross sections of the epithelium. Sections 60-90 nm, were cut on an Ultramicrotome (Ultracut E; Reichert Scientific Instruments, Buffalo, NY) and mounted on formvar coated grids. Grids were stained in 2% uranyl acetate in 50% ethanol for 15 minutes and Reynolds' lead citrate (Reynolds, 1963) for 60 seconds. Specimens were examined at 60-80 kV, using a 30 um objective aperature with a Philips 410 LS transmission electron microscope.

PART III. ANALYTICAL CHARACTERIZATION OF FIBRILLIN FRAGMENTS

1. Rotary shadowing

Rotary shadowing of molecules was accomplished by modification of standard techniques (Tyler et al., 1980). Samples containing 0.5 to 1.0 mg/ml in 0.5 M acetic acid or 0.2 M ammonium bicarbonate were diluted with glycerol to a final concentration of 70% glycerol. 100 µl of solution were sprayed through an air brush at an acute angle onto freshly cleaved 6-mm mica discs. Droplet sizes were 50 to 200 µm in diameter. Samples were dried in a Balzers BAE 250 evaporator (10^{-6} Torr). The sample was rotated at 100 rpm. Platinum was evaporated from an electron beam gun at a 6^{o} angle relative to the mica surface. The stage was then tilted 90^{o} relative to a carbon source, and 50 Å of carbon were evaporated onto the surface of the mica. The carbon replica was immediately floated off the mica surface in doubled-distilled water and mounted onto 400-mesh grids. The samples were examined at 80 kV, with a 30 µm objective aperture in a Philips 410 LS transmission electron microscope.

2. Electrophoresis

SDS-Polyacrylamide gel electrophoresis was performed according to the method described by Laemmli (1970) and the proteins visualized by Coomassie blue staining. Gradient gels of 5-10%, 3-10%, or 8-19% acrylamide were chosen for optimum separation. Molecular weight standards used were myosin (200kd), β-galactosidase (116kd), phosphorylase B (95.5kd), glutamate dehydrogenase (55kd), ovalbumin (43kd), lactate dehydrogenase (36kd), carbonic anhydrase (29kd), lactoglobulin (18.5kd), and cytochrome c (12.4kd).

3. Peptide mapping

Analytical quantities of PF1 and PF2 were cleaved with cyanogen bromide, trypsin, and V8 protease digestions, and analyzed on polyacrylamide gel electrophoresis to produce peptide maps (Trypsin: Sigma T-8642, 11,500 α-N-benzoyl-l-arginine ethyl ester (BAEE) units/mg enzyme; V8 protease: Sigma P-8400, 500 units/mg enzyme). The V8 protease digest was carried out using 1:50 enzyme to protein ratio in 50 mM Tris-HCl pH 7.5 containing 5 mM $CaCl_2$ at 37°C for 24 hours. The trypsin digest conditions were the same as for V8 protease except that the enzyme to protein ratio was 1:100 and no $CaCl_2$ was added. Cyanogen bromide reaction was performed using equal amounts (W/W) of cyanogen bromide and peptide in nitrogen-purged 70% formic acid for 4 hours at 30°C.

4. Cysteine derivitization

Disulfide bonds were reduced and blocked with vinyl pyridine (Friedman et al., 1970). The molar content of sulfhydryl groups was calculated from the moles of peptide in a given solution and residues of cysteine per peptide. Peptides were reduced in 100-fold molar excess of β-mercaptoethanol to moles of sulhydryl groups overnight at room temperature in 0.5 M Tris-HCl buffer, pH 7.5, containing 8 M urea, 0.2 M NaCl and 5 mM EDTA. Equimolar amounts of vinyl pyridine to β-mercaptoethanol were added and incubated another 90 minutes at room temperature. The peptides were separated from excess reagents by desalting on a BioRad P2 desalting gel in 0.5 M acetic acid, or by dialysis against 0.5 M acetic acid.

5. Amino acid composition

Amino acid analyses were carried out using phenylthiocarbamyl (PTC) amino acid derivatives and the Pico Tag system (Waters) with slight modifications (Morris et al., 1986) to detect the presence and achieve resolution of hydroxyproline and hydroxylysine. The reverse-phase column used was a C18 Ultrasphere 4.6 X 150 mm (Beckman Instruments). Buffer A: 19 g/l sodium acetate trihydrate, 1 ml/l triethylamine adjusted to pH 5.7 with acetic acid. Buffer B: 60% acetonitrile in water. Elution was performed at 50°C, 1.4 ml/min using the following linear gradient sequence: initial, 9% B; 6 min, 11% B; 11 min, 42% B; 15 min, 45% B; 18 min, 100% B; 22 min, 100% B; 22.5 min, 9% B; and 28 min, 9% B.

6. Sedimentation velocity and equilibrium sedimentation

Sedimentation coefficients were determined in a Beckman Model E ultracentrifuge equipped with a photoelectric scanner. Fragments were centrifuged at 52,000 (PF1 and PF2) and 48,000 (PF3) revolutions per minute at 20°C. The buffers used for PF1 and PF2 were 50 mM Tris pH 7.0 containing 100 mM NaCl. Centrifugation of PF3 was performed in three buffer conditions: 50 mM phosphate containing 100 mM NaCl, 0.1% HCl containing 100 mM NaCl, and 3 M guanidine-hydrochloride pH 7.8. Equilibrium centrifugation was performed at 13,000 rpm and analysis at 234 nm.

PART IV. AMINO ACID SEQUENCING

Amino acid sequences were determined using a gas-phase sequencer (Applied Biosystems Model 470A) with an average repetitive yield of 92%. The samples were applied to a glass fiber filter previously precycled with polybrene

(Applied Biosystems) and standard operating programs were used (run cycle RUN470-L). The PTH amino acids were identified using a dedicated on-line analyzer (Applied Biosystems Model 120A).

In addition to the amino-terminal sequences from PF1 and PF2, a considerable amount of internal sequences from short peptides have been generated. Enzyme digests using conditions and enzyme to protein ratios described under peptide mapping were used. Several chromatographic separation systems were used including TSK-DEAE anion exchange (BioRad), C18 reverse phase (Vydac TP201), and TSK2000 (BioRad) column chromatography. PF3 was digested further with pepsin (Sigma, 2500 units/mg) with the intention of producing a more homogeneous fragment, at a 1:50 protein-enzyme ratio in 0.5 M acetic acid, at 50°C for one hour followed by overnight at 37°C. The peptides were separated on two BioSil TSK2000 columns in tandem, equilibrated in TSK-urea buffer described above. Resulting peaks were pooled and separated further on a C18 reverse-phase column. Baseline separated peaks were pooled and lyophilized. Peptides were then reduced and alkylated, desalted and reapplied to the reverse-phase column prior to sequence analysis.

A newer preparative method for peptide sequencing was also applied that combines the high resolving power of SDS gel electrophoresis with electroblotting onto a polyvinylidine difluoride membrane (PVDF, Immobilon, by Millipore) according to the method by Matsudaira (1987). A CNBr peptide mixture from PF1 was separated by SDS-PAGE on a 8-19% polyacrylamide gradient gel. Following electrophoresis, the gel was equilibrated in CAPS transfer buffer for 15 minutes (10 mM 3-cyclohexylamino-1-propanesulfonic acid, pH 11.0 with 2.0M NaOH). A section of Immobilon was cut to gel-size, wetted with methanol and equilibrated with transfer buffer for at least 5 minutes. A

blotting apparatus was assembled with the gel oriented between the negative electrode and the Immobilon membrane. The peptides were electrotransfered at 70V for 1 hour at 4°C. The membrane was then washed for 5 minutes with distilled water, stained with Coomassie blue for 5 minutes to visualize the peptide bands, destained for 10 minutes and rinsed with distilled water. The bands of interest were cut out and directly sequenced according to Edman chemistry.

Computer programs were used to analyze sequence data. These included RELATE and SEARCH, programs provided by Protein Sequence Query (PSQ), the communication and retrieval service of Protein Identification Resource (PIR), (Orcutt and Dayhoff, 1985; Dayhoff, 1979). The RELATE program was designed to detect similarity between sequences by comparing all possible segments of a given length from one sequence to a second sequence. A score is determined by the pairing of residues at corresponding positions within the two segments. RELATE was used to locate regions of identity between the cDNA and peptide sequences, thus providing a way to identify correct reading frames, and maintain alignment. SEARCH was designed to identify sequence homologies with known protein sequences from the protein database. Fibrillin cDNA sequences were used to search the database to locate sequence similarities.

PART V. HIGHER LEVELS OF STRUCTURE

1. Circular dichroism

Circular dichroism (CD) spectra were taken on a Jasco J-500A CD spectrophotometer. Measurements were made using a 50 or 100 µm pathlength cell thermostatted at 20°c. The instrument was calibrated using (+)-10-camphorsulfonic acid, $\Delta\varepsilon$ = +2.37 $M^{-1}cm^{-1}$ at 290.5 nm and -4.95 at 192.5 nm.

Data points were collected by a microcomputer at 0.1 nm intervals using a 4 second time constant and a 5 nm/min scanning speed throughout the experiments. Absorbance measurements were made on a Cary 2000 spectrophotometer. Protein concentrations were determined by amino acid analysis (see analytical methods above). The protein concentrations varied from 1.0-2.0 mg/ml. PF1, PF2 and PF3 were analyzed in 25 mM Tris, pH 8.0. Digitized CD spectra for 20 repeated runs of each protein sample were averaged and analyzed for secondary structure by the variable selection methods of Manavalan (1987) using 161 data points at 0.5 nm intervals from 260-180 nm. Digitized CD spectra for PF1 and PF2 in 50 mM Tris, 100 mM NaCl, pH 7.8 were analyzed in a similar fashion from 260-180 nm.

2. Prediction from sequences

Computer predictions of secondary structure were applied to regions of PF2. This is not to imply that the empirical methods of structure prediction describe accurate structures but rather are useful as a means of evaluating circular dichroism. CHOFAS, a program that is part of the Protein Identification Resource (PIR), was used to predict secondary structure in two segments of PF2 amino acid sequence. It is based on the statistical analysis of the frequency of occurrence of amino acid residues found in known protein structures. Regions of alpha-helix and beta-sheet secondary structures are calculated according to the methods of Chou-Fasman (Chou and Fasman, 1978a, Chou and Fasman, 1978b). Hydrophobicity data was used to analyze beta-turn, as calculated by Nozaki and Tanford (Nozaki and Tanford, 1971) with modifications (Rose, G.D., 1978).

3. Isolation of disulfide-linked peptides

Purified, lyophilized PF1 and PF2 were subject to harsh enzyme digest conditions to generate short, disulfide bonded peptides. These were isolated and purified, then reduced and alkylated, desalted, and applied to a reverse-phase chromatgraphy column to separate the formerly crosslinked components. Pepsin (Boehringer Mannheim, 2500 units/mg) was added to a 50°C solution of PF1 and PF2 (concentration, 2 mg/ml) 0.5 M acetic acid at a enzyme to protein ratio of 1:50 and incubated at 50°C for 1 hour, then overnight at 37°C. The digest was applied to a Vydac C18 reverse-phase column, 25 cm, buffers as previously described. Fractions representing baseline separated peaks were pooled and lyophilized. Reduction and alkylation with β-mercaptoethanol and vinyl pyridine was performed as described (see above, cysteine derivitization). A 20 cm X 0.5 cm P2 BioRad desalting gel was used to desalt the peptides in 50 mM acetic acid. The peptide peak was directly injected onto the same reverse-phase column; fractions were lyophilized, an aliquot removed for composition and sequencing. See above for methods.

Peptides that were not well separated following pepsin digestion were pooled, lyophilized and digested with trypsin as described previously. The resulting peptides were collected and treated as above: peptides reduced and aklylated, desalted, and applied to a C18 reverse-phase column to separate resulting peptides of formerly crosslinked components. Aliquots were removed for composition and sequencing.

RESULTS

PART I. ISOLATION AND IDENTIFICATION OF PEPSIN FRAGMENTS OF FIBRILLIN

Initially monoclonal antibody 201 was used to search for fibrillin fragments. A component in a pepsin-digested preparation of human amnion demonstrated immunoreactivity with the previously characterized antibody (Sakai et al., 1986). Pepsin solubilized tissue was fractionated with sodium chloride and presence of the antigen was monitored by immunoblotting with mAb201 at each consecutive salt step (Fig. 1). Immunoreactive material remained in solution after fractional salt precipitation of the solubilized proteins at 4M NaCl (Fig. 1). Dialyzing this solution extensively against water caused the formation of a heavy precipitate which contained a complex mixture of proteins (Fig.2A). The dialysis supernatant however, gave one major Coomassie blue stained band after electrophoresis which split into two major components after disulfide-bond reduction (Fig. 2A). Western blot analysis of unreduced samples showed that both dialysis supernatant and precipitate contained immunoreactive material and that the separation of a major component into the supernatant was incomplete (Fig.2B). However, sufficient amounts of protein were recovered from the less complex supernatant to allow further characterization of this material.

1. Isolation of PF1 and PF2 from the water dialysis supernatant

The supernatant was lyophylized and chromatographed on a molecular sieve column which gave rise to two major fractions called PF1 and PF2 (Fig. 3A). When compared to globular standard proteins, the fractions demonstrated apparent molecular weights of 260k and 150k respectively. Each fraction was further

purified using reverse phase chromatography (Fig. 5A and 5B), and analyzed by SDS-PAGE on a 5-10% polyacrylamide gel (Fig. 3B). On Coomassie blue stained electrophoresis gels they both exhibited apparent molecular weights of 74,000. After reduction, PF1 decreased in mobility corresponding to an apparent molecular weight of 94,000 while mobility of PF2 increased slightly corresponding to 68,000. This suggested that PF1 has a disulfide-stabilized conformation that is more compact than in a reduced state.

2. Isolation of PF3 and PF1B from the water dialysis precipitate

The precipitate was resuspended in TSK buffer and chromatographed on a molecular sieve column as shown in figure 4A. Fraction 1 contained high molecular weight material that did not enter a gel (not shown); fraction 2 contained material that remained near the top of a 3-10% polyacrylamide gel (Fig. 4B). Electrophoresis under reducing conditions produced a complex pattern of nondiscrete bands with apparent molecular weights of 30-50k, indicating that the large structure present in fraction 2 was maintained by disulfide bonds. Fraction 3, after further purification by reverse-phase chromatography (Fig. 5C), demonstrated an apparent molecular weight of 200kD by SDS-PAGE (Fig. 4C). Electrophoresis of PF1B in the presence of reducing agents, produced a ladder of discrete bands (Fig. 4C) suggesting that there are internal cleavage sites from the initial pepsin digest but that the fragment was held together by disulfide bonds. However, the amount of internal cleavage varied. This particular digest demonstrated more extensive cleavage than seen in subsequent preparations.

3. Characterization of new antibodies and identification of fragments as fibrillin

The original immunoreactivity of a component in the water dialysis supernatant with mAb201 was shown to identify PF1 as the antigen by ELISA. Though no antigenicity of PF2 was observed with this, and another fibrillin antibody (mAb F2), it was speculated that it too might be another fragment. Antiserum was made using PF2 as the immunogen, in an attempt to produce antibodies that would crossreact with fibrillin, thus identifying it as part of the molecule. Purified antisera pAb7075, made against PF2, demonstrated specific reactivity to fibrillin by immunoblotting (Fig. 6), and indirect immunofluorescence labeling of several bovine tissue sections (Fig. 7) produced a staining pattern characteristic of a fibrillin distribution (Sakai et al., 1986). Immunoelectron microscopic localization using pAb7075 as the primary antibody and gold-conjugated secondary antibody (Fig. 9B) verified that the structure recognized was that of the microfibril previously found to contain fibrillin (Sakai et al., 1986).

Due to the complex and interesting structure of PF3 as observed by rotary shadowing (described below) its molecular origin was of interest, although its relationship to fibrillin was not indicated. There was no immunoreactivity of PF3 detected with existing antibodies to fibrillin and collagen types VI and VII. Monoclonal antibodies were made against PF3 and one antibody mAb69 selected for further characterization. This antibody reacted specifically with intact fibrillin in Western blot analysis (Fig. 6) and gave characteristic indirect immunofluorescent staining patterns on several bovine tissue sections (Fig. 8). Immunoelectron microscopy, using gold conjugated antibodies, showed the labeling to be specific in skin for microfibrils, similar to that for pAb7075 (Fig. 9A).

One way to determine the relationship of fragments to each other is by determining crossreactivity of the antibodies. Western blot analysis was performed on PF1, PF1B, PF2, and PF3 with antibodies mAb201, the original fibrillin antibody, pAb7075, made against PF2, and mAb69, made to PF3. There was no crossreactivity noted (Fig. 10A): mAb201 recognized only PF1 and PF1B, antiserum pAb7075 reacted only with PF2, and mAb69 recognized only PF3. This lack of crossreactivity indicates that although they are all fragments of fibrillin, they are probably from different regions of the parent molecule.

PF1B demonstrated immunoreactivity with only mAb 201, demonstrating a relationship with PF1, at least sharing an epitope to the fibrillin antibody (Fig. 10B). Amino acid sequence analysis of PF1 and PF1B revealed that the fragments have the same amino-terminal sequence (Table I).

Material in pool 1 of figure 4A did not enter a 3% polyacrylamide gel and therefore could not be analysed using immunoblotting but did react strongly and exclusively with mAb69 in ELISA assays.

4. Rotary shadowed images of the pepsin fragments

Electron micrographs of rotary shadowed preparations of PF1, PF2, and PF1B showed rod shaped molecules (Fig. 11A,B,C). PF2 images appeared to be a segmented rod while PF1 was more uniform, thinner and longer. PF1B appeared to be almost twice as long as PF1. Electron microscope pictures of rotary shadowed PF3 preparations revealed a complex structure (Fig. 11D). A crab-like unit was observed which consisted of a central dense region surrounded by flexible "arms", giving the impression of several protein chains uniting to form a central core. In pool 1 of the TSK separation of water precipitate (Fig.4A), most of the material was in an aggregated form, containing from two

to several units of PF3, as indicated by rotary shadowed images (Fig. 11E,F), apparently covalently bound since they were chromatographed in the presence of 6M urea. In contrast pool 2 consisted mainly of single complexes, and this oligomer is referred to as PF3. The number of projecting chains was difficult to determine, however as many as 8 chains have been observed. Extraction of the fragments may have damaged PF3 units in a heterogeneous manner so that the number and lengths of the arms varied from crab to crab. From the broad band on SDS-PAGE it also appeared that there was heterogeneity of size.

PART II. CHARACTERIZATION OF FIBRILLIN FRAGMENTS

1. Peptide mapping of PF1 and PF2

Although PF1 and PF2 did not share mAb201 and pAb7075 epitopes, it was still possible that they contained common sequences, that is, they were overlapping fragments. To determine this peptide maps produced by trypsin, V8 protease and CNBr cleavage of PF1 and PF2, were analyzed using SDS-PAGE (Fig. 12). Fragments with intact disulfide bonds were cleaved and run reduced and unreduced on gels. A comparison of peptide bands that showed a similar pattern would indicate significant overlap of the fragments. Comparing fragmentation patterns PF1 and PF2 (Fig. 12), there is little similarity, indicating that there is very little if any overlap of sequences.

2. Amino acid composition and amino terminal sequencing

The amino acid compositions of PF1, PF1B, PF2, and PF3 are shown in Table I. Noteworthy is the high content of acidic amino acids. Unfortunately aspartic and glutamic acid quantitative values includes asparagine and glutamine which are oxidatively deaminated to the acid form during the hydrolysis process. The

absence of hydroxyproline[1] and hydroxylysine excluded the presence of a collagenous domain. All fragments contained significant amounts of cysteine.

Amino terminal amino acid sequencing of PF1, PF1B, and PF2, is shown in Table I. Due to the complexity of PF3 a single amino terminal sequence could not be determined. Presumably there were several amino termini, but none dominated to produce a sequence signal that could be detected. PF1, PF1B, and PF2 contained a single polypeptide chain. No homologous sequences were found in searches of protein sequence data banks. The fifth residue of PF1 was not identified in the sequencer but the amino acid composition of a tryptic peptide corresponding to positions 1 to 10 contained a serine. This position is probably occupied by a glycosylated serine. Especially significant is the amino terminal sequence identity between PF1 and PF1B. Although both fragments reacted with mAb201, the relationship between the two fragments was not clear. The molecular weight of PF1B determined by SDS-PAGE, was twice that of PF1 (Fig. 3 and 4). The extent of internal cleavages as indicated by a ladder of peptides in the presence of reducing agents varied between preparations. The sample analyzed by SDS-PAGE in figure 4 indicates considerably more cleavage than the sample that demonstrated a single amino terminus (Table I).

3. Biophysical properties of the fibrillin fragments

The sedimentation profile of PF1 and PF2 was determined in 50 mM Tris, pH 7.0 containing 100 mM NaCl. At a speed of 52,000 rpm, a single sedimenting

---

1/ it is uncertain whether the small amount of hydroxyproline in the composition of PF3 was a small contaminant or actually present in the sequence of the fragment

boundary was observed. Sedimentation was repeated at two additional concentrations of fragments in solution, and the sedimentation coefficient values were extrapolated to zero concentration. This yielded a sedimentation constant of $s^0_{20,w}$ = 3.4 and 2.7S, respectively (Table II).

The sedimentation constant is a useful value to determine molecular weight and hydrodynamic properties of proteins. The frictional coefficient (f) is a term that describes the drag of a molecule in solution and was determined for PF1 and PF2 according to:

$$s = \frac{M(1-\nu\rho)}{Nf} = \frac{\nu}{\omega^2 r}$$

The minimun value for f (f_o) is that of a spherical molecule. It is calculated using Stokes Law: $f_o = 6\pi\eta R$. The frictional ratio, f/f_o, for a particular molecule is always greater than 1. Based on f/f_o, a molecule can assume a prolate (cigar shape), an oblate (disc shape) ellipsoid conformation, or that of a rod (van Holde, 1985). The dimensions of the fragments were calculated for each of these possibilities (Table II), with **a** ≡ 1/2 of the length, **b** ≡ 1/2 of the width of the assumed conformation. Comparison of the calculated dimensions with estimated dimensions from rotary shadow micrographs supports a rod-like structure being the actual shape.

As mentioned above, molecular weight can be approximated using sedimentation coefficient. A more accurate measurement than sedimentation velocity is sedimentation equilibrium based on:

$$M = \frac{2RT}{(1-\nu\rho)\omega^2} \frac{d\ \ln C}{d(x^2)}$$

where: ν (partial specific volume based on compositions of the fragments) = 0.705; ρ (density of buffer) = 1.1442 gm/ml; ω (angular velocity) = 1368 rads/sec; R (gas constant) = 8.313 X 10^7 g cm^2/deg mol sec^2; d ln c/d(x^2) is the slope of a curve with O.D. (c) plotted on a semilog scale on the vertical axis and distance from the axis of rotation (x) squared, on the horizontal axis. The molecular weights of PF1 and PF2 were determined to be 110,000 and 51,300, respectively (Table II).

The sedimentation profile of PF3 was difficult to obtain. In 10 mM phosphate buffer, pH 7.8 containing 100 mM NaCl, and 0.1% HCl buffer, the fragment sedimented at such a phenomenal rate that it was rumoured in the lab to be a virus particle. An approximate s and molecular weight could not be determined from this sort of sedimentation behavior. By SDS-PAGE the apparent molecular weight of the fragment is 750kD to 900kD, which would not account for the sedimentation rate that was observed. It was speculated that aggregation of the fragments occurred. In 3 M guanadine-hydrochloride, sedimentation occurred at a much slower rate, although it was very broad indicating heterogeneity in the population of PF3 units. From this data an s value of 25.6S was determined at a speed of 48,000 rpm (Table II). A molecular weight based on that of a sphere at this s value was estimated at approximately 800,000, similar to the apparent molecular weight position from SDS-PAGE.

PART III. SEQUENCE DATA

In addition to the amino-terminal sequences from PF1 and PF2, considerable sequence data from short peptides has been generated from enzyme digests. Due to the complexity of the fragment, an amino terminal sequence of PF3 could not be determined. The majority of sequenced peptides from PF1, PF2, and PF3 were

purified by HPLC reverse-phase chromatography, at least at the last step of a separation protocol. This provided a way to desalt the peptides prior to sequence analysis.

The peptides that compose PF3 were disulfide bonded and although they were heterogeneous, they were difficult to separate by chromatographic methods described above as they are so similar in size, charge, and hydrophobic properties following reduction. When PF3 was further digested with pepsin, a disulfide bonded peptide approximately 30kd was produced by SDS-PAGE (Fig. 13A), which reduced to a band migrating further than the 16kd molecular weight marker. Although the pepsin digestion was not complete by gel analysis, two well defined bands were blotted with mAb69 with approximate molecular weight of 25-30kd (Fig. 13B).

Peptide mixtures of PF1 and PF2 that were difficult to separate by conventional chromatography methods were prepared differently, following a method described by Matsudaira (1987) for electroblotting and sequencing. Electrotransfer of peptide bands from SDS-PAGE onto an Immobilon membrane that is compatible with Edman chemistry was successful in separating and sequencing several CNBr peptides of PF2 (Fig. 14). Sequences from PF1, PF2, PF3 isolated by both HPLC and electrotransfer are listed in Appendix I. Approximately 700 residues have been sequenced from peptides.

Dr. Cheryl Maslen, a postdoctoral fellow in the laboratory of Dr. Lynn Sakai, is investigating the relationship of fibrillin to Marfan syndrome. Using oligonucleotide probes representing the degenerate sequences of candidate regions of PF1 and PF2, she has identified several positive clones in a λgt11 cDNA library made from human placenta (purchased from Clontech). The hybridization procedure was base composition-independent of fully degenerative

probe sequences (Wood et al., 1985). cDNA sequences were compared with protein sequences to identify correct reading frames, and both sequences were used to confirm or correct each other. This was especially important in regions of peptide that could not be identified by protein sequences, such as glycosylated residues. As longer stretches of amino acids were translated from cDNA sequencing, the short peptides determined by Edman chemistry were ordered and aligned into longer sequences. Up to 4000 bases will be sequences from nonoverlapping clones identified with a PF2 probe (underlined in PF2 sequence section in Appendix I). Two stretches of significant length (Fig. 16) were used for secondary structure predictions (see Part IV).

PART IV. OTHER STRUCTURAL ANALYSES

1. Circular dichroism

Circular dichroic analysis was applied to obtain information on the secondary structure of fibrillin fragments. PF1 and PF2 were initially analyzed in Tris buffer containing 100 mM NaCl. Unfortunately absorbance at 180 nm could not be determined in the NaCl-containing buffer. The spectra of PF1, PF2, and PF3 in 25 mM Tris, pH 8.0 are shown in figure 15. Calculated contributions of α-helix, β-sheet, parallel and antiparallel, β-turn and unidentified "other" structures are presented in Table III. The spectra of PF1 and PF2 in high salt indicated more β-sheet and less α-helix than buffer without NaCl. It appears that NaCl stabilizes β-sheet structure in the two smaller fragments, so that it more closely resembles PF3 which contains considerable antiparallel β-sheet and β-turn.

2. Prediction from sequences

Computer predictions of secondary structure were applied to sequences of PF2. cDNA sequences from two clones, CLM1 and CLM2, were used to order peptide sequences and produced longer regions of sequence than peptide sequences alone. Two stretches of sequence data were amenable to secondary structure prediction. Results indicate mostly beta-sheet with frequent beta-turns in one sequence (Fig. 16A), and a long stretch of beta-sheet in another (Fig. 16B).

3. Isolation of disulfide crosslinks

Disulfide crosslinks have been shown to play a role in maintaining the tertiary conformation of the fibrillin molecule (Sakai et al., 1986), as well as playing a major role in the integrity of microfibrils (Ross and Bornstein, 1969). From amino acid composition we know that there is a large contribution of cysteine residues in the fibrillin fragments isolated (Table I). Whether or not they are involved in intrachain crosslinks or available for intermolecular crosslinks has not been determined, although it is clear from enzyme digestions and subsequent peptide maps before and after reduction that disulfide links play a role in intrachain stabilization. With the goal of developing a protocol for isolation of disulfide bonded peptides (see METHODS), several peptides from PF1 were successfully isolated by HPLC following enzymatic digestion (Fig. 17A). These were reduced and rechromatographed, although only two peptides (peaks 1 and 2, Fig. 17A) were of sufficient length following reduction to separate from the reagents eluted in the final peak during desalting. In one case, a single peptide eluted, suggesting an intra-peptide bond, or possibly an intermolecular bond between aligned molecules (Fig. 17B).

In another case, two peptides were eluted and their sequences determined (Fig. 17C). These specific sequences were not previously known, so that ordering these peptides along the intact molecule will have to wait for much more extensive cDNA sequencing.

DISCUSSION

PREPARATION AND CHARACTERIZATION OF FRAGMENTS

Difficulties in extraction and characterization of connective tissue macromolecules are common. The structural stability that enables extracellular matrix components to function in the extracellular space also imparts insolubility. Progress in the isolation and characterization of elastin for example, has been tremendously hampered because of its insolubility, the result of extensive crosslinking. Nonreducible lysine-derived crosslinks are characteristic of elastin. Methods of isolation were designed to destroy all other connective tissue components by boiling tissues in sodium hydroxide or autoclaving, thus leaving behind an elastin residue. Isolation of collagens has utilized treatment of tissue with proteolytic enzymes such as pepsin. Cleavage occurs at pepsin sensitive sites that flank the proteolytic resistant helical domain which is then easily extracted.

Extracellular matrix microfibrils have also been difficult to isolate and characterize. The tissue most frequently studied has been the nuchal ligament due to its availability and high elastic fiber content. The standard method of tissue extraction has been that of Ross and Bornstein's (1969) which utilized chaotrophic agents in the presence of reducing agents. By ultrastructural analysis following "reductive GuHCl" extraction, the microfibrils disappear, indicating solubilization. Unfortunately these extracts have been shown to contain a mixture of proteins. In addition to the difficulties caused by insolubility of the microfibrils, and a heterogeneous extract, a third significant problem was lack of a specific marker to identify individual components. Cleary and coworkers have produced polyclonal antisera to pooled

fractions from molecular sieve chromatography and were able to use antibodies to identify their components. However, they have not demonstrated that their antisera are monospecific or how the components are structurally related. Monoclonal antibody technology identified fibrillin as an integral component of the microfibrils. Other groups have produced monoclonal antibodies that recognize a microfibrillar pattern but have not isolated a specific protein responsible for the antigenicity (Schmitt et al., 1986; Kambe and Hashimoto, 1987).

An objective of this thesis project was to isolate human fibrillin that could be used for structural studies. Components extracted with denaturing and reducing agents as from previous methods, were of no use for analyses other than composition and amino acid sequences. Additionally, the fibrillin marker that was available was a monoclonal antibody that recognized only a native, nonreduced conformation. However, intact fibrillin secreted into cultured fibroblast medium rapidly aggregated to an insoluble matrix (Sakai, 1990) so that the monomer pool was very small. This was of limited use as larger quantities were needed.

Attempts were made to extract fibrillin from tissues using PBS, salt buffers, and 8 M GuHCl with no reducing agent present, and were not successful. Previous studies of the elastic fiber had shown that the microfibrils were solubilized with enzyme digestion using trypsin and chymotrypsin (Ross and Bornstein 1969). With this in mind, a protocol based on collagen preparations utilizing a pepsin digest of human amnion was applied. Placenta was an available tissue and known to contain fibrillin (Sakai et al. 1986).

Four fragments of fibrillin were isolated following tissue digestion, differential salt fractionation and dialysis against water. Two smaller

fragments, PF1 and PF2, were isolated from the water supernatant; two larger fragments from the water precipitate. These pepsin-resistant domains demonstrated further resistance to proteolytic processing for peptide sequencing. Internal disulfide bonds apparently maintain this stability, as indicated by increased enzyme sensistivity following reduction of the fragments.

Yields of the fragments were more than adequate for the proposed studies. 5 and 10 mg per 100 g wet weight of tissue was obtained for PF1 and PF2, respectively. The yield of PF1B and PF3 varied with different preparations from 0 to 0.5 mg, and from 0.5 to 2 mg per 100 g wet weight, respectively. Yields of PF1 and PF2 are higher than those for any glycoproteins Cleary reported (Gibson et al., 1989; Gibson et al., 1986). Reductive GuHCl extractions of nuchal ligament produced 0.8 to 1.0 mg of MAGP per 100 g wet weight, and 1.6 t0 1.8 mg MP340. As these components were extracted from a different tissue than amnion, it is difficult to directly compare the yields per 100 g wet weight.

Of interest is the degree of solubilization of the microfibrils using either of these techniques. Reduction of disulfide bonds clearly results in extractability of microfibrillar glycoproteins from tissue, but how much of the microfibrils is solubilized is not known. Sakai has observed in biosynthetic studies that high molecular weight aggregates of fibrillin contain crosslinks that cannot be reduced (Sakai, 1990). These crosslinks may form between fibrillin molecules or between fibrillin and other matrix components, thus holding the microfibrils in tissues. It is tempting to speculate that there are lysine-derived crosslinks between elastin and the microfibrils that form an elastic fiber. These crosslinks are characteristic of elastin, and the enzyme

responsible has been localized to the interface of the amorphous core and the surrounding microfibrils (Kagan et al., 1986).

Analytical methods have been useful in determining three dimensional structural features, such as size and shape of the fragments. Rotary shadowed images of PF1, PF2, and PF1B show these to be rod shaped linear fragments. PF1 is approximately 40 nm, and PF2 approximately 32 nm in length. PF1B appears to be at least twice as long as PF1, although it was difficult to measure. Intact fibrillin monomer isolated from fibroblast culture medium is also an extended linear molecule by rotary shadowing, measuring approximately 130 nm (Sakai, unpublished observation). In contrast to these fragments and the parent molecule, the rotary shadowed image of PF3 is quite dramatic. It is a highly complex structure with a predominant central globular region and arms extending outwards. There is nothing about the structure that would suggest asymmetry or could represent sidedness. The arms look similar to PF1 and PF2 in that they are flexible rod-like segments. It is certainly not obvious what the center portion is composed of. It almost looks as though there is a hole in the middle of some beads, although the metal deposits on a high profile structure could lead to such an artifact.

Results obtained from analytical ultracentrifugation studies provide additional information concerning the size and shape of the fragments. From sedimentation velocity and equilibrium data, accurate molecular weights, frictional coefficients and dimensions of possible conformations were determined. Comparison of the hydrodynamic parameters for PF1 and PF2 to rotary shadowed images confirms that the rod-like shape observed approximates the size and shape in solution. Because PF3 was centrifuged in a denaturing solution, hydrodynamic parameters could not be determined for the native

structure. The molecular weight is approximated from the frictional coefficient of a spherical particle at the extrapolated sedimentation coefficient of 25.6S (Tanford, 1961). The apparent molecular weight from SDS-PAGE is similar to the value from sedimentation velocity, suggesting most of the mass is contributed by the very dense globular region.

PF3 analyzed by SDS-PAGE demonstrated a 800,000 dalton protein band that reduced to 10 to 20 bands, with approximate molecule weight of 30 to 60 kDa. These bands are narrow and well defined, suggesting little glycosylation. No immunological relationship of the peptides to each other has been determined since mAb69, the antibody made to PF3, does not recognize reduced material. Separating so many peptides for sequence analysis to determine sequence overlap was impossible. The peptides are similar in size, charge, and hydrophobic properties so that conventional HPLC separation methods have not been helpful. Methods to digest PF3 to a more uniform shape with less peptide heterogeneity has proved somewhat successful so that a few peptides have been purified and sequenced.

It is clear that the peptides that compose this large, oligomeric structure are held together through disulfide bonds, indicating that PF3 may represent a major crosslinking region. It is not known whether the fibrillin monomer forms this structure alone or with another component. Other proteins that may be covalently attached to this oligomer have not yet been identified. In the process of making monoclonal antibodies to PF3, mAb69 as well as many other clonal hydridomas resulted. All the antibodies that produced a microfibrillar immunofluorescent pattern, also recognized fibrillin and PF3 as the antigen. Theoretically, if other components were present they should have generated an immunogenic response and produced antibodies as well. However,

some proteins are not very immunogenic. For example, several attempts were made to produce monoclonal antibodies to PF2, but were unsuccessful. Even so, this evidence supports that fibrillin is the sole component of PF3.

PF1B and PF2 are linear and nonoverlapping fragments. The sum of the molecular weights of PF1B and PF2 (200,000 and 51,300, respectively) is at least 250,000, which is 70% of the total molecular weight. That leaves 30% of the molecule contained in the crosslinked domain, or roughly 110,000 daltons. PF3 estimated at 800,000 daltons, would contain 8 such fibrillin peptides. This is consistent with the observation that there are 6 to 10 arms extending from the globular region of PF3. These fragments may be a useful way of reconstructing assembly events toward a concept of macromolecular structure.

Information concerning the secondary structure of the fragments obtained from circular dichroic analyses was disappointing. An initial run of PF1 and PF2 in 50 mM Tris, pH 7.8 containing 100mM NaCl, demonstrated significant structure, especially in antiparallel β-sheet and β-turn. The spectra of PF1 and PF2 looked similar to each other. In the presence of NaCl, it was difficult to determine the absorbance at 180λ so that in repeated experiments, NaCl was not included. However, there was less structure without NaCl. Samples from four different preparations were analyzed with the same results. As purification of PF1 and PF2 required use of denaturing buffers containing urea and organic solvents, the possibility that the fragments were irreversibly denatured was considered. Therefore, a sample containing PF1 and PF2 prior to separation in urea buffer was analyzed and the spectra compared to that for purified fragments. If the fragments had been altered by the procedures, then the spectra of the mixture would have indicated more total structure. However, the results were the same as the others, all demonstrating less structure than

the initial run. PF1 and PF2 have some α-helix, less β-sheet, and more β-turn. PF3 has much more β-sheet, and practically no α-helix. These results are reminiscent of fibronectin. CD analysis of fibronectin indicates essentially no α-helix and a high proportion of β-structure (Mosesson et al., 1975).

Comparison of the secondary structure profiles of the linear (PF1 and PF2) and globular fragments (PF3) indicates some general similarities and differences. All three fibrillin fragments have a major proportion in "other" structure which could be random coil or some sort of secondary structure not yet quantitated by CD from X-ray crystallography. Of the little structure available, there is more β-sheet in PF3, and more α-helix in PF1 and PF2. There also appears to be a correlation between the size of the fragments and the degree of structure, although the addition of NaCl seems to stabilize the β-structure in PF1 and PF2 so that they more resemble PF3. Samples were rerun after sitting at 4^{o} for variable periods of time and exhibited even less structure, possibly indicating disulfide exchange over time, or just unstable globular structure.

The positions of the fragments along the length of the molecule is not known. Information from immunochemistry, peptide mapping, and sequence analysis does not indicate significant, if any, overlap of fragments, with the exception of establishing that PF1 and PF1B have the same amino terminal sequence. Of course, when more complete protein sequence data is available the positions of the fragments will be known. To determine the entire amino acid sequence of fibrillin, it will be necessary to rely on a combination of cDNA and peptide sequences. Approximately 700 residues have been sequences from peptides, and a significant region of the fibrillin message has been sequenced as well. Probes from other regions are currently being synthesized and will be

used to screen the λgt11 cDNA library that was used for the isolation of PF2 clones.

For the time being, mapping the fragments to regions of the molecule would be helpful in speculating about the assembly process and designing experiments to test possible hypotheses. One method to determine orientation of the fragments in relation to one another is by antibody labeling of the molecule. Antibodies are easily visualized as they bind at the epitopes along the surface of an extended molecule such as fibrillin (Dieringer et al., 1985). The relative positions of the epitopes can be determined, thus fixing the relative positions of the fragments. This has been attempted unsuccessfully several times with the intact molecule. It is hoped that by altering conditions, binding will be increased, and the fibrillin monomer will be more efficiently labeled.

MACROMOLECULAR STRUCTURE

A large beaded structure has been isolated by Dr. Robert Glanville and rotary shadowing performed by Doug Keene in the Research Department at Shriners Hospital. A manuscript describing the isolation and ultrastructural analysis of the fibrillar structure is in preparation (Keene et al., see Appendix II). It was extracted from a number of tissues without the use of proteolytic enzymes. The length of the structure varies from 10 to 100 bead units per chain with thin filaments spanning the distance between the beads. Short flexible arms also extend from the bead perpendicular to the fibril axis. What is immediately noticeable is the resemblance of the beaded subunits to PF3. To detect immunoreactivity and possibly determine the molecular origin, the beads-on-a-string was used as antigen in an ELISA assay with mAb69. The positive

reaction needed confirmation since there were other components present in the solution.

The beaded structure was labeled with mAb69 and negatively stained to provide contrast with the background for better visualization. It was clear from electron micrographs that mAb69 localized to the structure, and specifically to an area adjacent to the globular domain. The characterization of a fibrillin antibody presented in this thesis, and its recognition of the beaded, fibrillar structure was important. This evidence strongly suggests that these beads-on-a-string represent the macromolecular form of fibrillin. However, the microfibrils in tissue observed by immunolocalization did not look like the beaded chains in that the ultrastructural features were not visible. It was thought perhaps that the harsh methods involved in tissue preparation, including fixing, dehydration, and embedding, might be responsible for altering the finer details of the microfibrillar structure. To compare the observed microfibrils found in tissue sections with the isolated beads-on-a-string, a homogenate of ligament containing immunolabeled beaded chains was exposed to similar conditions of tissue preparation. The result was embedded, immunolabeled microfibrils indistiguishable from those in tissues.

The fact that fibrillin antibodies labeled microfibrils in immunolocalization studies was well known. This additional information about the detailed structure of the microfibrils is new and exciting. The demonstration of mAb69 localizing to the beads-on-a-string is significant in two ways: PF3 oligomers are now thought to be the beaded unit of the beaded chains, and the beaded chains appear to be isolated microfibrils.

Isolated structures such as Glanville's have been observed before. Many years earlier this structure was described in preparations from chick vitreous

humor (Matoltsy et al, 1951). Wright and Mayne (1989) also described a similar beaded chain extracted from chick vitreous humor in PBS. Although the amino acid composition and molecular origin was not determined, based on morphology they suspected that these might be related to the beaded zonular fibrils. Ciliary zonules demonstrated a periodicity of 49 nm (Raviola, 1971) which agreed with 49.8 nm observed for the beaded chains. The reported diameter of zonule fibrils is 11 - 12 nm (Raviola, 1971), significantly lower than the 22.6 nm observed in rotary shadowed images of the beaded structures. Wright speculated that the preparative techniques of extraction and rotary shadowing might account for an artifactually large diameter.

A study of the zona pellucida, the extracellular coat of mammalian eggs, likewise revealed a beaded chain structure (Greve and Wassarman, 1985). Three glycoproteins were isolated, although how they are organized into the filament is not clear. These are thought to play a role in fertilization by acting as species-specific sperm receptors, participating in a secondary block to polysperm, and later to protect embryos traveling down the oviduct to the uterus. To date, fibrillin has not been immunolocalized to the zona pellucida, so that a relationship between the two beaded structures has not been established. Information about fibrillin does not currently support this sort of physiological role, but a possible interaction between sperm receptors and the coat matrix might be interesting to explore if it is determined that fibrillin is present in the zona pellucida.

A question worthy of comment is whether fibrillin is a structural component of the microfibrils or is an associated protein. The evidence to support that it is indeed a major structural component of microfibrils, is substantial, the criteria being that the component is present in all

microfibrils, regardless of tissue or developmental stage. Microfibrils are present in many connective tissues and matrices within the body and are easily observed at the electron microscope level. Immunoreactivity to fibrillin antibodies has been demonstrated in every tissue in which microfibrils are present. Tissue distribution studies with mAb201 and F2 were previously described (Sakai et al., 1986), and in this thesis two more antibodies, recognized antigen in all the tissues studied. If fibrillin was not a structural component of the microfibrils, one would not expect to see this exact correlation between tissue distribution patterns and presence of microfibrils. More likely, the pattern would indicate a limited distribution, such as only recognizing the microfibrils surrounding an elastic fiber in elastic tissue, or with the microfibrils of the ciliary zonules.

Another supporting indication is that in the immunolocalization studies using fibrillin antibodies and conjugated gold particles, microfibrils are labeled in a regular, repeated fashion with a periodicity of 67 nm. It would seem unlikely that an antibody would recognize a random association with such regularity. A third significant observation comes from immunolocalization of antibodies to negatively stained isolated beaded chains (Keene et al., see Appendix II). mAb69 appears to recognize an epitope to one side of the bead. The preparation of the beaded chains involves extraction with guanidine hydrochloride, a chaotropic agent that would remove associating components not covalently linked to the microfibrils, significantly reducing the possibility that the immunoreactivity is due to recognition of an associated element.

Other proteins that have been characterized in the literature as possible microfibril components are serum amyloid P (SAP), lysyl oxidase, fibronectin, and MAGP. These proteins have all been immunolocalized to the microfibrils.

SAP has been ruled out as a covalent component of microfibrils because expression of the protein is later than the appearance of the microfibrils in developing tissues (Khan and Walker, 1984). Lysyl oxidase antibodies localize to the interface between microfibrils and the elastin core, rather than to the microfibrils themselves (Kagan et al., 1986). Analysis of amino acid composition has also ruled out the possibility that SAP and lysyl oxidase are structural components as they lack cysteine, regarded as essential since the microfibrils are stabilized by disulfide bonds. Fibronectin is an odd candidate to suggest as a microfibrillar protein. It localizes to the vicinity surrounding cells and is well characterized as a cell binding protein from functional assays. It may codistribute and associate with the microfibrils noncovalently in some tissues (Schwartz et al., 1985), but does not meet the criteria for being a structural component.

Recently a new microfibrillar protein was described and isolated from porcine aorta (Kobayashi et al., 1989). Antiserum raised against the purified protein demonstrated immunohistochemical and immunolocalization to the microfibrils surrounding elastic fibers in aorta adventitia exclusively (Kobayashi et al., 1989). The antibodies did not detect the presence of antigen in skin, placenta or esophagus, tissues that are rich in fibrillin. Based upon this restricted tissue distribution, the new protein is definitely not fibrillin or another structural element of the microfibrils. It may turn out to be a tissue-specific associated protein and perform an interesting biological function, possibly interacting with fibrillin or other microfibrillar structural components.

For a number of years, Cleary and coworkers have investigated the components of the microfibrils, and until recently, exclusively the "elastin-

associated microfibrils," regarding them as a different class of structural element from those found independent of elastin in tissues. Tissue distribution studies of antiserum to MAGP, Cleary's first microfibrillar protein described, demonstrated immunoreactivity to microfibrils of the elastic fiber as well as those in nonelastic tissues (Gibson and Cleary, 1987; Gibson et al., 1986). A total of three proteins have been isolated that demonstrate a relationship to the microfibrils by immunochemical characterization. These are MAGP (31kDa microfibril-associated glycoprotein), MP78 and MP340 (microfibrillar proteins 78kD and 340kD, respectively), the molecular weight approximation based on SDS-PAGE protein bands (Gibson et al., 1989; Gibson et al., 1986). MP78 and MP340 are immunologically related, as is MAGP and MP340. MP78 and MAGP did not demonstrate crossreactivity of antibodies prepared to their respective antigens. As their preparation was not a pepsin digest of tissue, it was not suggested that MAGP and MP78 were proteolytic fragments of MP340. Rather they speculated that MAGP and MP78 plus other polypeptides were crosslinked to form MP340 (Gibson et al., 1989; Cleary et al., 1990). They report no evidence for this and do not rule out the possible degradation of MP340 to the smaller peptides.

There are obvious similarities between MP340 and fibrillin. The apparent molecular weights, 340,000 and 350,000 are essentially the same. Both are extrapolated from gel electrophoresis positions rather than sedimentation equilibrium which would provide more accurate molecular weight measurements. Initial carbohydrate analyses indicates both are glycoproteins (Gibson et al., 1986, Sakai et al., 1986). Indirect immunofluorescent patterns in various tissues are similar, and immunolocalization of antibodies recognizes the same microfibrillar structures. No amino acid composition is available for

fibrillin to compare with the published MP340 (Gibson et al., 1989), and no peptide maps or sequence data have been presented for either. However, antibodies are available that recognize the two glycoproteins. It is important that crossreactivity of the antigens be determined and documented. If it is demonstrated that they are one molecule, one name should exist for the sake of consistency.

MFP II is a large (300,000) molecular weight glycoprotein isolated from cultured ligaments cells (Sear et al., 1981). It was not collagenase sensitive and did not contain hydroxyproline. Antibodies produced to the isolated material recognized a microfibrillar pattern in tissue and also recognized an epitope on MFP II, indicated by immunoprecipitation. However, the antiserum was raised to a heterogenous preparation and proteins identified by the antiserum were later shown to be nonfibrillar components. The size of MFP II is similar to fibrillin and MP 340, and it remains to be determined whether the molecules are related.

Microfibrils and the isolated beads-on-a-string are obviously very complex assemblies. Detailed models have not been described for the process of incorporation of a fibrillin molecule into the complex. What other, if any, additional proteins associate with fibrillin and are structurally contained in the microfibril, remain to be determined.

QUESTIONS CONCERNING ASSEMBLY AND FUNCTION

Two areas of intense interest in the fibrillin story are the biosynthesis of the microfibril and its biological function. A logical place to begin to study the macromolecular assembly is with the secreted monomer from cultured cells. Theoretically, the monomer should aggregate in an ordered fashion into the

microfibrils, and it should be possible to detect and capture intermediate species that are formed in the process. For example, if the monomer forms a dimer, then tetramer, octamer, 32-mer, then each of these species should be present in cell culture medium. Immunopurification and rotary shadowing, or a gel of crude medium would reveal a ladder of immunoreactive material representing multimers of 350,000. Dr. Lynn Sakai has devoted considerable effort to investigate this, and her observations do not support this concept of stepwise assembly. Instead the monomers rapidly disappear from the cell culture medium, and a very high molecular weight fibrillin-containing compound is formed. Perhaps this represents a PF3-like intermediate that aligns linearly to form the microfibrils.

One hypothesis to explain this behavior is that microfibril assembly occurs in two steps: the association of monomers into a PF3-like oligomer followed by the linear alignment of the beaded units. This would suggest that specific areas within the molecules are involved in interactions that precede covalent crosslinking. Antibodies to discrete regions of the molecule may interfere with specific interactions and could be added to a cell culture system during active synthesis. For example, mAb69 binds to the PF3-like region in isolated, labeled beads-on-a-string, and may inhibit or block interactions that are responsible for aggregation of monomers prior to disulfide bond stabilization. Likewise, pAb7075 may block an interaction between ends of the molecule, assuming that PF2 is a terminal domain of fibrillin.

Since the macromolecular form of fibrillin is based on association and covalent crosslinking of PF3-like domains, any tendency to aggregate is worth investigating. Sedimentation studies of PF3 were difficult, presumably due to

tendency toward aggregation. It is not known whether this is a physiological phenomenon or an artifact of the ultracentrifugation conditions. It would be useful to know if the antibody binding site is close to a self-aggregation region. It might provide information about an in vivo assembly.

Another important topic of fibrillin assembly and function is that of interactions with other proteins. Fibronectin and laminin are two matrix glycoproteins that function by interacting with several components in connective tissue through functional domains along the length of the polypeptide chain. Domains can be cleaved off with proteolytic reagents and their activities determined individually. Since isolated domains of fibrillin are available, it would be useful to investigate physiological functions and localize the activity to the particular region of the molecule. Elastin is an obvious choice for interaction studies as it associates with fibrillin to form an elastic fiber. In elastogenesis microfibrils make an earlier appearance than amorphous elastin (Fahrenbach et al., 1966; Jaques and Serafini-Fracassini, 1985) and it would be significant to determine an association or crosslink. It has been speculated that an association of elastin with microfibrillar proteins occurs via the carboxyl domain of tropoelastin (Cicila et al., 1985). This region contains several basic amino acids and a cysteine. Other proteins that are candidates for investigating a possible interaction with fibrillin include fibronectin which colocalizes in isolation procedures, and basement membrane components such as collagen types IV, VII, and laminin since microfibrils appear to intersect the basement membrane in skin (Daroczy and Feldman, 1981; Briggaman and Wheeler, Jr., 1975).

Cell binding is a phenomenon that is often evaluated as a function of matrix molecules. Cell adhesion to a matrix network can lead to changes in

cell shape for some types of cells and matrix molecules. Fibrillin has not been demonstrated to effect cell binding. The available fragments would be a good place to start investigating a possible cell interaction, or any of the protein interactions suggested above. Fibrillin fragments that have been described, antibodies to the fragments, and oligonucleotide probes that have been synthesized to regions of fragment sequence, are available tools to begin investigations of interactions toward an understanding of biological activity.

MODEL OF CONNECTIVE TISSUE MICROFIBRILS

A model has been suggested to graphically relate the fragments isolated and described in this thesis with the beads-on-a-string, isolated by Glanville (Fig. 18). The evidence provided by labeling the beaded chains with mAb69, and reconstructing immunolabeled matrix-looking microfibrils from these labeled chains, leads to the assumption that the chains are, in fact, isolated microfibrils. Of course, tissue manipulations involved in the extraction of the microfibrils, including homogenization and extraction, may damage the "beads-on-a-string." This may result in the short fibers that extend perpendicular to the axis of the microfibril. In the tissue, all the filaments may connect the beads and appear more homogeneous. From the assumption that the isolated beaded chains are microfibrils, it follows that the fragments are domains of microfibrils that are released into solution by the action of pepsin on tissues and produce PF1, PF1B, PF2, and PF3, as well as other uncharacterized fragments (Fig. 18).

Further speculation leads to questions concerning the formation of the microfibril. Preliminary data mentioned above suggests that fibrillin is secreted as an extended, flexible molecule. Several monomers may organize

themselves into a PF3-like intermediate which then align end to end. To explain the asymmetry of mAb69 binding preferentially to one side of the beaded unit, requires that one side of PF3 be different from the other. The morphology appears symmetrical from rotary shadowing. It may be that the arms extending on one side are the amino termini of the molecule, and the arms extending on the other side are the carboxyl termini. The linear alignment could therefore be head to tail, with the amino termini from one bead associating with the carboxyl termini from a second bead forming the spanning filaments between the beaded units. This would maintain the asymmetrical orientation of the beaded unit in the microfibril. Figure 19 depicts the major events suggested here in the formation of the microfibrils. It is not meant to accurately detail fibrillogenesis, but to provide a model for lively discussion of these very complex events.

IMPLICATIONS OF FIBRILLIN ABNORMALITIES IN MARFAN SYNDROME

With most extracellular matrix macromolecules the structural characterization precedes the determination of a functional role. What biological role fibrillin and the microfibrils play in the structure of connective tissue, or dynamic cell-matrix interactions is unknown. When speculating about possible functions of a molecule, it is always advantageous to have a mutated system to illustrate defects. Some defects in collagen molecules that result in connective tissue diseases have been well documented. These include Osteogenesis Imperfecta (O.I.), Ehlers Danlos Syndrome (E.D.S.), and Epidermolysis Bullosa (E.B.), examples that represent a heterogenous group of genetic diseases that involve collagen types I, III, VII, respectively. Amino acid deletions, additions, and substitutions can lead to a change in structure

or stability of a molecule that causes the formation of a defective fiber. Weight or stress bearing tissues like bone and aorta require maximum strength from bundles of fibers. Defects can result in the brittle bone disorder (O.I.), and ruptured aortas, a common cause of death in E.D.S. In certain forms of Epidermolysis Bullosa, type VII collagen and its macromolecular form, the anchoring fibrils, appear to be affected. It is clinically characterized by skin blistering caused by separation of the epidermis from the underlying dermal stroma. Anchoring fibrils span this zone in normal tissues (Keene et al., 1987). While the molecular defect and primary cause of E.B. is not known, the data correlating anchoring fibril defects with the clinical diagnosis of E.B., is rather convincing. The function of type VII collagen appears to be structurally involved in maintaining the integrity of the epidermal-dermal junction.

Marfan syndrome is a more common connective tissue disease that has made news with the recent deaths of two outstanding young athletes, Flo Hyman and Chris Patton. It is characterized by a number of clinical features that involve the ocular, cardiovascular, pulmonary and musculoskeletal systems, and is inherited in an autosomal dominant manner. Life expectancy is 2/3 of normal. Cardiovascular complications are responsible for the 85% mortality rate. Death usually results from dissection and rupture of the aorta, or aortic or mitral valvular disease which causes congestive heart failure. The classical body type, known as "Marfanoid habitus" is a tall stature, with long thin limbs and arachnodactyly and joint hypermobility. Often the chest cavity and spinal column are deformed (asymmetric pectus deformity and kyphoscoliosis, respectively). Common ocular abnormalities include retinal detachment and dislocation of the lens (ectopia lentis) caused by ruptured or overly extended

fibers that compose the ciliary zonules.

Histological, ultrastructural and biochemical abnormalities have been described for Marfan syndrome, although the cause of the disease remains elusive. Defects in the collagen molecule have long been considered to be an underlying cause of the disease. Recent gene linkage studies using DNA probes for types I and II have ruled out primary structural defects involving these collagens (Boileau et al., 1990). Fibrillin has been immunolocalized to the ciliary zonules, and as Marfan syndrome is associated with dislocated lenses, a possible relationship is of interest. Indeed, indirect immunofluorescent studies of Marfan patients and their families with fibrillin antibodies show abnormal results. There appears to be a decrease in overall fluorescence in Marfan patient skin sections, and cultured fibroblasts grown in chamber slides (Godfrey et al., 1990). These studies suggest that there is a defect in the synthesis of fibrillin or the assembly of the matrix microfibrils. Whether this is a consistent finding or coincidental to this particular study group remains to be determined.

There could be a number of explanations for these abnormal results. A decrease in fluorescence indicates that the epitope of the molecule is not accessible to the antibody in tissue sections, or that the matrix that is secreted and assembled by the cultured fibroblasts does not contain microfibrils. This could be due to an overall decreased synthesis of the molecule leading to a deficient accumulation, or a sequence alteration that prohibits recognition of the epitope. However, it is suggestive that a structural defect has occurred leading to a decrease of the microfibrillar network. It is also possible that the epitope is masked by an excess of another matrix component, for example hyaluronic acid. A normal pattern in a

Marfan patient could indicate accessibility of the epitope but says nothing concerning other defective regions that result in a less stable molecule. Antibody labeling studies are extremely valuable. However, abnormal results suggest only gross defects in the molecule.

cDNA probes to the PF2 region of the molecule have been synthesized and are being used in Northern and Southern blot analyses. Hybridization of the radiolabelled probes to the fibrillin message would normally result in appropriate 10kb message size. Likewise in a Southern blot, genomic DNA fragments would hybridize to a normal pattern from an endonuclease digest. If a defect has not occurred specifically within the region of the probe, it will hybridize and blot normally. If there is a large deletion in the message, indicating major structural abnormalites, the correct message size will show a decrease in the amount, and an additional smaller band will be present. As with antibody labeling there are difficulties in interpretation of results, so that only gross defects or deletions will be apparent. Molecules with subtle base sequence changes can produce unstable fibrils, these would be undetected in these analyses.

Gene linkage analysis using chromosomal markers called restriction fragment length polymophisms (RFLPs), is an approach that is currently being used to evaluate complex genetic diseases. RFLPs are short sequences of genetic material that display differences among individuals within a population. They can be applied to family studies; individuals that have a disease may show a particular variant. A polymorphism that occurs in high frequency with a disease is known as gene linkage. From peptide sequences of PF2, probes have been synthesized that have identified positive fibrillin clones. These and other cDNA probes will be used to determine if polymorphisms

occur that "link" differences in RFLPs of Marfan syndrome patients to the fibrillin gene. Gene linkage studies will greatly increase the likelihood of detecting the gene alterations that lead to the disease, and establish the connection between Marfan syndrome and fibrillin.

Information from studies of Marfan patients and families will be helpful in deciphering the function of fibrillin. Presumably, afflicted individuals will produce a mutant protein and the defect can be pinpointed to a characterized domain. Analyses of the stability and sequence changes of these defective molecules will aid in determining biological functions.

CONCLUSIONS

The major objective of this project was to isolate human fibrillin in sufficient quantity for structural studies. The isolation and characterization of four large structural domains has enabled probes to be synthesized and fibrillin cDNA clones to be identified. From this information, a link between fibrillin and Marfan syndrome can be investigated at the molecular level. Information about the fragments has provided evidence that recently isolated fibrillar structures from connective tissues, are the macromolecular form of fibrillin. Unique features about the fibrillin microfibrils have been elucidated. Based on analyses of the fragments, a model to explain the relationship between the pepsin fragments and the microfibrils has been presented. Major events speculated to occur in fibrillogenesis are described in a second model.

An underlying concern of biological chemistry is the relationship between protein structure and function. This thesis has addressed structural features of an extracellular matrix element. The isolation and analytical characterization of four fibrillin fragments has contributed significantly toward a better understanding of the architecture of the connective tissue microfibrils. It is hoped that the tools provided by these investigations will be useful in studying functional aspects of the microfibrils and also be of use in applying the basic science information to medical science.

REFERENCES

1. Boileau, C., Jondeau, G., Bonaiti, C., Coulon, M., Delorme, G., Dubourg, O., Bourdarias, J.-P., and Junien, C. (1990) Linkage analysis of five fibrillar collagen loci in a large French Marfan syndrome family. J. Med. Genet. 27, 78-81.

2. Briggaman, R.A., and Wheeler, Jr., C.E. (1975) The epidermal-dermal junction. J. Invest. Dermatol. 65, 71-84.

3. Bruckner-Tuderman, L., Mitsuhashi, Y., Schnyder, U.W., and Bruckner, P. (1989) Anchoring fibrils and type VII collagen are absent from skin in severe recessive dystrophic epidermolysis bullosa. J. Invest. Dermol. 93, 3-9.

4. Bruns, R.R., Press, W., Engvall, E., Timpl, R., and Gross, J. (1986) Type VI collagen in extracellular, 100-nm periodic filaments and fibrils: identification by immunoelectron microscopy. J. Cell Biol. 103, 393-404.

5. Chou, P.Y. and Fasman, G.D. (1978a) Empirical predictions of protein conformation. Ann. Rev. Biochem. 47, 251-276.

6. Chou, P.Y. and Fasman, G.D. (1978b) Prediction of secondary structure of proteins from their amino acid sequence. Adva. Enzymol. 47, 45-148.

7. Cleary, E.G., Gibson, M.A., Kumaratilake, J.S., and Fanning, J.C. (1990) The microfibrillar component of the elastic fibers. In Elastin: Chemical and Biological Aspects. Proc. Internatl. Congr. Italy (Eds: A.M. Tamburro and J.M. Davidson) Galatina Congedo.

8. Cleary, E.G., and Gibson, M.A. (1983) Elastin-associated microfibrils and microfibrillar proteins. Int. Rev. Conn. Tiss. Res. 10, 97-209.

9. Cotta-Pereira, G., Rodrigo, F.G., and Bittencourt-Sampaio, S. (1976) Oxytalan, elaunin, and elastic fibers in the human skin. J. Invest. Derm. 66, 143-148.

10. Daróczy, J., and Feldmann, J. (1981) Microfilaments of the human epidermal-dermal junction. Front. Matrix Biol. 9, 155-174.

11. Dayhoff, M.O. (1979) Survey of new data and computer methods of analysis, In Atlas of Protein Sequence and Structure. Natl. Biomed. Res. Found. 5, 353-358

12. Dieringer, H., Hollister, D.W., Glanville, R.W., Sakai, L.Y., and Kühn, K. (1985) Structural studies of human basement-membrance collagen with the use of a monoclonal antibody. Biochem. J. 227, 217-222.

13. Dempsey, E.W. and Lansing, A.I. (1954) Elastic tissue. Int. Rev. Cytol. 3, 437-453.

14. Engel, J., Odermatt, E., Engel, A. (1981) Shapes, domain organizations and flexibility of laminin and fibronectin, two multifunctional proteins of the extracellular matrix. J. Mol. Biol 150, 97-120.

15. Fahrenbach, W.H., Sandberg, L.B, Cleary, E.G. (1966) Ultrastructural studies on early elastogenesis. Anat. Rec. 155, 563-568.

16. Friedman, M., Krull, L.H., Cavins, J.F. (1970) The chromatographic determination of cystine and cysteine residues in proteins as S-B-(4-Pyridylethyl)cysteine. J. Biol. Chem. 245:15, 3868-3871.

17. Furthmayr, H., Widemann, H., Timpl, R., Odermatt, E., Engel, J. (1983) Electron-microscopical approach to a structural model of Intima Collagen. Biochem J. 211, 303-311.

18. Gibson, M.A., and Clearly, E.G. (1982) A collagen-like glycoprotein from elastin-rich tissues. Biochem. Biophys. Res. Comm. 105, 1288-1295.

19. Gibson, M.A., Cleary, E.G. (1985) CL glycoprotein is the tissue form of type VI collagen. J. Biol. Chem. 260, 11149-11159.

20. Gibson, M.A., Cleary, E.G. (1983) Distribution of CL glycoprotein in tissues: an immunochistochemical study. Collag. Rel. Res. 3, 469-488.

21. Gibson, M.A., Hughes, J.L., Fanning, J.C., Cleary, E.G. (1986) The major antigen of elastin-associated microfibrils is a 31 kDa glycoprotein. J. Biol. Chem. 261:24, 11429-11436.

22. Gibson, M.A., Kumaratilake, S., and Cleary, E.G. (1989) The protein components of the 12-nanometer microfibrils of elastic and nonelastic tissues. J. Biol. Chem. 264, 4590-4598.

23. Gibson, M.A., and Cleary, E.G. (1987) The immunohistochemical localization of microfibril-associated glycoprotein (MAGP) in elastic and non-elastic tissues. Immunol. Cell Biol. 65, 345-356.

24. Godfrey, M., Menashe, V., Weleber, R., Koler, R., Bigley, R., Lovrien, E., Zonana, J., and Hollister, D. (1990) Cosegregation of elastin-associated microfibrillar abnormalities with the Marfan phenotype in families. Am J. Hum. Genet. 46, 652-660.

25. Greenlee, T.K., Jr., Ross, R., and Hartman, J.L. (1966) The fine structure of elastic fibers. J. Cell Biol. 30, 59-71.

26. Hall, D.A. (1957) Chemical and enzymatic studies on elastin. In Connective Tissue (Ed: R.E. Tunbridge) pp 238-253. Blackwell, Oxford.

27. Jaques, A., and Serafini-Fracassini, A. (1985) Morphogenesis of the elastic fiber: an immunoelectronmicroscopy investigation. J. Ulstructr. Res. 92, 201-210.

28. Jaques, A., and Serafini-Fracassini, A. (1986) Immunolocalization of a 35K structural glycoprotein to elastin-associated microfibrils. J. Ultrastruct. Mol. Struct. Res. 95, 218-227.

29. Johnson, Jr., W.C. (1988) Secondary structure of proteins through circular dichroism spectroscopy. Ann. Rev. Biophys. Biophys. Chem. 17, 145-166.

30. Kagan, H.M., Vaccaro, C.A., Bronson, R.E., Tang, S.-S., and Brody, J.S. (1986) Ultrastructural immunolocalization of lysyl oxidase in vascular connective tissue. J. Cell Biol. 103, 1121-1128.

31. Kambe, N. and Hashimoto, K. (1987) Anti-elastofibril monoclonal antibody NKH-1: production and application. J. Invest. Derm. 3, 253-258.

32. Karrer, H.E. (1958) The fine structure of connective tissue in the tunica propria of bronchioles. J. Ultrastr. Res. 2, 96-121.

33. Keene, D.R., Engvall, E., and Glanville, R.W. (1988) Ultrastructure of type VI collagen in human skin and cartilage suggests an anchoring function for this filamentous network. J. Cell Biol. 107, 1995-2006.

34. Keene, D.R., Sakai, L.Y., Lunstrum, G.P., Morris, N.P., Burgeson, R.E. (1987) Type VII collagen forms an extended network of anchoring fibr ils. J. Cell Biol. 104, 611-621.

35. Kewley, M.A., Steven, F.S., Williams, G. (1977) Preparation of a specific antiserum towards the microfibrillar protein of elastic tissues. Immunology 32, 483-489.

36. Kewley, M.A., Williams, G., and Steven, F.S. (1978) Studies of elastic tissue formation in the developing bovine ligamentum nuchae. J. Pathol. 124, 95-101.

37. Khan, A.M., and Walker, F. (1984) Age related detection of tissue amyloid P in the skin. J. Pathol. 143, 183-186.

38. Kobayashi, R., Tashima, Y., Masuda, H., Takeshi, S., Yukiko, N., Ken-ichi, M., Hayakawa, T. (1989) Isolation and characterization of a new 36-kDa microfibril-associated glycoprotein from porcine aorta J. Biol. Chem. 264, 17437-17444.

39. Laemmli, U.K. (1970) Cleavage of structural proteins during the assembly of the head of bacteriophage T4. Nature 227, 680-685.

40. Low, F.N. (1962) Microfibrils: fine filamentous components in the tissue space. Anat. Rec. 142, 131-137.

41. Manavalan, P., and Johnson, Jr., W.C. (1987) Variable selection method improves the prediction of protei secondary structure from circular dichroism spectra. Anal. Biochem. 167, 76-85.

42. Matsudaira, P. (1987) Sequence from picomole quantities of proteins electroblotted onto polyvinylidene difluoride membranes. J. Biol. Chem. 262, 10035-10038

43. Mayer, B.W., Hay, E.D., Hynes, R.O. (1981) Immunocytochemical localization of fibronectin in embryonic chick trunk and area vasculose. Develop. Biol. 82, 267-286.

44. Mecham, R.P. (1981) Elastin biosynthesis: a look at the current scene. Conn. Tiss. Res. 8, 155-160.

45. Mendler, M., Eich-Bender, S.G., Vaughan, L., and Winterhalter, K.H. (1989) Cartilage contains mixed fibrils of collagen types II, IX, and XI. J. Cell Biol. 108, 191-197.

46. Morris, N.P., Keene, D.R., Glanville, R.W., Bentz, H., and Burgeson, R.E. (1986) The Tissue form of type VII collagen is an antiparallel dimer. J. Biol. Chem. 261, 5638-5644.

47. Mosesson, M.W., Chen, A.B., and Huseby, R.M. (1975) The cold-insoluble globulin of human plasma: studies of its essential structural features. Biochim. Biophys. Acta 386, 509-524.

48. Muir, L.W., Bornstein, P., and Ross, R. (1976) A presumptive subunit of elastic fiber microfibrils secreted by arterial smooth-muscle cells in culture. Eur. J. Biochem. 64, 105-114.

49. Nozaki, Y. and Tanford, C. (1971) The solubility of amino acids and two glycine peptides in aqueous ethanol and dioxane solutions. J. Biol. Chem. 246, 2211-2217.

50. Orcutt, B.C., and Dayhoff, M.O. (1985) Scoring Matrices, PIR Report MAT-0285. Natl. Biomed. Res. Found.

51. Raviola, G. (1971) Fine structure of the ciliary zonule and ciliary epithelium. Investig. Ophthal. 10, 851-869.

52. Reynolds, E.S. (1963) The use of lead citrate at high pH as an electron-opaque stain in electron microscopy. J. Cell Biol. 17, 208-215.

53. Rose, G.D. (1978) Predictions of chain turns in globular proteins on a hydrophobicity basis. Nature 272, 586-590.

54. Ross, R., and Bornstein, P. (1969) The elastic fiber: I. separation and partial characterization of its macromolecular composition. J. Cell. Biol 40, 366-381.

55. Ross, R. (1973) The elastic fiber: a review. J. Histochem. Cytochem. 21, 199-208.

56. Sakai, L.Y., Engvall, E., Hollister, D.W., and Burgeson, R.E. (1982) Production and characterizatin of a monoclonal antibody to human type IV collagen. Amer. J. Path. 108, 310-318.

57. Sakai, L.Y., Keene, D.R., Engvall, E. (1986) Fibrillin, a new 350-kD glycoprotein, is a component of extracellular microfibrils. J. Cell Biol. 130, 2499-2509.

58. Sakai, L.Y. (1990) Disulfide bonds crosslink molecules of fibrillin in the connective tissue space. In Elastin: Chemical and Biological Aspects. Proc. Internatl. Congr. Italy (Eds. A.M. Tamburro and J.M. Davidson). Galatina Congedo.

59. Sandberg, L.B., Weissman, N. and Smith, D.W. (1969) The purification and partial characterization of a soluble elastin-like protein from copper-deficient porcine aorta. Biochemistry 8, 2940.

60. Sandberg, L.B., Weissman, N., Gray, W.R. (1971) Structural features of tropoelastin related to the sites of cross-links in aortic elastin. Biochem. 10, 52-56.

61. Schmitt, D., chignol. M., Brochier, J. and Thivolet, J. (1986) HB8: a monoclonalantibody recognizing elastic fiber microfibrils. Brit. J. Derm. 114, 661-665.

62. Schwartz, E., Goldfischer, S., Coltoff-Schiller, B., and Blumenfeld, O.O. (1985) Extracellular matrix microfibrils are composed of a core proteins coated with fibronectin. J. Histol. Cytochem. 33, 268-274.

63. Sear, C.H.J., Grant, M.E., and Jackson, D.S. (1981) The nature of the microfibrillar glycoproteins of elastic fibres. Biochem. J. 194, 587-598,

64. Sear, C.H.J., Jones, C.J., Knight, K.R., and Grant, M.E. (1981) Elastogenesis and microfibrillar glycoprotein synthesis by bovine ligamentum nuchae cells in culture. Conn. Tiss. Res. 8, 167-170.

65. Streeten, B.W., and Gibson, S.A. (1988) Identification of extractable proteins from the bovine ocular zonule: major zonular antigens of 32kD and 250kD. Curr. Eye Res. 7, 139-146.

66. Tanford, C., (1961) In Physical Chemistry of Macromolecules John Wiley, New York.

67. Tyler, Jr., J.M., and Branton, D. (1980) Rotary shadowing of extended molecules dried from glycerol. J. Ultrastr. Res. 71, 95-102.

68. van Holde, K.E. (1985) In Physical Biochemistry Prentice-Hall, Inc., New Jersey.

69. Wood, W.I., Gitschier, J., Lasky, L.A., and Lawn, R.M. (1985) Base composition-independent hybridization in tetramethylammonium chloride: A method for oligonucleotide screening of highly complex gene libraries. Proc. Natl. Acad. Sci. 82, 1585-1588.

70. Wright, D.W., and Mayne R. (1988) Vitreous humor of chicken contains two fibrillar systems: an analysis of their structure J. Ultrastruct. Mol. Struct. Res. 100, 1-11.

LIST OF FIGURES

Fig. 16. Predicted secondary structure from peptide sequences of PF2.

Fig. 17. Isolation of disulfide bonded peptides from PF1 pepsin digest for sequence analysis.

Fig. 18. A model of the preparation of fibrillin fragments PF1, PF2, PF1B, and PF3 from pepsin digest of connective tissue microfibrils.

Fig. 19. A model representing the synthesis of a microfibril from a fibrillin molecule.

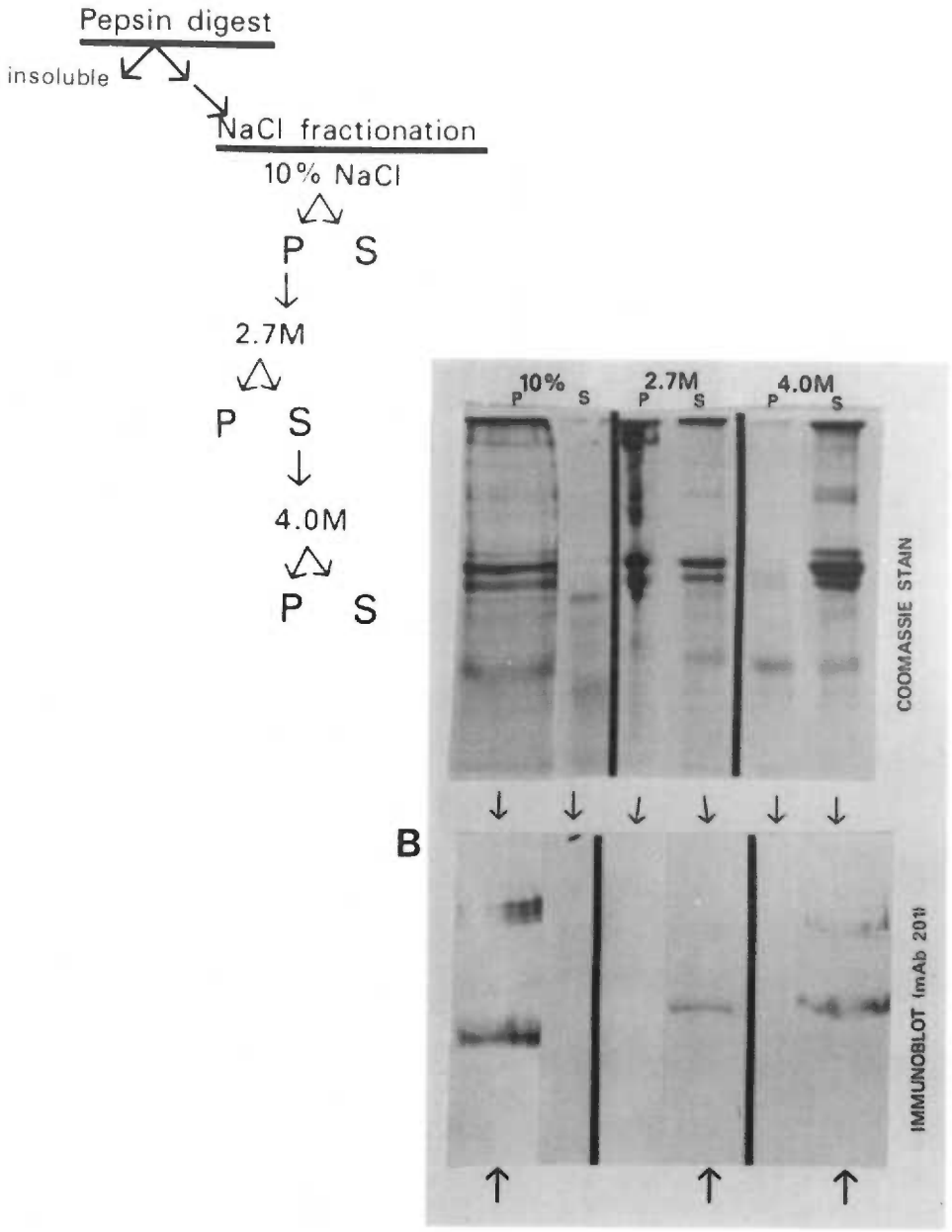

Figure 1. Monitoring immunoreactivity of NaCl precipitated fractions with mAb 201. Human amnion was digested with pepsin and fractionated as shown. Both precipitate and supernatant were analyzed by SDS-PAGE at each stage of the fractionation, on a 5-10% gradient polyacrylamide gel. (A) Coomassie blue stained gel. (B) Western blot analysis using fibrillin antibody mAb201 following electrotransfer onto nitrocellulose. Aliquots of the fractions were only electrophoresed without reducing agents as the antibody does not recognize reduced samples. Precipitate - P, Supernatant - S.

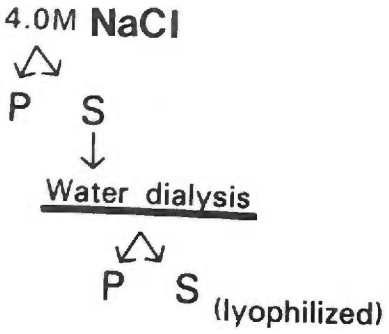

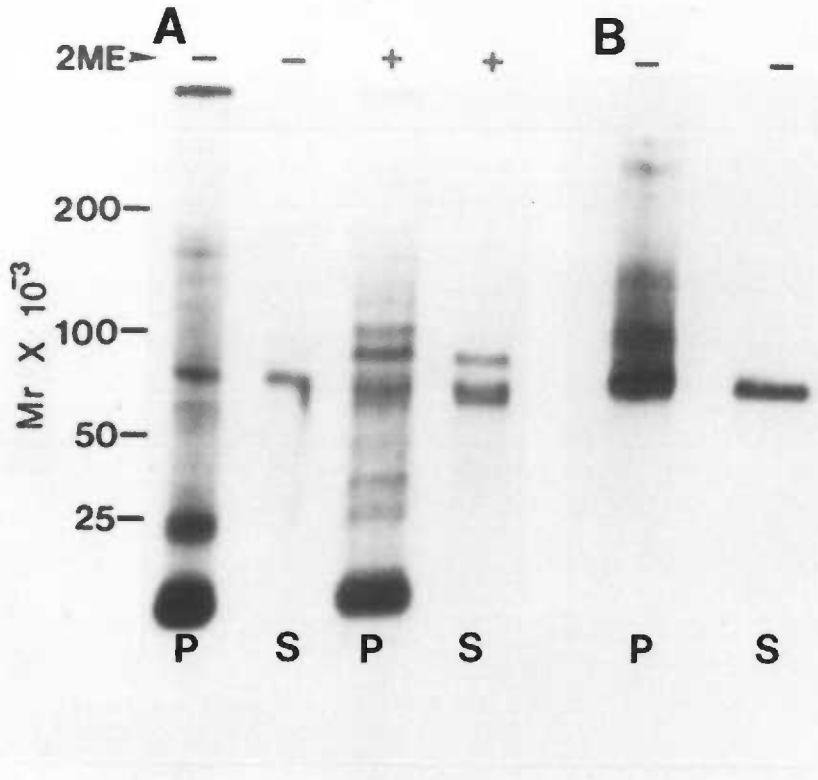

Figure 2. Immunoblotting of water dialysis fractions. Components of the water precipitate and supernatant were separated on a 5-10% gradient polyacrylamide gel, with (+) and without (-) 2-mercaptoethanol (2ME). Gel lanes stained with Coomassie blue are shown on the left (A). Separated components were also electrotransferred to nitrocellulose and immunoblotted with mAb201 to identify fibrillin fragments (B). The antibody does not recognize reduced samples. Precipitate - P, Supernatant - S.

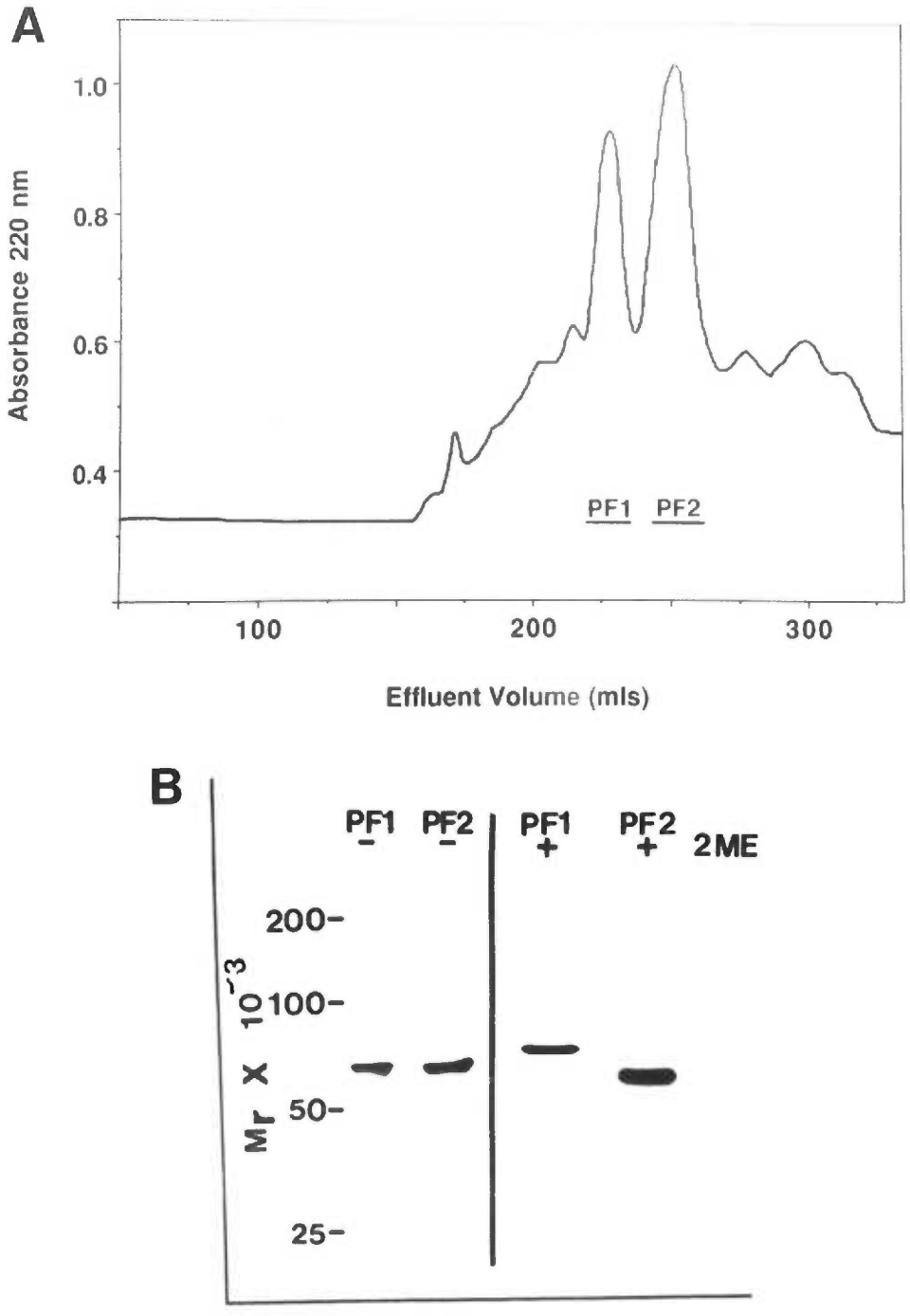

Figure 3. Purification of PF1 and PF2 by molecular sieve chromatography. A: separation of the water supernatant fraction on a TSK3000 column into two major components, PF1 and PF2. Fraction was collected as indicated by bars underneath the peaks and further purified using reverse-phase chromatography (not shown). B: SDS-PAGE of PF1 and PF2 on a 5-10% gradient acrylamide gel. The fragments were electrophoresed with (+) and without (-) 2-mercaptoethanol (2ME) and stained with Coomassie blue. The apparent molecular weight scale was determined by using globular standards.

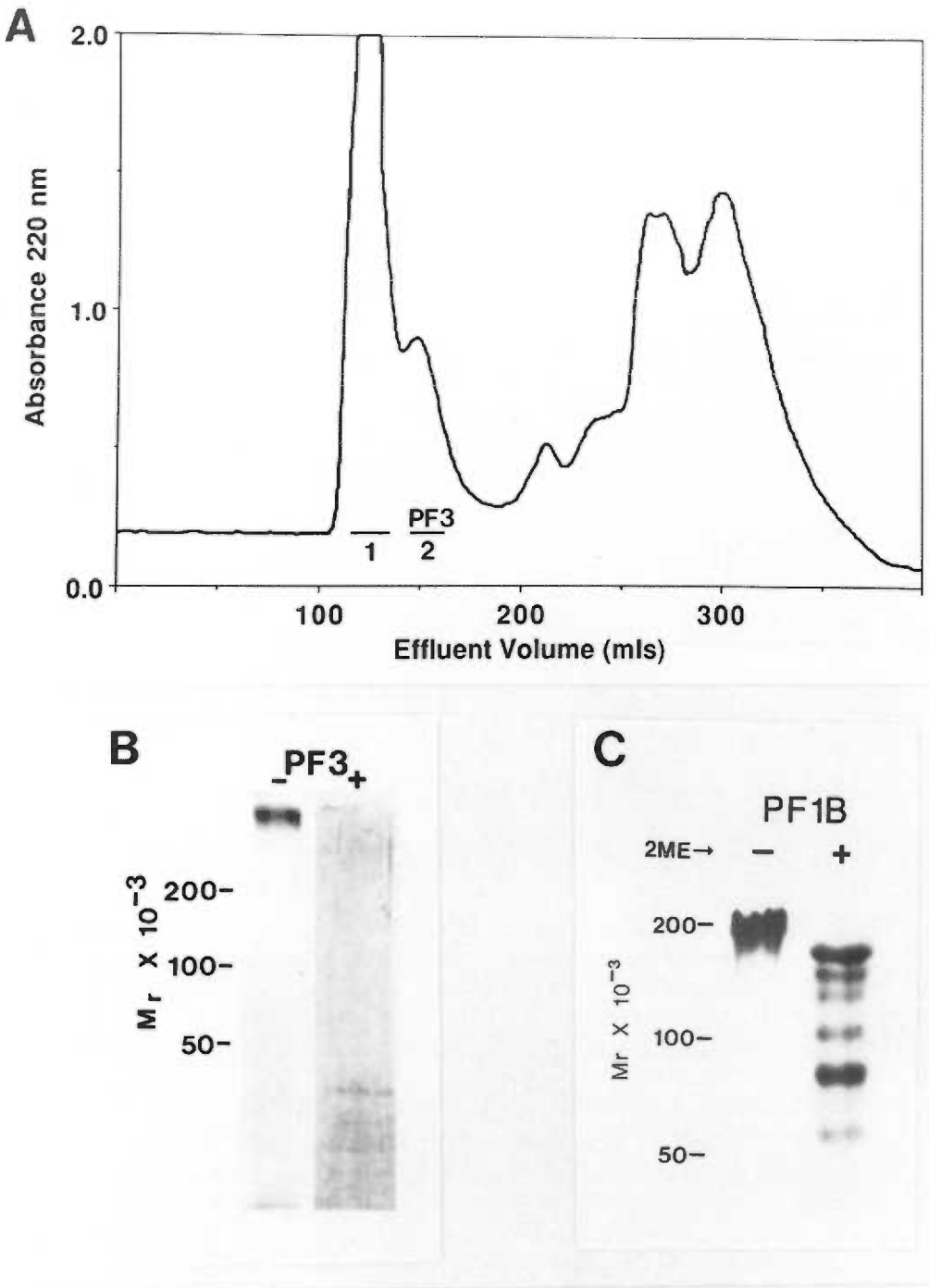

Figure 4. Purification of PF3 and PF1B by molecular sieve chromatography. (A): Absorbance profile of the water precipitated fraction on a TSK4000 column; fractions representing PF3 and PF1B were pooled as indicated by bars. PF3 was further purified using an antibody affinity column (see materials and methods for details) and PF1B was applied to a PLRP-S reverse phase chromatography column (Fig. 5). SDS-PAGE of an aliquot from peak 2 containing PF3 on a 3-10% acrylamide gel (B); peak 3 containing PF1B on a 5-10% gradient acrylamide gel (C). The fragments were electrophoresed with (+) and without (-) 2-mercaptoethanol (2ME) and stained with Coomassie blue. The apparent molecular weight scale was determined by using globular standards.

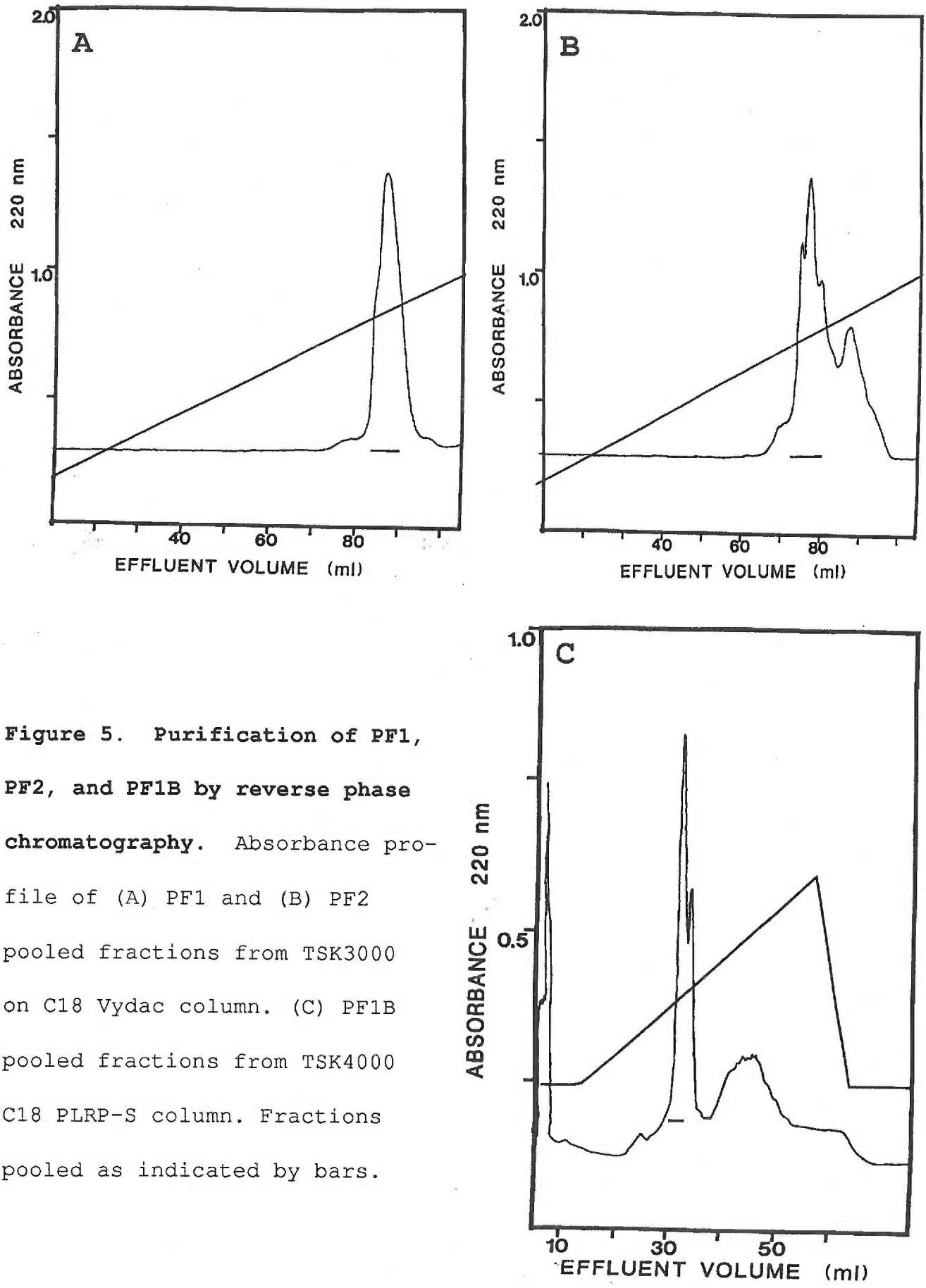

Figure 5. Purification of PF1, PF2, and PF1B by reverse phase chromatography. Absorbance profile of (A) PF1 and (B) PF2 pooled fractions from TSK3000 on C18 Vydac column. (C) PF1B pooled fractions from TSK4000 C18 PLRP-S column. Fractions pooled as indicated by bars.

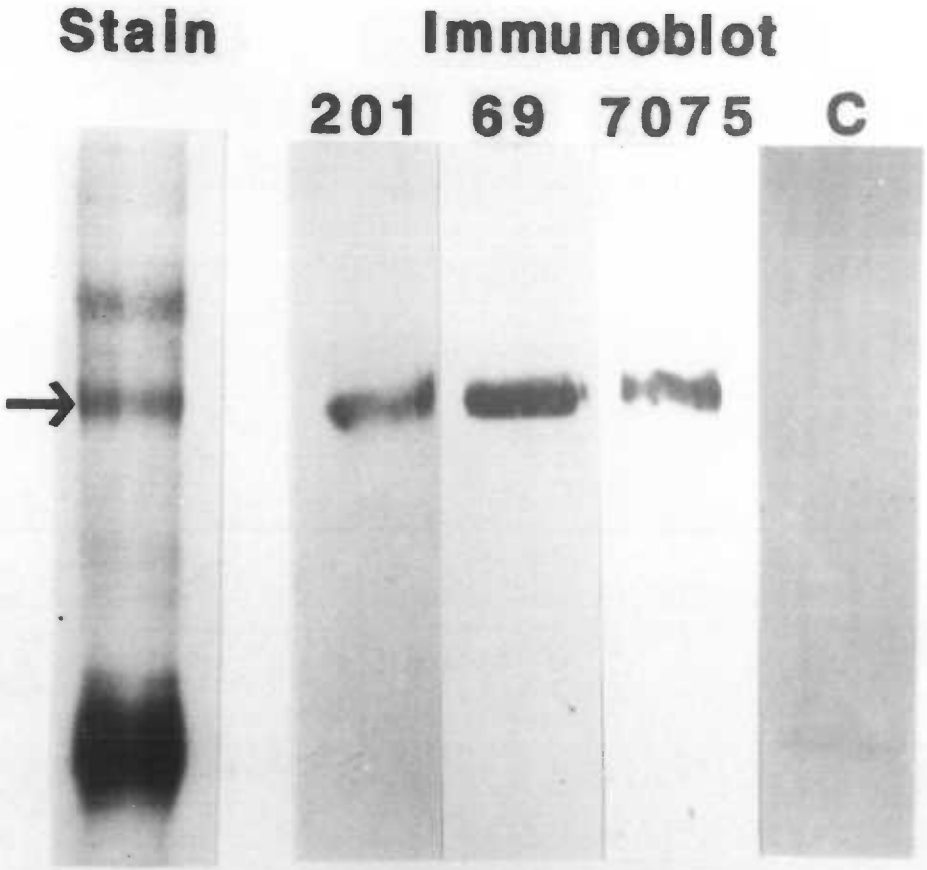

Figure 6. Immunoblot analysis of new antibodies mAb69 and pAb7075 using intact fibrillin. Fibroblast cell culture medium containing fibrillin, was separated on a 3-5% polyacrylamide gel and stained with coomassie blue. The proteins were transferred to nitrocellulose and immunoblotted with the antibodies, along with mAb201 as a positive control. Lane C is blotted with normal serum as a negative control. The arrow indicates the position of fibrillin.

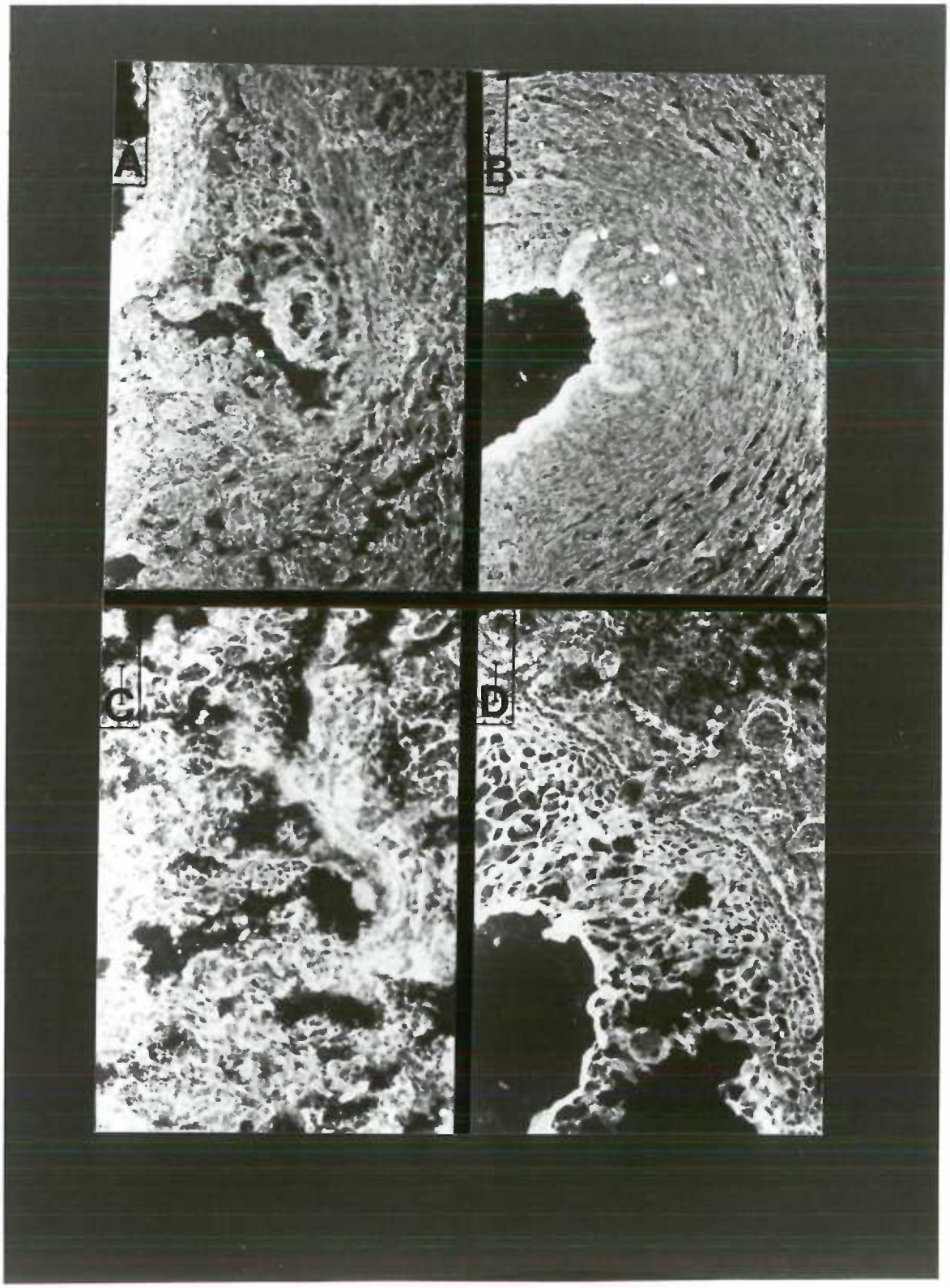

Figure 7. Indirect immunofluorescent staining of bovine tissues using pAb7075. Fetal bovine tissues were sectioned, labeled with pAb7075, and stained with fluorescein isothiocyanate (FITC) conjugated to rabbit-specific anti-IgG. A) kidney, B) aorta, C) ligament D) ear.

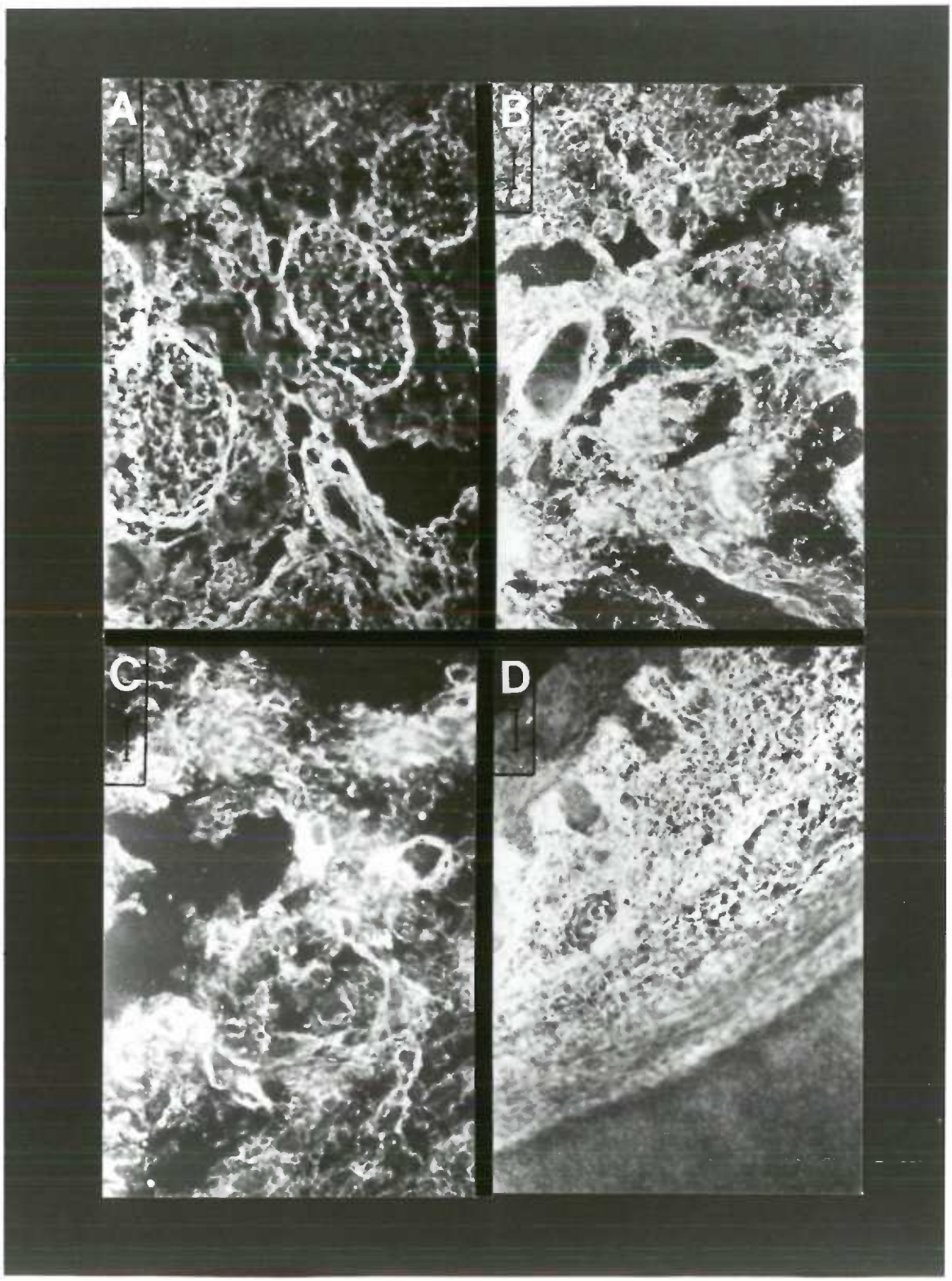

Figure 8. Indirect immunofluorescent staining of bovine tissues using mAb69. Fetal bovine tissues were sectioned, labeled with mAb69 and stained with fluorescein isothiocyanate (FITC) conjugated to mouse-specific anti-IgG. A) kidney, B) ligament, C) lung, D) ear.

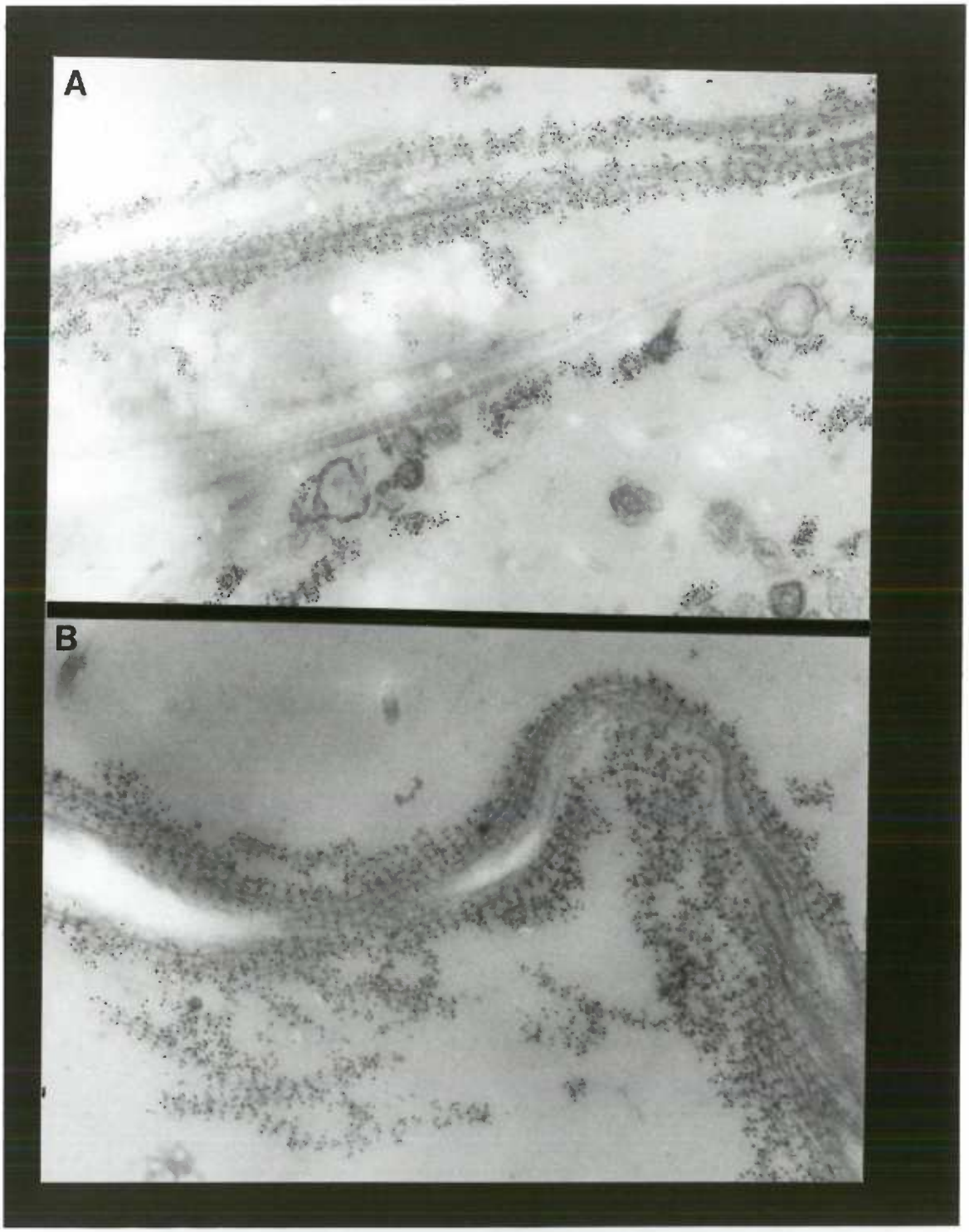

Figure 9. Immunolocalization of mAb69 and pAb7075 to microfibrils in human skin. Electron micrographs of 5-nm gold particles around (A) bundles of microfibrils labeled with mAb69 and (B) microfibrils surrounding amorphous core of elastic fiber labeled with pAb7075.

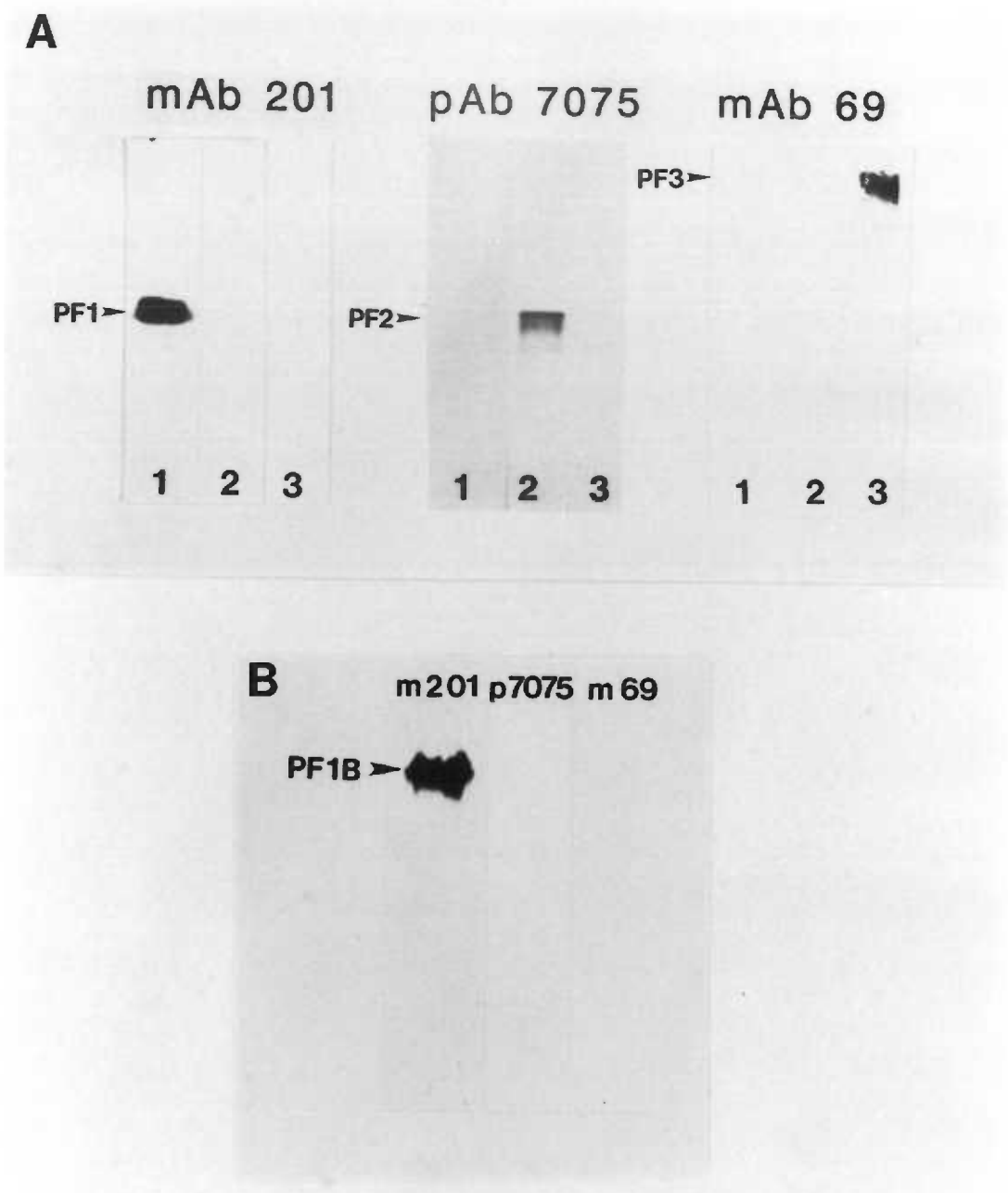

Figure 10. Immunoblot analysis of PF1, PF2, PF3 and PF1B. Purified fragments were separated by SDS-PAGE on a 3-10% polyacrylamide gradient gel, electrotransferred to nitrocellulose, and immunoblotted with mAb201, pAb7075, and mAb69. (A) Lanes 1, 2, and 3 are PF1, PF2, and PF3 respectively. Each set of three lanes was immunoblotted with the antibody indicated. (B) PF1B immunoblotted with mAb201, pAb7075, and mAb69.

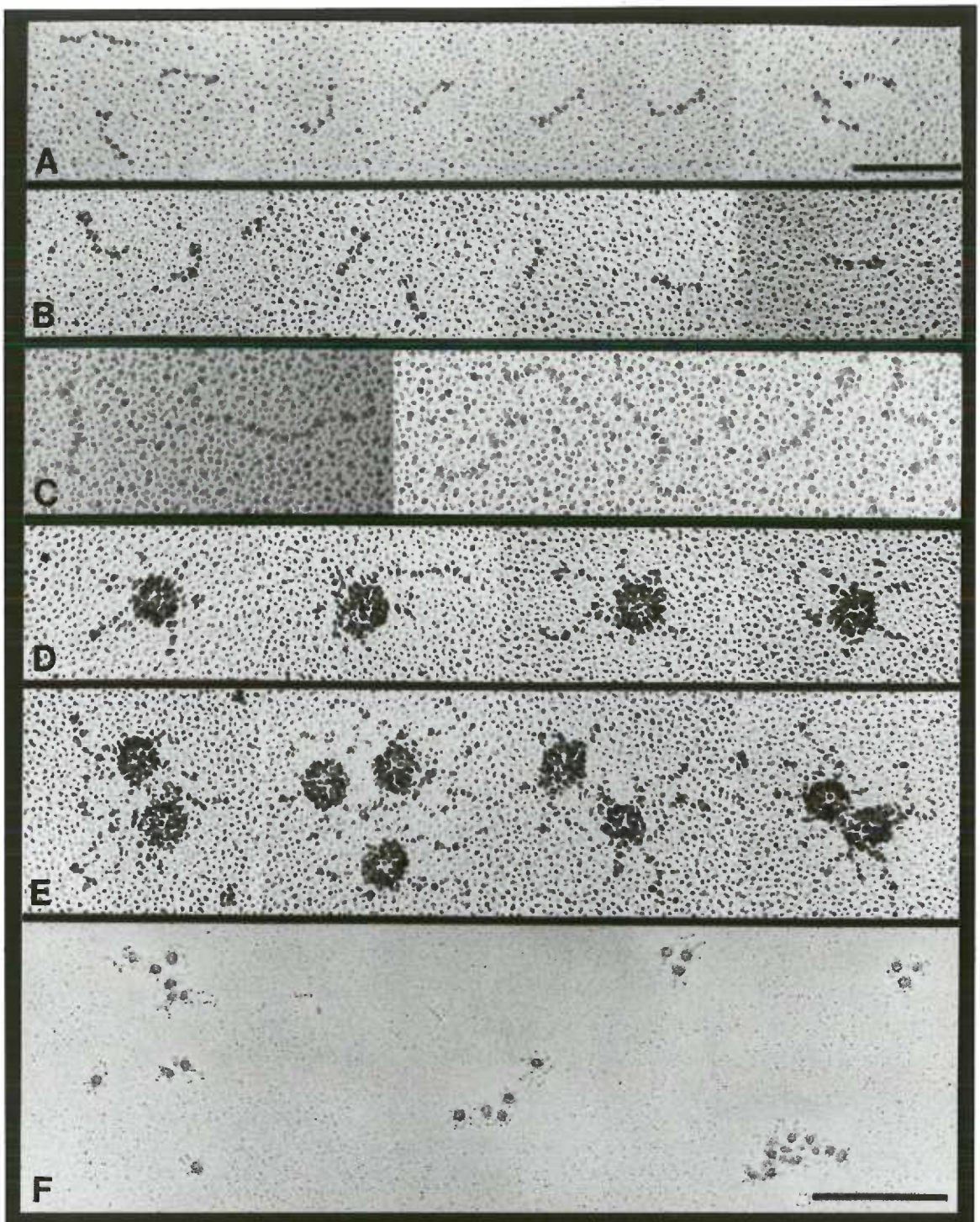

Figure 11. Rotary shadowing of fibrillin fragments. Representative micrographs of (A) PF1, (B) PF2, (C) PF1B, (D) PF3, (E) aggregates of PF3 from peak 1 in Fig. 4A, and (F) aggregates at a lower magnification. For A to E bar = 50 nm. For F bar = 250 nm.

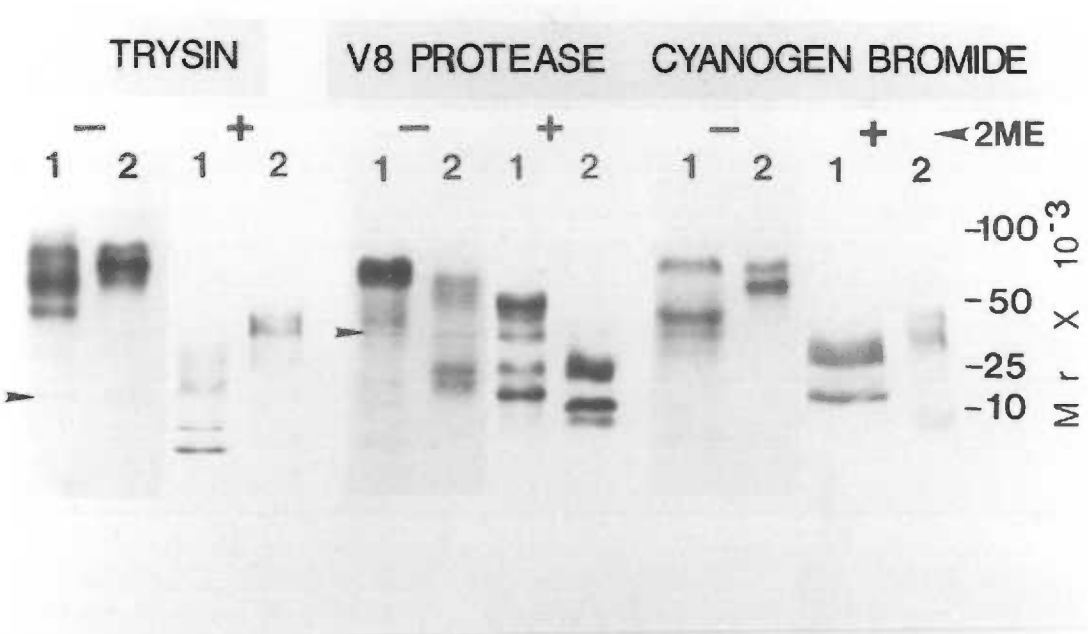

Figure 12. Comparison of PF1 and PF2 by peptide mapping on SDS-PAGE. PF1 (1) and PF2 (2) were treated with trypsin, V8 protease, and cyanogen bromide, and separated in an 8 to 19% polyacrylamide gel with (+) and without (-) 2-mercaptoethanol (2me).

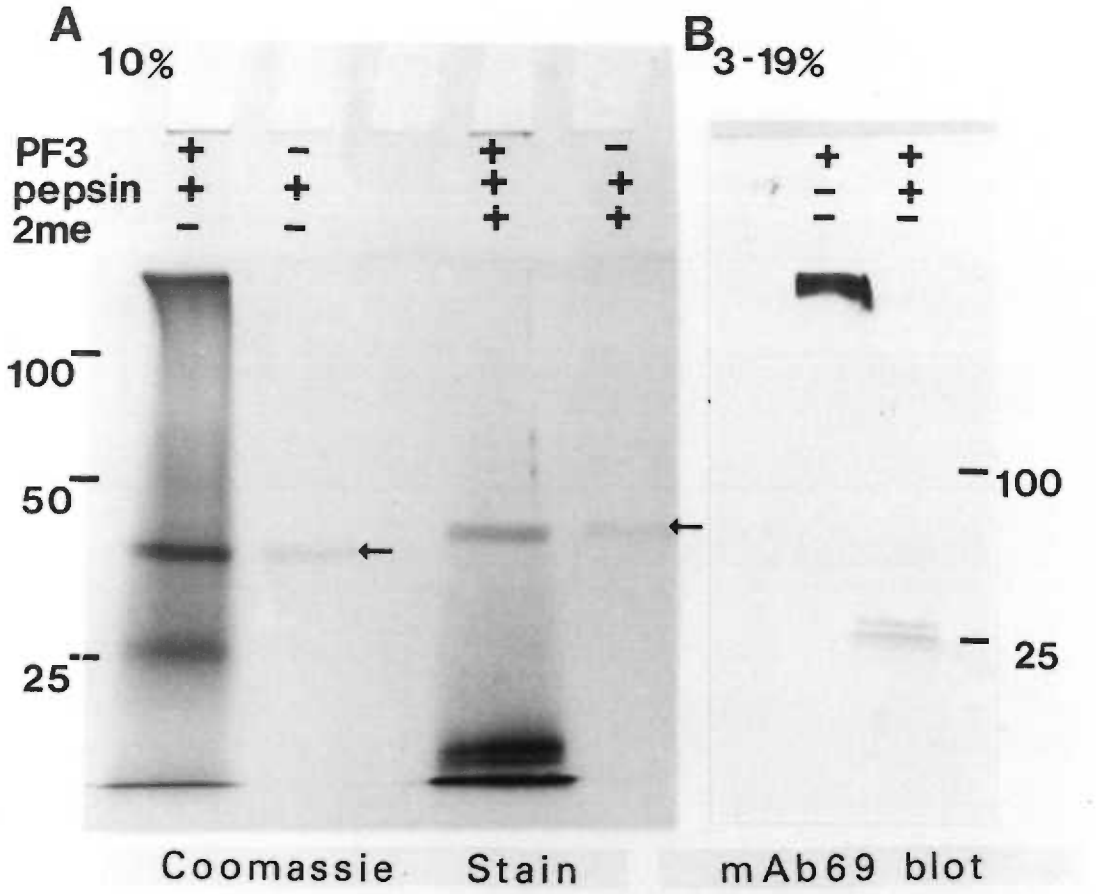

Figure 13. SDS-PAGE and Western blot analysis of PF3 digested with pepsin. (A) Coomassie blue stained 10% polyacrylamide gel of PF3, with (+) and without (-) pepsin, and β-mercaptoethanol (2me). The position of pepsin is noted by arrow. (B) mAb69 immunoblot of PF3 +/- pepsin on a 3-19% polyacrylamide gel.

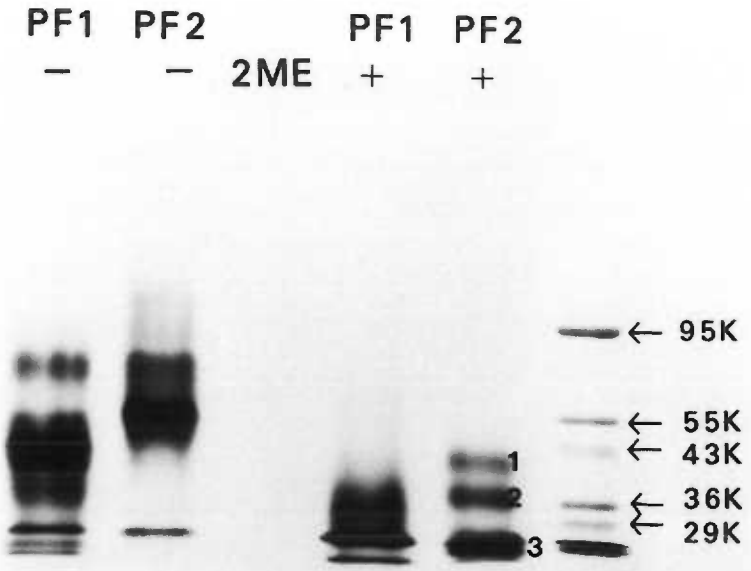

BAND 1: val-gly-ser-phe-arg- ? -glu-asp-pro-val-gly-phe-phe-tyr-asn-asp-
-lys-leu-leu-val- ? -glu-asp-ile-asp-

BAND 2: val-leu-asp-ile-asn-glu- ? -glu-arg-asp-ala-phe-glu-tyr-asn-gly-
-leu-arg-

BAND 3: gly-tyr-ser-tyr-ala-lys-phe-glu-gly-gly-lys-phe-ser-ser-pro-pro-

Figure 14 Electroblot analysis of CNBr peptides from PF1 and PF2 for sequencing. PF1 and PF2 were treated with CNBr, peptides separated on a 5 to 10% polyacryalmide gel with (+) and without (-) β-mercaptoethanol (2me), and electrotransferred to a PVDF membrane and stained with Coomassie blue. Bands labeled 1, 2, 3 were sequenced as indicated.

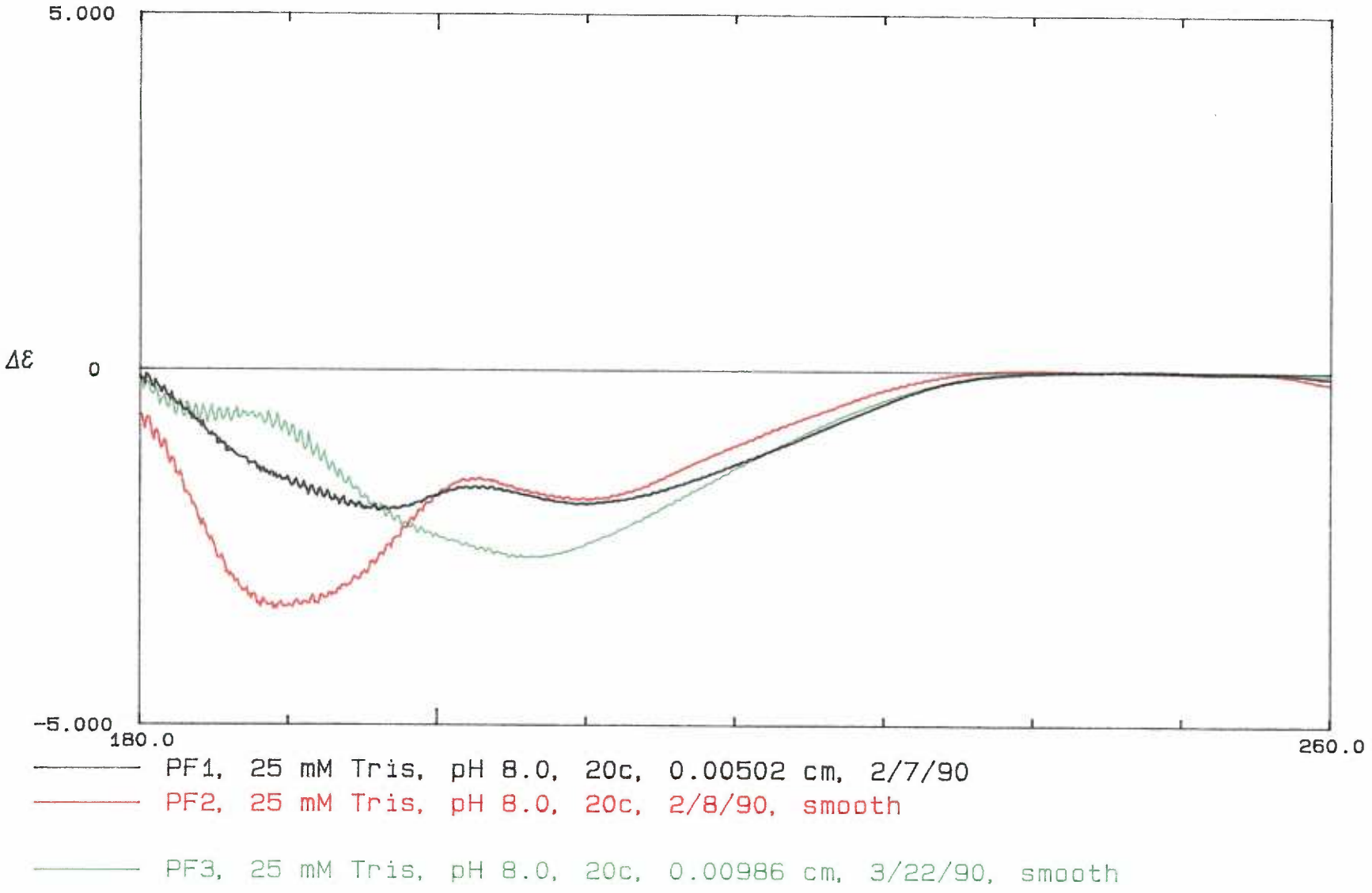

Figure **15.** CD spectra of PF1, PF2, PF3.

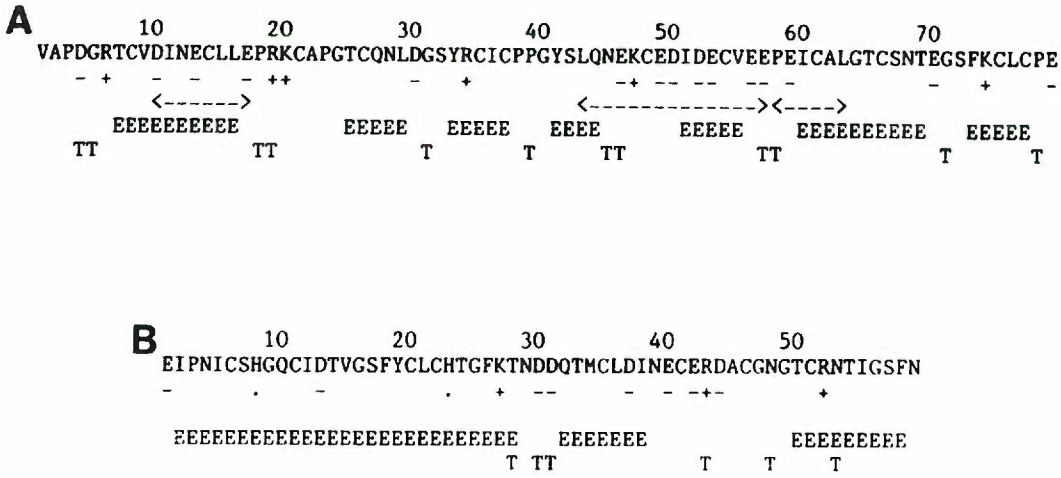

Figure 16. Predicted secondary structure from peptide sequences of PP2. cDNA sequences used to align peptide sequences into longer stretches. CHOFAS structure prediction program of PIR protein databanks recognizes regions of

α-helix <-------->
β-sheet EEEEEEE
β-turn TTTTTTT
(+) positively charged residues
(-) negatively charged residues

(A) from CLM1 clone, beginning at residue 40, (B) from CLM2 clone, position 1.

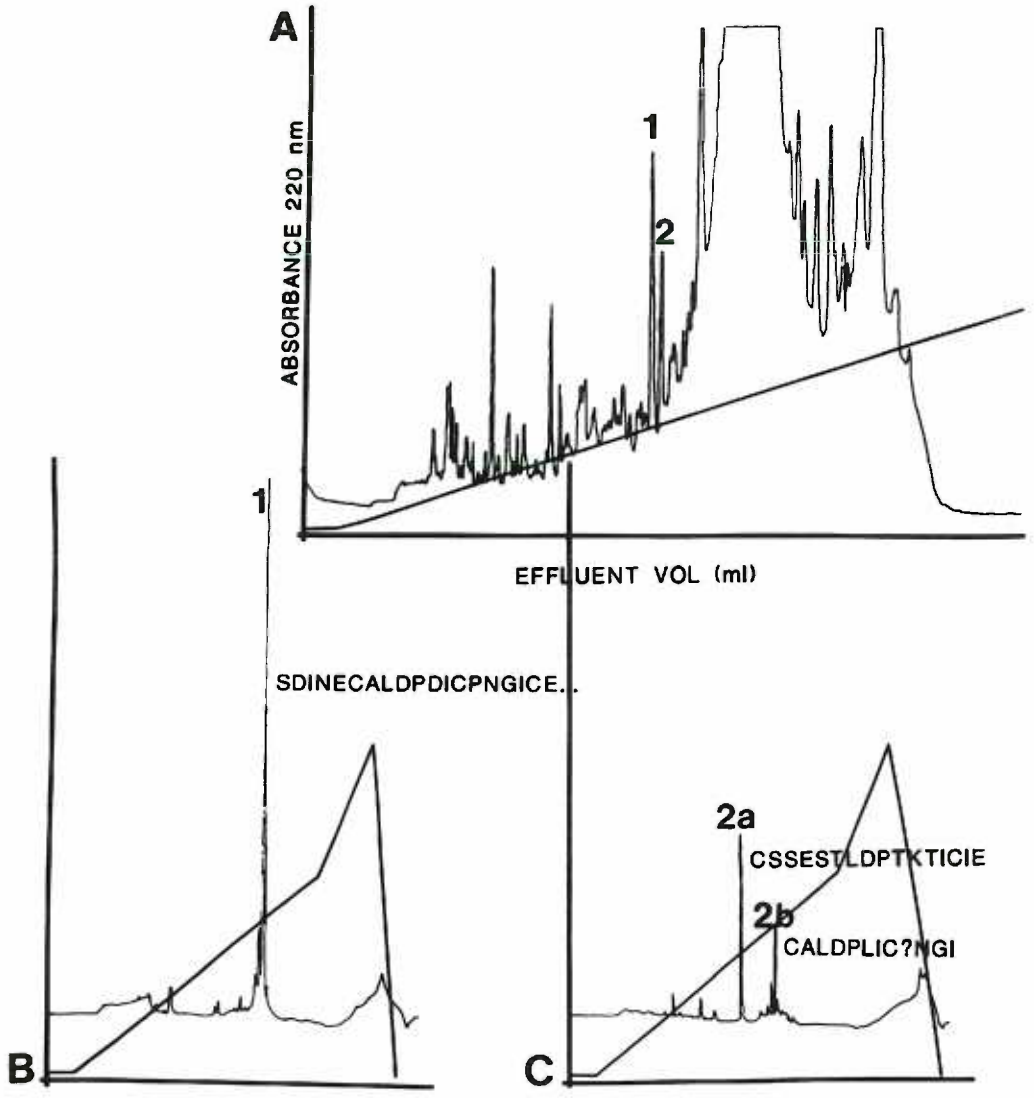

Figure 17. Isolation of disulfide bonded peptides from PF1 pepsin digest for sequence analysis. (A) absorbance profile of C18 reverse phase separation of PF1 pepsin peptides. Fractions from peaks 1 and 2 were pooled as indicated by bars. Peak 1 (B), and peak 2 (C) were reduced, alkylated, desalted and the resulting peptides separated. Fractions B1, and C2a and b were sequenced as indicated.

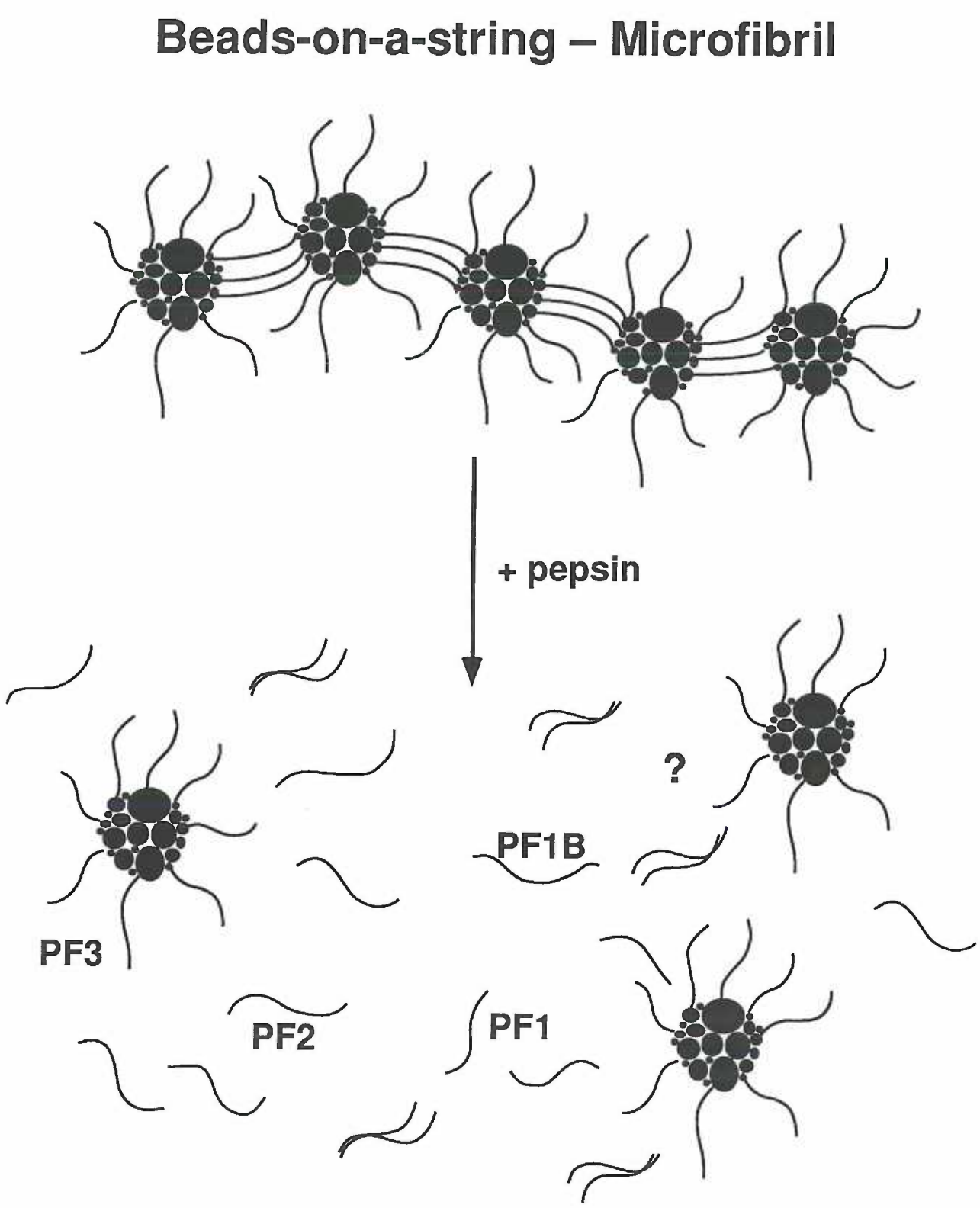

Figure 18. A model of the preparation of fibrillin fragments PF1, PF1B, PF2, PF3 from pepesin digest of connective tissue microfibrils.

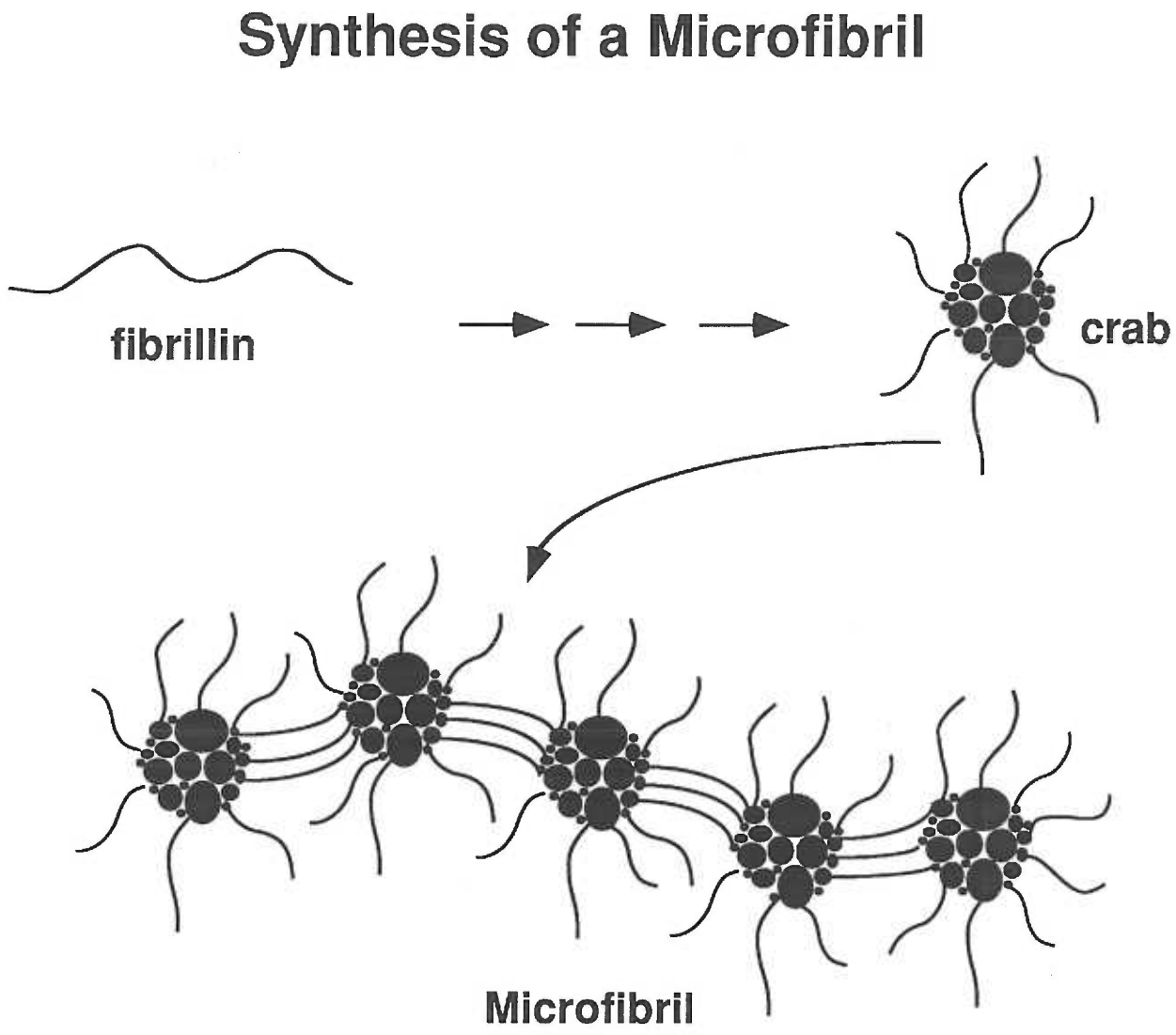

Figure 19. A model representing the synthesis of a microfibril from a fibrillin molecule. Major events are depicted including formation of an oligomeric beaded unit and alignment of the beaded units into a microfibril.

LIST OF TABLES

Table I

AMINO ACID COMPOSITION OF FIBRILLIN FRAGMENTS

Cysteine residues were determined as pyridylethylcysteine. Amino acids are expressed per 100 residues.

Amino acid	PF1	PF2	PF1B	PF3
aspartic acid	13.6	14.2	10.8	11.0
glutamic acid	13.0	13.4	10.0	11.8
hydroxyproline	0.1	0.0	0.0	0.4
serine	7.7	7.4	7.2	7.5
glycine	11.7	11.0	10.3	12.8
histidine	1.2	1.4	1.5	2.1
arginine	6.3	5.3	4.2	4.8
threonine	5.2	3.8	6.2	4.6
alanine	4.0	3.6	4.0	4.3
proline	6.9	6.2	5.6	7.4
tyrosine	2.4	1.9	2.9	2.1
valine	4.8	3.2	3.4	4.1
methionine	0.8	0.7	2.2	1.2
cysteine	8.2	11.5	15.2	10.8
isoleucine	4.5	4.9	5.2	4.4
leucine	5.2	4.9	4.6	4.8
phenylalanine	2.7	3.7	2.8	2.7
lysine	1.7	2.9	3.7	3.2

N-terminal sequences of PF1, PF1B, and PF2

PF1: Tyr - Leu - Tyr - Pro - Ser - Arg - Glu - Pro - Pro - Arg - Val -

PF1B: Tyr - Leu - Tyr - Pro - Ser - Arg - Glu - Pro - Pro - Arg - Val -

PF2: Ile - Tyr - Thr - Ile - Leu - Pro - Val - Asp - Ile - Asp - Glu -

Table II

BIOPHYSICAL PROPERTIES OF FIBRILLIN FRAGMENTS

Fragment	s	MW_{kd}	f^1	f/f_o		prolate	oblate	rod
PF1	3.3S	110	16.4	2.39	a/b	30.91	50.79	35.7
					2a	61.7	23.2	59.4
					2b	2.0	0.5	1.7
PF2	2.6S	51.3	9.9	1.86	a/b	16.82	23.17	19.0
					2a	31.9	13.8	30.2
					2b	1.9	0.6	1.6
PF3	25.6S	800[2]	N.D.	N.D.				

Refer to METHODS for ultracentrifugation conditions, and RESULTS for definition of terms. N.D. = not determined.

1/ x $10^{-8}gs^{-1}$

2/ molecular weight approximated based on value of globular proteins using sedimentation coefficient of 25S

TABLE III

SECONDARY STRUCTURAL ANALYSIS OF CIRCULAR DICHROISM DATA FOR FIBRILLIN FRAGMENTS

FRAGMENT	α-HELIX	β-sheet$_{AP}$	β-sheet$_{P}$	β-turn	OTHER	TOTAL
PF1	0.22	0.05	0.11	0.22	0.42	1.01
PF1$_{+NaCl}$	0.08	0.22	0.10	0.18	0.38	0.97
PF2	0.19	0.01	0.18	0.28	0.35	1.01
PF2$_{+NaCl}$	0.07	0.27	0.10	0.14	0.38	0.96
PF3	0.04	0.26	0.03	0.20	0.43	0.97

APPENDIX I

PF1 SEQUENCES

N-TERMINAL SEQUENCE

tyr-leu-tyr-pro-(ser)-arg-glu-pro-pro-val-leu-pro-val-(asn)-val-thr-asp-tyr-
-cys-gln-leu-val-arg-tyr-leu-leu-gln-asn-gly-arg-?-ile-pro-thr-asp-tyr-cys-gln-
-leu-val-arg

Cyanogen Bromide peptides:

CB1 -(met)-asn-gly- ? -cys-val-asn-thr-asp-ala- ? -tyr-arg-cys-glu-cys-
-phe-pro-gly-leu-ala-val-gly-leu-asp-gly-cys-

CB2 -(met)-arg-asn-thr-pro-glu-tyr-glu-glu-leu-cys-pro-arg-gly-pro-gly-
-phe-ala-thr-lys-glu-

Miscellaneous Peptides:

T-1 -(arg/lys)-asp-ile-asp-glu-cys-leu-gln-pro-pro-arg

T-2 -(arg/lys)-tyr-glu-asp-glu-glu-cys-thr-leu-pro-ile-ala-gly-arg

T-3 -(arg/lys)-gly-thr-gln-cys-glu-asp-ile-asp-glu-cys-glu-thr-?

T-4 -(arg/lys)-ala-gly-thr-gln-ser-thr-leu-thr-arg

T-5 -(arg/lys)-asp-glu-cys-ile- ? -glu-

T-6 -(arg/lys)-gly-pro-cys-pro- ? -val-

T-7 -(arg/lys)-asn-cys-glu-asp-met-asp-glu-cys-ser-ile-arg

T-8 -(arg/lys)-ala-val-gly-leu-asp-gly-arg

T-9 -(arg/lys)-gly-glu-phe-glu-glu-lys

T10 -(arg/lys)-met-glu-gln-cys-tyr-

T11 -(arg/lys)-met-asp-ala-cys-cys-cys-ser-val-gly-ala-ala- ? -gly-thr-
-glu-glu-cys-

T12 -(arg/lys)-gly- ? -pro-gly-tyr-tyr- ? -cys-

T13 -(arg/lys)-ile-cys-asn-asn-gly-arg

T14 -(arg/lys)-tyr-leu-cys-gln-asn-gly-arg

T15 -(arg/lys)-val-cys-val-asp-thr-his-met-arg-ser-thr-cys-tyr-gly-gly-
-tyr-lys

T16 -(arg/lys)-leu-tyr-arg-pro-tyr-

T17 -(arg/lys)-ser-glu-cys-cys-ala-thr-leu-

T18 -(arg/lys)-gly-val-asn-ile-

P1 -ser-asp-ile-asn-glu-cys-ala-leu-asp-pro-asp-

P2a -cys-ser-ser-glu-ser-thr-leu-asp-pro-thr-lys-thr-ile-cys-ile-glu-

P2b -cys-ala-leu-asp-pro-leu-ile-cys- ? - asn-gly-ile-

PT3 -asn-pro-cys-ala-gly-gly-glu-cys-ile- ? - asn-gln-gly- ? - tyr-thr-
-cys-gln-cyr-arg-

PF2 SEQUENCES

N-TERMINAL SEQUENCE

ile-tyr-thr-gly-leu-pro-val-asp-ile-asp-glu- ? -val-glu-ile-pro-gly-val-

Cyanogen Bromide peptides:

CB1

-(met)-val-gly-ser-phe-arg-cys-glu-cys-pro-val-gly-phe-phe-tyr-asn-asp-
-lys-leu-leu-val-cys-glu-asp-ile-asp-cys-gln- ? - gly-lys-ile-ser-
<---------->

CB1 peptides

-(arg)-ala-glu-cys-ile-asn-thr-ala-gly-asp-tyr-arg-

-(asp/glu)-ile-ile-ala-leu-ala-gly-cys-tyr-arg-cys-asp-cys-lys-
-pro-gly-tyr-arg-phe-thr-ser-thr-gly-gln-cys-asn-asp-arg-asn-asp-
-cys-glu-ile-pro-asn-ile-cys-

CB2

-(met)-val-leu-asp-ile-asn-glu-cys-glu-arg-asp-ala-cys-gly-tyr-asn-gly-
-lys-leu-arg-

CB2 peptide

-(lys)-thr-leu-asp-ile-asn-glu-cys-glu-arg-

CB3

-(lys)-thr-asn-asp-asp-gln-thr-(met)-cys-leu-asp-ile-asn-glu-cys-glu-
-arg-asp-ala-cys-gly-leu-gly-thr-cys-arg- ? -thr-ile-gly- ? -phe-asn-

CB4

-(met)-ser-tyr-cys-tyr-ala-lys-phe-glu-gly-gly-lys-cys-ser-ser-pro-lys-

Miscellaneous PF2 peptides

V8-1 -(asp/glu)-cys-ala-ser-gly-asp-gly-asn-leu-cys-arg-asn-gly-gln-cys-ile-

-asn-thr-val-gly-asp-phe-gln- ? -gln-asn-asp

V8-2 -(asp/glu)-cys-leu-leu-glu-pro-arg-lys-cys-ala-pro-gly- ? -cys-gln-asn-
-leu-asp-gly-ser-tyr-arg- ? -ile- ? -pro-gly-tyr-ser-leu-gln-asp-glu-
-lys-

V8-3 -(asp/glu)-val-ala-pro-asp-gly-arg-thr-cys-val-asp-ile-asn-glu-

V8-4 -(asp/glu)-gly-asp-phe-lys-cys-leu-cys-pro-glu-

V8-5 -(asp/glu)-val-ala-lys-met-ser-arg-pro-

V8-6 -(asp/glu)-ile-ile-ala-leu-ala-gly-cys-arg-cys-asp-cys-lys-pro-
-gly-tyr-arg-

V8-7 -(asp/glu)-ile-cys-ala-leu-gly- ? -cys-ser-asn-thr-glu-

V8-8 -(asp/glu)-cys-gln-asp-gly-pro-val-cys-gln-arg-arg-

-asp-glu-ser-tyr-arg- ? -ile-pro-gly-tyr-ser-leu-gln-asn-glu-lys

PF3 SEQUENCES

Pepsin-derived peptides

P1 ala-cys-tyr-cys-arg-ile-pro-ala- ? -cys-ile-ala-gly-glu-arg-tyr-

P2 asn-thr-glu-gly-ile-tyr-gln-cys-ser-cys-pro-lys-

P3 leu-gln-his-tyr-gln-

P4 gly-pro-pro-gly-pro-pro-gly-ala- ? - ? -leu-

P5 gly-gly-gly-gly-

P6 gly-gly-ile-pro-leu-

P7 gly-gly-arg-pro-glu-tyr-

P8 val-asp-met-asp-glu-

APPENDIX II

Extraction of Extendable Beaded Structures and Their Identification as Fibrillin Containing Extracellular Matrix Microfibrils

Douglas R. Keene[#], B. Kerry Maddox[#*], Huey-Ju Kuo[#], Lynn Y. Sakai[#*] and Robert W. Glanville[#*]

Running Title: Fibrillin Beaded Structure

Shriners Hospital for Crippled Children, Portland, Oregon 97201

* Department of Biochemistry, Oregon Health Sciences University, Portland, Oregon 97201

Address for correspondence:

Robert W. Glanville

3101 S.W. Sam Jackson Pk. Rd.

Portland, Oregon 97201

(503) 241-5090 Ext. 507

ABSTRACT

High molecular weight aggregates were extracted from human amnion using buffers containing 6M guanidine hydrochloride. Rotary shadowed preparations and negatively stained samples examined in the electron microscope showed that each aggregate appeared to be a string of bead like structures joined by fine filaments. The periodicity of the beads was variable. A mouse monoclonal antibody, directed against a previously characterized pepsin fragment of fibrillin, was used with gold conjugated secondary antibody and immunoelectron microscopy to show that the aggregates contained fibrillin. Similar structures were found in non-denaturing extracts of skin, tongue, ligament, ciliary zonule, cartilage, and vitreous humor. When immunogold labeled beaded structures were prepared for electron microscopy in the same manner as tissue, no beaded structures could be identified. Instead, gold labeled structures were found which appeared to be the same as the fibrillin containing matrix microfibrils observed in connective tissues and often associated with elastin. When skin was stretched and prepared for electron microscopy while still under tension, beaded filaments were seen in the tissue sections but were not visible in non-stretched controls, and when stretched ligament was immunolabeled while still under tension with antibody directed against fibrillin, the periodicity of microfibrils was shown to be elongated. Thus fibrillin is present in tissues as a high molecular weight, extendable, beaded polymer that is a major structural component of microfibrils and whose appearance may be altered depending upon the protocol applied for investigation.

INTRODUCTION

Fibrillin is an extracellular matrix glycoprotein that is a constituent of microfibrils, which are found in practically all connective tissues. It was first isolated from the medium of human fibroblast cell cultures and shown to be a noncollagenous intramolecularly disulfide bonded glycoprotein with an apparent molecular weight of 350k (Sakai et al., 1986). Monoclonal antibodies were used with immunofluorescence microscopy to show its widespread distribution in tissues, and with immunoelectron microscopy to localize it to structural elements called microfibrils. Fibrillin containing microfibrils are approximately 10 nm in diameter and in cross section often appear to be hollow (Low, 1962; Cleary and Gibson, 1983). They are found associated with amorphous elastin, for example in skin and ligament, and also in tissues which lack amorphous elastin such as hyaline cartilage and ciliary zonule. They appear to have a periodic structure, as several fibrillin monoclonal antibodies bind to the surface of microfibrils, giving rise to an induced 54 nm periodic banding pattern, equivalent to that of banded collagen fibrils in the same preparations observed in the electron microscope following tissue dehydration and embedding (Sakai et al., 1986; Maddox et al., 1989).

Studies on the biosynthesis of fibrillin and its extractability in cultured chick aorta have revealed that the monomer quickly assembles, initially into a disulfide bonded aggregate and then a non-reducible structure (Sakai, 1990). A pepsin fragment of the tissue form of fibrillin has been recently characterized which appears to be composed of six to eight crosslinked fragments of fibrillin (Maddox et al., 1989). Here we describe a polymeric structure that can be

extracted from tissues and appears to be related to this pepsin fragment. It is shown that this structure contains fibrillin, is an extendable beaded structure, and is related to the connective tissue microfibrils observed in tissues prepared for electron microscopy.

MATERIALS AND METHODS

Preparation of Fibrillin Aggregates

Fibrillin aggregates were isolated from 6M guanidine hydrochloride extracts of human amnion using a procedure recently described for the isolation of type VI collagen (Kuo et al., 1989). Briefly, the extract was dialyed against 1% acetic acid, the precipitated material collected, taken up in a neutral buffer containing 6 M urea, and passed through DEAE cellulose. Proteins which did not bind were size fractionated in the presence of 6 M urea using Sephacryl S-500 and the first fraction, eluting at the void volume of the column, contained the fibrillin aggregates while type VI collagen was in another fraction (Figure 2 in Kuo et al., 1989). The fibrillin containing fraction, which was slightly opalescent, was centrifuged at 18000g for 60 minutes. A small gelatinous residue was collected and resuspended in 0.2 M ammonium bicarbonate. This suspension, which contained fibrillin aggregates, was contrasted either by rotary shadowing or negative staining, or immunolabeled as described below before viewing in the electron microscope.

Preparation of Antibodies

Monoclonal antibody mAb69 has been previously characterized and shown to be specific for the pepsin resistant "PF3" domain in human and bovine fibrillin (Maddox et al., 1990). The control monoclonal antibodies used recognized type III collagen (Keene et al., 1987a), type VI collagen (Keene et al., 1988) and a polyclonal antibody to type VII collagen (Keene et al., 1987b) was also used.

Preparation of Tissue Homogenates

Bovine nuchal ligament, aorta, femoral head cartilage, tongue, skin, and suspensory ligaments of the eye were obtained from 10 week old fetal calves within 28 hours following death. Fetal calf vitreous humor was obtained by cutting the eye globe at the equator and allowing a portion of the vitreous body to fall free. This was combined with an equal volume of 0.2 M ammonium bicarbonate buffer, pH 7.4. The mixture was gently shaken but not homogenized. Small pieces of bovine nuchal ligament, femoral head cartilage, isolated suspensory ligaments, tongue, skin, and aorta were homogenized in 0.2 M ammonium bicarbonate buffer on ice using a polytron tissue homogenizer (Brinkman Instruments) until no visible tissue fragments remained. The resulting homogenates were centrifuged briefly at 500g to remove large tissue debris. Each sample was deposited on a carbon coated grid and negatively stained with 2% phosphotungstic acid pH 7.0 and also sprayed, using an airbrush, from 70% glycerol onto freshly cleaved mica and rotary shadowed as previously described (Morris et al, 1986).

Immunolabeling

Each tissue homogenate (150ul) was incubated, overnight at 4^{o}C, with 50ul of undiluted antibody. Excess primary antibody was rinsed away by washing the sample pellet three times in 500ul of 0.2 M ammonium bicarbonate buffer and centrifuging at 11,600g for 15 minutes. The washed pellet was resuspended in the appropriate goat anti-mouse or anti-rabbit 5-nm gold conjugate (Janssen Life Sciences Products, Piscataway, N.J.) diluted 1:3 in BSA buffer (20 mM

Tris-HCl, 0.9% NaCl, 1 mg/ml BSA, 20 mM NaN3), pH 8.0 and incubated overnight at 4°C. Unbound secondary conjugate was washed away as above. Following incubation in primary and secondary antibodies, the samples were deposited on carbon coated 600 mesh grids and contrasted with 2% PTA, pH 7.0. One sample of immunolabeled ligament homogenate was pelleted, fixed, dehydrated in acetone and embedded following the same protocol described below for intact tissues. All samples were examined using a Philips 410 L.S. operated at 60 KV with a 30 um objective aperture.

Preparation of Tissues for Electron Microscopy

Human amnion was obtained shortly after term delivery and fixed in buffered 3% gluteraldehyde/3% paraformaldehyde followed by 1% OsO4, then dehydrated and embedded in Spurrs epoxy for TEM. Additionally, fetal calf nuchal ligament and neonate human foreskin were cut into strips measuring approximately 1 mm x 10 mm, then placed under tension in the following way. One end of a tissue strip was tied to a wooden dowel and the other end was pulled, using forceps, so that the tissue was effectively stretched. Maintaining tension, this end was also secured to the dowel. Tension was maintained throughout the subsequent protocol until embedding. Enbloc immunolabeling of relaxed and stretched tissue was carried out using modifications of a protocol described previously (Sakai et al., 1986). Briefly, tissue pieces were submersed overnight at 4°C in ascites fluid containing the appropriate antibody, diluted 1:5 in PBS. Following washing, tissues were incubated overnight in goat anti-mouse 5-nm gold conjugate (Janssen Life Sciences Products, Piscataway, N.J.) diluted 1:3 in BSA buffer,

pH 8.0. Tissues were then washed, fixed in buffered 3% gluteraldehyde/3% paraformaldehyde followed by buffered 1% OsO4, then dehydrated and embedded in Spurrs epoxy. Stretched tissues were sectioned in a plane parallel with the direction of tension. All sectioned material was contrasted with uranyl acetate (2% in 50% EtOH for 15 minutes) followed by Reynolds lead citrate (Reynolds, 1963).

RESULTS

Although they were passed through two chromatography columns, the beaded aggregates of fibrillin were not in solution. They could easily be sedimented out of a buffer containing 6 M urea along with fragments of collagen fibers and other unidentifiable material. The beaded structures were clearly visible in rotary shadowed samples as shown in figure 1a. Strings with more than 60 beads were frequently seen. The strings of beads are clearly very flexible, although individual beads within a string never touch. In rotary shadowed preparations, the diameter of the beaded portion of the strings measures approximately 22 nm, whereas in negative stain preparations the beaded portion measures approximately 15 nm. At higher magnification it appears that each bead is surrounded by a network of fine filaments (figure 1b). The periodicity of the beads along a string varies. The periodicities along the strings in figures 1b and 1c average 33 nm and 94 nm respectively and periodicities as high as 165 nm have been measured. Figure 1d shows a negatively stained preparation where the periodicities clearly vary along the length of individual strings. In what appear to be stretched regions the periodicity averages 62 nm and in the two relaxed ends the periodicity averages 26 nm.

To demonstrate that the beaded string was a physiological structure and not induced by the harsh procedure used to extract amnion, various tissues were homogenized in non-denaturing buffers and examined in the electron microscope after rotary shadowing or negative staining. Figure 2 shows two examples, a negatively stained sample from fetal calf vitreous humor and a rotary shadowed preparation from fetal calf femoral head cartilage. In both pictures, the

beaded structure is clearly identifiable. Similar results (not shown) were obtained from all other tissues investigated (see Methods).

Although preparations of the guanidine extracted beaded aggregates could not be purified, it was possible to show that they contained fibrillin by using immunogold labeling techniques in combination with negative staining. Figure 3a shows a preparation of beaded aggregates in which gold particulate label is directed by mAb69, a monoclonal antibody specific for fibrillin. Only the beaded structures were labeled with gold, indicating that they are fibrillin containing structures. Controls using primary antibodies specific for types III, VI and VII collagens did not result in gold labeling of the beaded strings.

To confirm that the beaded strings observed in tissue homogenates are the same as those found in guanidine extracts of human amnion, some of the homogenates were immunolabeled as described above. Ligament, which contains large numbers of microfibrils, contained masses of beaded strings which could be specifically labeled using the fibrillin antibody mAb69 (figure 3b). Further, close examination of individual immunolabeled strings (figure 3c) shows that the binding site for the antibody is located consistently to one side of a bead, indicating that the beaded area is asymmetric.

After conventional fixation, dehydration and embedding, matrix microfibrils present in tissues measure approximately 10 - 12 nm in diameter. Typically, in longitudinal section, a scalloped appearance to the microfibrils can be resolved, but a definitive substructure or periodicity is difficult to distinguish (figure 4b). As the beaded structure is not visible in tissue sections it is probably altered by the processing, particularly dehydration, necessary to prepare tissues for conventional electron microscopy. To

investigate this, a pelleted immunolabeled ligament homogenate, similar to that shown in figure 3b, was subjected to fixation, dehydration, and embedding. Prior to pelleting, it was confirmed by negative staining that the only labeled structures in the homogenate were beaded strings. TEM revealed that the beaded strings were no longer apparent in the embedded preparation (figure 4a). Instead, the only immunolabeled structures present were those which were indistinguishable from matrix microfibrils as normally visualized in fixed, dehydrated, and embedded tissues (figure 4b).

Tissues were manually stretched, then fixed and embedded while still under tension to determine if the appearance of tissue microfibrils present in sections could be altered. Although difficult to adequately contrast, figure 4c shows a beaded microfibril in stretched skin. These structures were not observed in unstretched tissues.

When microfibrils are immunolabeled, a banding pattern, probably induced by the primary antibody, is apparent regardless of the antibody used (Sakai et al., 1986; Maddox et al., 1989). Following fixation, dehydration, and embedding the periodicity measures about 54 nm, the same as banded collagen fibrils present in similarly processed tissues. When stretched tissue was immunolabeled, the periodicity of the microfibrils increased as compared to the periodicity observed in unstretched tissues. In some areas the periodicity was measured to be over 75 nm, demonstrating that even though a definitive beaded appearance was not evident in this preparation, the periodicity of the microfibril was never the less extended (figure 4d).

DISCUSSION

The ultrastructure of connective tissue microfibrils was described in early literature as being an approximately 10 nm diameter fibril with a vesicular cross-section and a 3-4 nm lucent core (Low, 1962; Greenlee et al., 1966; Fahrenbach et al., 1966; Cleary et al., 1981). The longitudinal section was variously described as a "light and dark staining pattern" (Cleary et al., 1981), "beaded appearance" (Fahrenbach et al., 1966), or "chain-like aggregates of tiny vesicles" (Haust, 1965). Their periodicity was not uniformly reported. In one report (Fahrenbach et al., 1966), "pre-elastin filaments" were extracted from fetal nuchal ligament and after negative staining, the segmented appearance of "swollen" microfibrils could be more clearly seen. They were described as 13 nm long by 13 nm wide cylindrical segments separated by an electron-opaque region 10 nm long by 15 nm wide. More recently, similar beaded structures were found in rotary shadowed samples of chick vitreous humor, where the beads were clearly visible and had a diameter of 22 nm with a spacing of 50 nm (Wright and Mayne, 1988). The measured diameters of the beaded structures visualized in this report, either by rotary shadowing or negative staining, are consistent with these earlier studies.

Several proteins including fibronectin, vitronectin, and amyloid P have been found to associate with microfibrils, but are not considered true structural components of microfibrils (Schwartz et al., 1985; Breathnach et al., 1981; Dahlbäck et al., 1989; Kobayashi et al., 1989). MAGP, a 31 kDa glycoprotein isolated from reductive extracts of bovine nuchal ligament, has been partially characterized (Gibson et al., 1986). Immunofluorescent studies using polyclonal antibodies prepared against MAGP labeled both elastin

associated microfibrils and microfibrils in non-elastin containing tissue in a similar manner as do monoclonal antibodies to fibrillin (Gibson and Cleary, 1987). A second 340 kDa fragment called MP340 was subsequently characterized and shown to be related to MAGP (Gibson et al., 1989). Because of the similar molecular weights of MP340 and fibrillin and the similarity of the antibody binding patterns of MAGP and fibrillin, it is likely that MP340 is fibrillin, and to date this is the only structural component of microfibrils identified.

The first indication that the beaded strings might contain fibrillin came from a study of three large pepsin fragments of fibrillin (Maddox et al., 1989). One of the fragments (PF3) appeared to be a single bead from the structure described by Wright and Mayne. Furthermore, other fractions contained several PF3 fragments joined into short strings. In this report, we used a monoclonal antibody, specific for fibrillin and directed against PF3, to show that the beaded fibrils present in homogenates of various tissues and in vitreous humor contain fibrillin. The beaded filaments in 6 M guanidine hydrochloride extracts of human amnion that had been partially purified by chromatographing in the presence of 6M urea were also recognized by the antibody, indicating that fibrillin must be a structural component of the beaded strings and not just associated with them.

Studies of the biosynthesis and assembly of fibrillin in embryonic chick aorta organ cultures have shown that fibrillin monomers quickly polymerize, within hours after initial secretion, into large multimers stabilized by intermolecular disulfide bonds (Sakai, 1990). With the exception of pools of newly synthesized fibrillin monomers, the tissue form of fibrillin has been shown to be multimeric. Estimates of the size of initially formed aggregates might accommodate more that 23 fibrillin molecules. The fibrillin-containing

beaded structure described in this report is consistent with these studies. However, the details of the initial assembly process and of the stabilization of the final linear polymer is still under investigation. In addition, whether other molecules participate in the formation of this structure is currently unknown.

The gold deposited at each binding location along a beaded string probably represents a cluster of primary and secondary antibodies. The actual epitope on the fibrillin molecule is likely positioned along the arms between each bead. Although binding at regular intervals along the beaded string, mAb69 bound consistently to only one side of the bead structure. For this asymmetric binding to occur the beads must contain either the amino terminal end of one molecule and the carboxy terminal end of an adjacent molecule (head to tail alignment), or the central region of the fibrillin molecule so that the amino terminal region of the molecule is on one side and the carboxy terminal region on the other side of the bead.

All monoclonal fibrillin antibodies bind to microfibrils in tissues in a 54 nm periodic manner, indicating that there is a regular arrangement of fibrillin molecules within this structure (Sakai et al., 1986; Maddox et al., 1989). The ultrastructural appearance of antibody labeled beaded strings can be effectively converted to antibody labeled microfibrils by processing beaded strings through a standard TEM fixation, dehydration, and embedding protocol as though they were tissue, indicating that the beaded strings and tissue microfibrils represent the same structural entity. However, the periodicity of the beaded strings present in guanidine extracts and tissue homogenates is variable, and significantly increases when subjected to tension. By stretching ligament prior to antibody labeling, the periodicity of microfibrils could be

increased significantly beyond that of the surrounding collagen fibrils, indicating a unique extendability of the microfibril structure. It is likely that the 54 nm period demonstrated in standard tissue biopsies represents the period present in relaxed tissue following standard processing for TEM.

It is probable that the true structural appearance and the extendability characteristics of microfibrils are close to that of the beaded strings, since this structure can be demonstrated with minimal tissue processing. It is likely that the ultrastructural appearance of microfibrils in tissue sections represents an artifact of tissue processing, particularly dehydration. As the normal physiological dimensions of the microfibrils are unknown, the results of the tissue stretching experiments are difficult to interpret since the microfibrils may have been stretched or, alternatively, prevented from shrinking during dehydration. However, all data support the conclusion that fibrillin is a major structural component of microfibrils and that this structure is beaded and extendable.

ACKNOWLEDGEMENTS

We gratefully acknowledge Kenine Comstock, Marie Spurgin, Noé Charbonneau and Bruce Donaldson for their excellent technical assistance. This work was supported by grants from the Shriners Hospital for Crippled Children. Electron microscope facilities were provided in part by the R. Blaine Bramble Medical Research Foundation and the Fred Meyer Charitable Trust Foundation. The type VI collagen monoclonal antibody (5C6) was the generous gift of Dr. Eva Engvall, LaJolla Cancer Research Foundation, LaJolla, CA. The type VII antibody was the generous gift of Dr. Robert Burgeson, Shriners Hospital for Crippled Children, Portland, Or.

LITERATURE CITED

Breathnach SM, Melrose SM, Bhogal B, de Beer FC, Dyck RF, Tennent G, Black MM, Pepys MB (1981): Amyloid P component is located on elastic fibre microfibrils in normal tissue. Nature 293:652

Cleary EG, Gibson MA (1983): Elastin-associated microfibrils and microfibrillar proteins. Int Rev Connect Tissue Res 10:97

Cleary EG, Fanning JC, Prosser I (1981): Possible roles of microfibrils in elastogenesis. Connect Tissue Res 8:161

Dahlbäck K, Ljungquist A, Löfberg H, Dahlbäck B, Engvall E, Sakai LY (1990): Fibrillin immunoreactive fibers constitute a unique network in the human dermis. J Invest Dermatol in press

Fahrenbach WH, Sandberg LB, Cleary EG (1966): Ultrastructural studies on early elastogenesis. Anat Rec 155:563

Gibson MA, Cleary EG (1987): The immunohistochemical localization of microfibril-associated glycoprotein (MAGP) in elastic and non-elastic tissues. Immunol Cell Biol 65:345

Gibson MA, Hughes JL, Fanning JC, Cleary EG (1986): The major antigen of elastin-associated microfibrils is a 31-kDa glycoprotein. J Biol Chem 261:11429

Gibson MA, Kumaratilake JS, Cleary EG, (1989): The protein components of the 12-nanometer microfibrils of elastin and nonelastic tissues J Biol Chem 264:4590

Greenlee TK, Ross R, Hartman JL, (1966): The fine structure of elastic fibers. J Cell Biol 30:59

Haust MD (1965): Fine fibrils of extracellular space microfibrils their structure and role in connective tissue organization. Am J Pathol 47:1113

Keene DR, Engvall E, Glanville RW (1988): The ultrastructure of type VI collagen in human skin and cartilage suggests an anchoring function for this filamentous network J Cell Biol 107:1995

Keene DR, Sakai LY, Lunstrum GP, Morris NP, Burgeson RE (1987): Type VII collagen forms an extended network of anchoring fibrils. J Cell Biol 104:611

Keene DR, Sakai LY, Burgeson RE, Bächinger HP (1987): Direct visulization of IgM antibodies bound to tissue antigens using a monoclonal anti-type III collagen IgM as a model system. J Histochem Cytochem 35:311

Kobayashi R, Tashima Y, Masuda H, Shozawa T, Numata Y, Miyauchi K-I, Hayakawa T (1989): Isolation and characterization of a new 36-kDa microfibril-associated glycoprotein from porcine aorta. J Biol Chem 264:17437

Kuo H-J, Keene DR, Glanville RW (1989): Orientation of type VI collagen monomers in molecular aggregates. Biochemistry 28:3757

Low FN (1962): Microfibrils: fine filamentous components of the tissue space. Anat Rec 142:131

Maddox BK, Sakai LY, Keene DR, Glanville RW (1989): Connective tissue microfibrils : isolation and characterization of three large pepsin resistant domains of fibrillin. J Biol Chem 264:21381

Morris NP, Keene RD, Glanville RW, Bentz H, Burgeson RE (1986): The tissue form of type VII collagen is an antiparallel dimer. J Biol Chem 261:5638

Reynolds ES (1963): The use of lead citrate at high pH as an electron opaque stain in electron microscopy. J Cell Biol 17:208

Sakai LY (1990): Disulphide bonds crosslink molecules of fibrillin in the connective tissue space. In Tamburro A, Davidson J, eds. Elastin: Chemical and Biological Aspects. Italy. Congedo Editore Galatina. 213

Sakai LY, Keene DR, Engvall E (1986): Fibrillin a new 350KD glycoprotein is a component of extracellular microfibrils. J Cell Biol 103:2499

Schwartz E, Goldfischer S, Coltoff-Schiller B, Blumenfeld OO, (1985): Extracellular matrix microfibrils are composed of core proteins coated with fibronectin. J Histochem Cytochem 33:268

Wright DW, Mayne R (1988): Vitreous humor of chicken contains two fibrillar systems: an analysis of their structure. J Ultrastruct Mol Struct Res 100:224

FIGURE LEGENDS

Figure 1. Beaded aggregates in guanidine extracts of human amnion. (a) Rotary shadowed preparation containing long segments of beaded strings interdispersed among partially denatured banded collagen fibers. (b) Higher magnification of relaxed rotary shadowed beaded strings showing the network of fine filaments surrounding the beads. The periodicity in these beaded strings averages about 33 nm. (c) Occasionally, some beaded strings become tangled among debris present in the sample and are stretched, causing the periodicity to increase. The periodicity of this beaded string averages 94 nm. (d) A negatively stained preparation in which the periodicity of individual beaded strings varies. In this field, each of two beaded strings (labeled X and Y) become tangled amongst additional strands which are held under tension at either end by debris. At the point of entanglement, the average periodicity of strand X elongates from approximately 23 nm to 72 nm, whereas the periodicity of strand Y elongates from 25 nm to 53 nm. Bars, 200nm.

Figure 2. Material in non-denaturing homogenates of tissues contain readily identifiable beaded aggregates and banded collagen fibrils. (a) Fetal calf vitreous humor visualized by negative staining (b) Fetal calf femoral head cartilage visualized by rotary shadowing. Bars, 150 nm.

Figure 3. Beaded aggregates labeled with fibrillin specific monoclonal antibody mAb69 and 5 nm gold conjugated secondary antibody and then negatively stained with 2% phosphotungstic acid, pH 7.0. (a) Beaded aggregates in a guanidine extract of human amnion. The beaded structure can clearly be seen

labeled with gold indicating that they are fibrillin containing structures. At the top of the picture, other fibrous material and a collagen fiber are not labeled. (b) Low magnification field of fetal calf ligament homogenate demonstrates that the antibody also labels the beaded string structures directly extracted from tissue under non-denaturing conditions. (c) At higher magnification, antibody labeling is seen to be located consistently to one side of the "beaded" area of the string, indicating that the structure is not symmetrical. Solid arrows point to beaded areas; open arrows point to antibody binding sites. Bars, 100 nm.

Figure 4 (a) Ultrathin sections of immunolabeled fetal calf ligament homogenate (as shown in figure 3b) observed following fixation, dehydration, embedding and sectioning do not contain the beaded string structures, but instead contain immunogold labeled microfibril-like structures (b) Normal tissue matrix microfibrils in well fixed human amnion. (c) Human skin placed under tension prior to and during conventional processing for TEM. Some of the microfibrils are sufficiently stretched to take on the appearance of beaded aggregates. The periodicity in these areas averages 76 nm. (d) Immunolabeling fetal calf ligament while under tension results in microfibrils with varying periodicity. Some microfibrils (upper left, solid white arrow) demonstrate a periodicity of approximately 50 nm and are apparently not under tension. The periodicity of other microfibrils (solid black arrows) is substantially increased (in this example, to 80 nm), suggesting that these microfibrils are under tension. Bars, 150 nm.

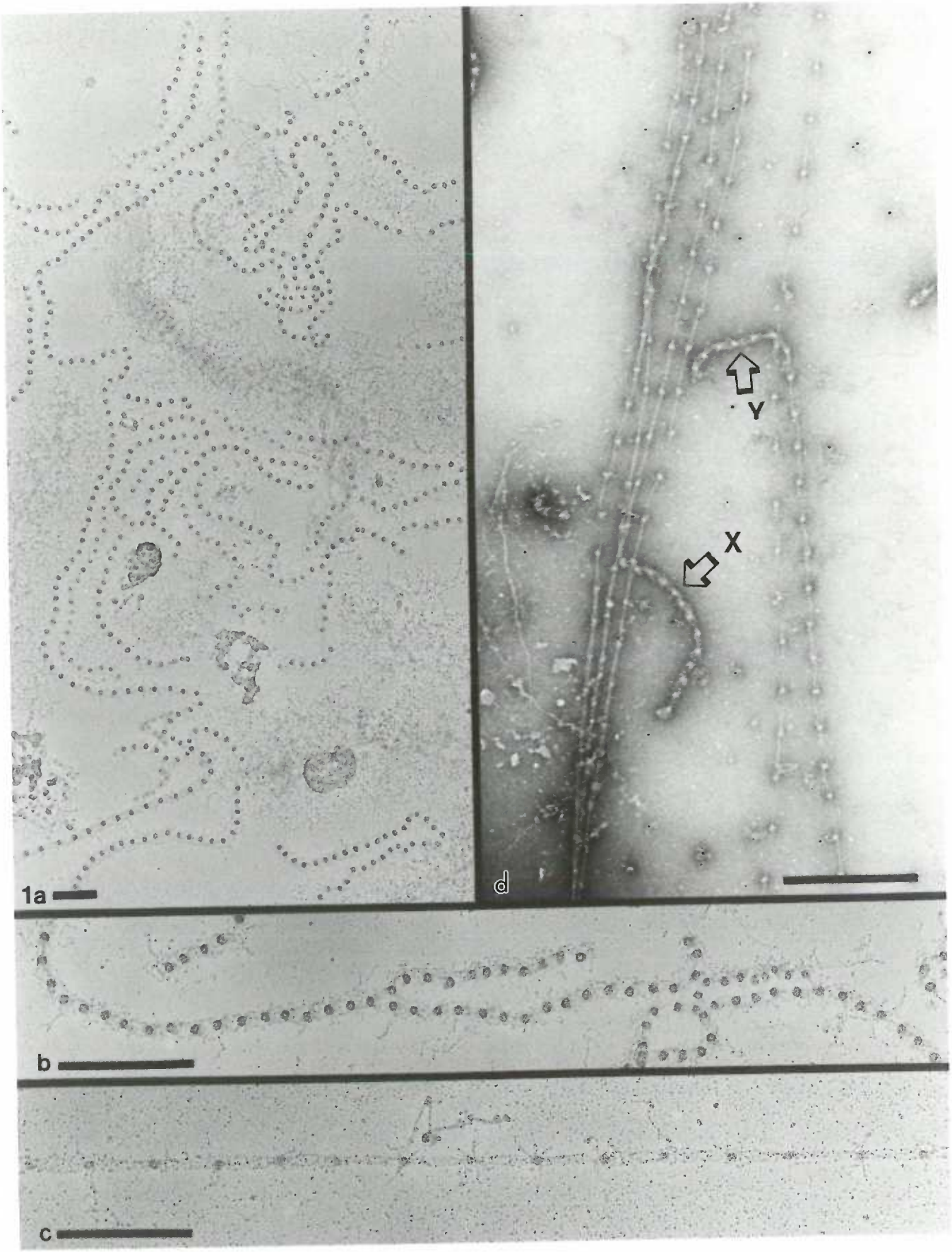
1a
d
Y
X
b
c

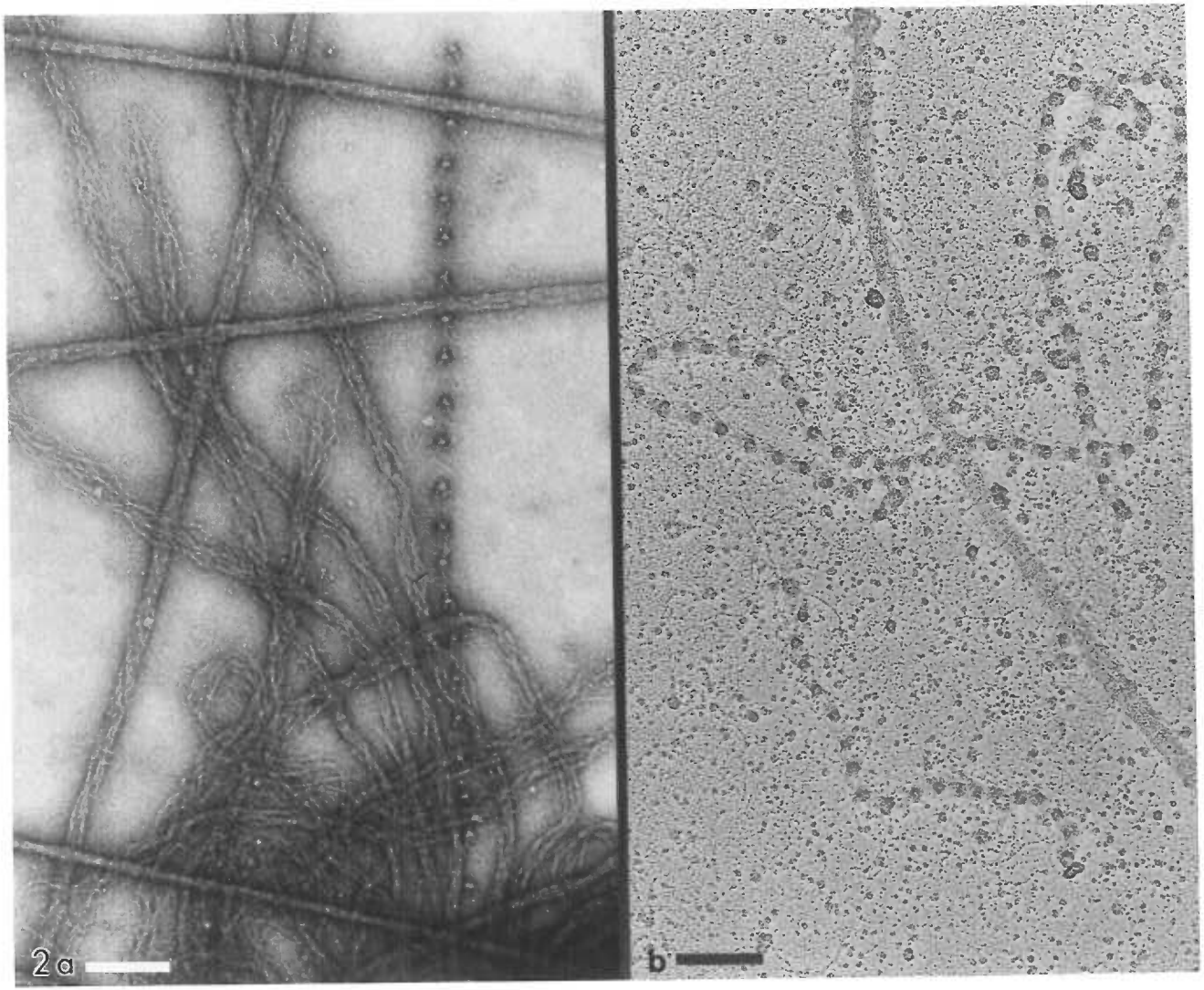
2a
b

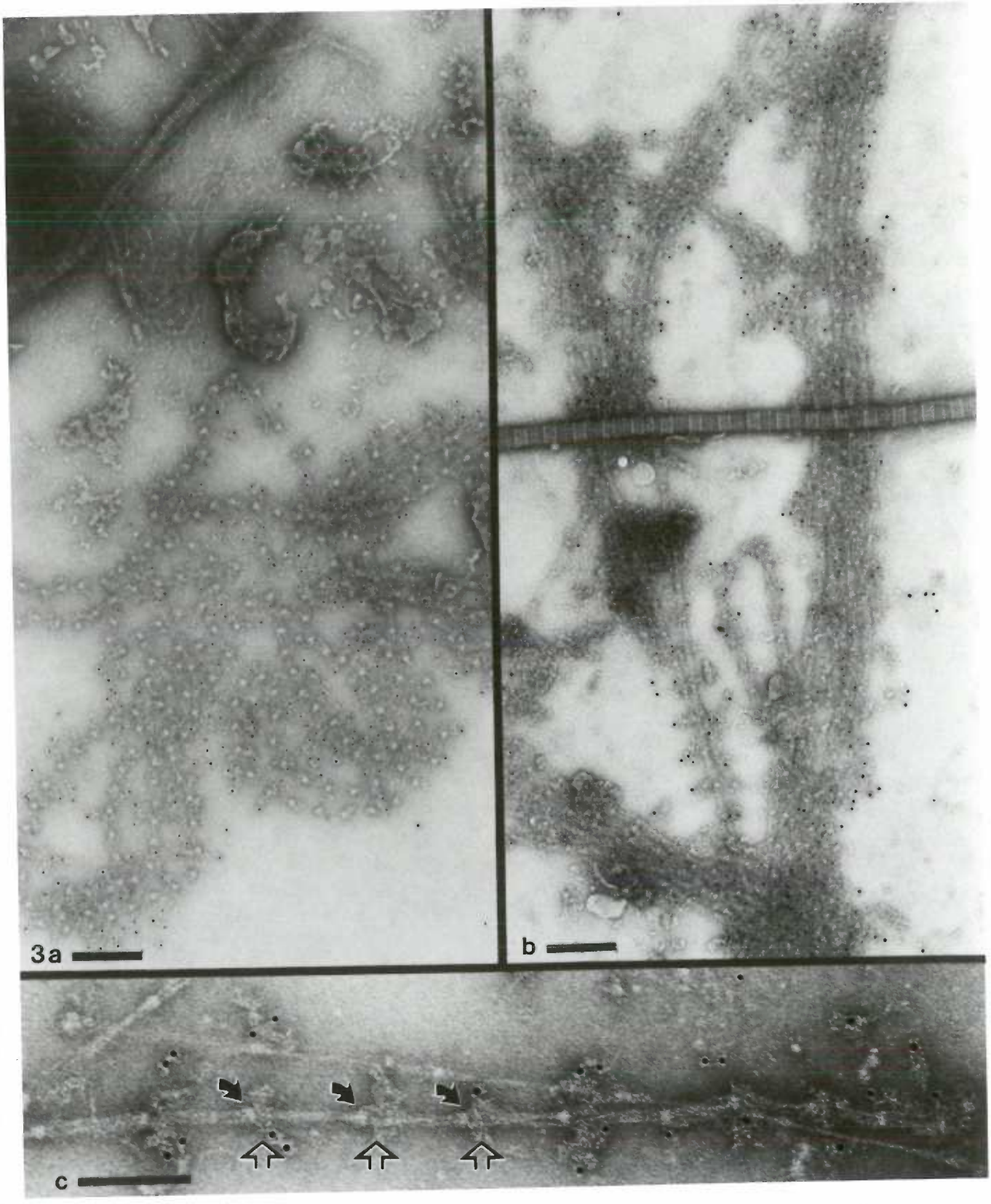
3a
b
c

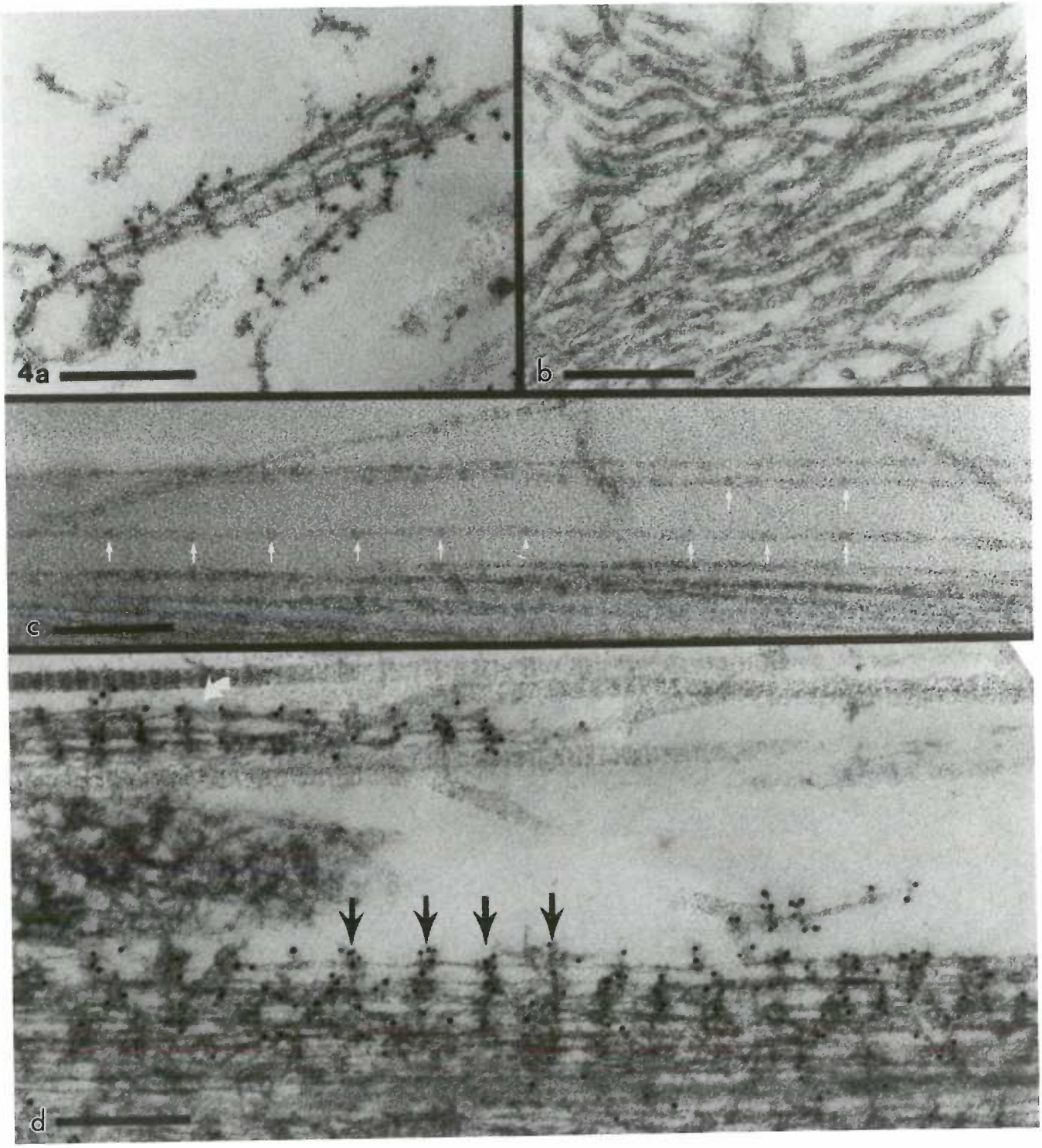
4a
b
c
d

APPENDIX III

THE JOURNAL OF BIOLOGICAL CHEMISTRY

Vol. 264, No. 35, Issue of December 15, pp. 21381-21385, 1989
Printed in U.S.A.

Connective Tissue Microfibrils

ISOLATION AND CHARACTERIZATION OF THREE LARGE PEPSIN-RESISTANT DOMAINS OF FIBRILLIN*

(Received for publication, July 18, 1989)

B. Kerry Maddox‡§, Lynn Y. Sakai‡§, Douglas R. Keene‡, and Robert W. Glanville‡§¶

From the ‡Shriners Hospital for Crippled Children, Portland, Oregon 97201 and the §Department of Biochemistry, Oregon Health Sciences University, Portland, Oregon 97201

Human amnion was solubilized using pepsin and the digest supernatant screened for fragments of fibrillin with a previously characterized monoclonal antibody (Sakai, L. Y., Keene, D. R., and Engvall, E. (1986) *J. Cell Biol.* 103, 2499–2509). One fragment (PF1), with an apparent molecular weight of 94,000, was isolated and characterized. Two other fragments, PF2 and PF3, were isolated and shown to be fragments of fibrillin by preparing a monospecific antisera to PF2 and a monoclonal antibody to PF3. Immunoelectron microscopy and immunoblotting showed that both antibodies were specific for fibrillin. Electron microscope pictures of rotary-shadowed PF1 and PF2 showed them to be short rod-shaped molecules while PF3 has a crab-like appearance and seems to be an aggregate of several fibrillin chain fragments. Amino-terminal amino acid sequencing of PF1 and PF2 gave single unique sequences. Each of the three antibodies used was specific for one fragment and peptide mapping of PF1 and PF2 showed that there was no significant amino acid sequence overlap. Aggregates of PF3 are described which provided insight into the assembly and macromolecular structure of fibrillin in microfibrils.

Connective tissue is composed of a variety of fibrillar structures, including microfibrils which have been the focus of research efforts for many years (Cleary and Gibson, 1983). The term microfibril (Low, 1961) specifies a particular subgroup of fibrils with a diameter less than 20 nm, and without the 67-nm banding pattern characteristic of interstitial collagen fibers. Microfibrils in the matrix of connective tissues can be subdivided into two classes with diameters of 3 to 5 nm and 6 to 18 nm. The smaller diameter fibrils were shown to be composed of type VI collagen (Furthmayr *et al.*, 1983; Bruns, 1986; Keene *et al.*, 1988). Common characteristics of the larger microfibrils include an average diameter of 10 nm, a cross-section that sometimes appears to have a hollow center, a beaded appearance with varying periodicity and proximity to basement membranes, or association with elastic fibers.

Ross and Bornstein (1969) attempted to isolate microfibrillar proteins in a series of steps which included collagenase digestion and guanidine extraction of tissue in the presence of an agent to reduce the disulfide bonds. The extraction steps were followed by ultrastructural analysis noting the apparent disappearance of the microfibrils. Disulfide bonds appeared to play a major role in maintaining the integrity of the microfibrillar network. Unfortunately, the method yields a heterogeneous mixture (Gibson and Cleary, 1982; Prosser *et al.*, 1984). Antisera that have been developed against such preparations and used to identify components of elastic microfibrils have identified several components ranging in molecular weight from 30,000 to 340,000 (Sear *et al.*, 1981; Gibson *et al.*, 1986; Jaques and Serafini-Fracassini, 1986; Kambe and Hashimoto, 1987; Streeten and Gibson, 1988; Gibson *et al.*, 1989). A major advance in determining the composition of microfibrils was made when a monoclonal antibody was characterized which identified a unique, single-chain component of microfibrils. This new protein was named fibrillin (Sakai *et al.*, 1986).

Immunofluorescent staining of tissues using the monoclonal antibody specific for fibrillin demonstrated the distribution of fibrillin in the extracellular matrix of skin, aorta, lung, muscle, cornea, placenta, and ciliary zonule (Sakai *et al.*, 1986). Immunoelectron microscopy localized fibrillin to the elastic fiber microfibrils and to morphologically similar microfibrils that are not associated with elastin. The antibody binds regularly along the microfibrils with a periodicity that corresponds to the periodicity of banded collagen fibers. Intact fibrillin was isolated from the medium of human fibroblast cell cultures. It was identified as a glycoprotein by the uptake of [^{3}H]glucosamine in cell culture and the staining of fibrillin with periodic acid/Schiff reagent. SDS-PAGE[1] showed that it contains a single chain with an apparent molecular weight, under reducing conditions, of 350,000. It also contains intrachain disulfide bonds.

In order to study the structure of fibrillin with a view to elucidating the structure and function of microfibrils, it was necessary to develop methods to isolate fibrillin from tissues. In the work described here, pepsin was used to solubilize tissue and antibodies specific to fibrillin were used to identify pepsin-resistant domains. A previously characterized monoclonal antibody identified one domain (PF1), antiserum was prepared against a second domain (PF2), and a third domain (PF3) was used to prepare a monoclonal antibody. Both new antibodies were shown to be specific for fibrillin. The isolation and characterization of the three domains, PF1, PF2, and

* This work was supported by grants from the Shriners Hospital for Crippled Children. Electron microscope facilities were provided in part by the R. Blaine Bramble Medical Research Foundation and the Fred Meyer Charitable Trust Foundation. The costs of publication of this article were defrayed in part by the payment of page charges. This article must therefore be hereby marked "*advertisement*" in accordance with 18 U.S.C. Section 1734 solely to indicate this fact.

¶ To whom correspondence should be addressed: 3101 S.W. Sam Jackson Pk. Rd., Portland, OR 97201. Tel.: 503-241-5090. Ex. 507.

[1] The abbreviations used are: SDS-PAGE, sodium dodecyl sulfate-polyacrylamide gel electrophoresis; PBS, phosphate-buffered saline; mAb, monoclonal antibody; pAb, polyclonal antibody.

Western blotting of unreduced samples showed that both dialysis supernatant and precipitate contained immunoreactive material. Although recovery of the major component in the supernatant was incomplete (Fig. 1), as the same material was also present in the precipitate, sufficient amounts of protein were recovered from the supernatant to allow further characterization.

Isolation of PF1 and PF2 from the Water Dialysis Supernatant—The supernatant was lyophilized and chromatographed on a molecular sieve column which gave rise to two major fractions called PF1 and PF2 (Fig. 2*A*) which, when compared to globular standard proteins, had apparent molecular weights of 260,000 and 150,000, respectively. Each fraction was further purified using reverse-phase chromatography and analyzed on SDS-PAGE (Fig. 2*A*, *inset*). On stained electrophoresis gels they both exhibited apparent molecular weights of 74,000. After reduction, PF1 decreased in mobility corresponding to an apparent molecular weight of 94,000 while mobility of PF2 increased slightly to 68,000.

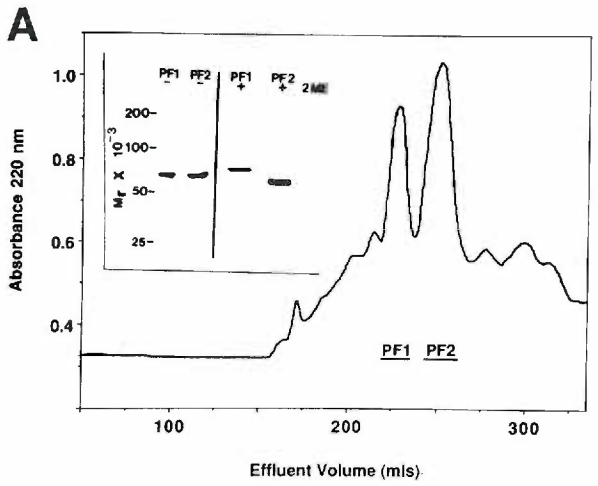

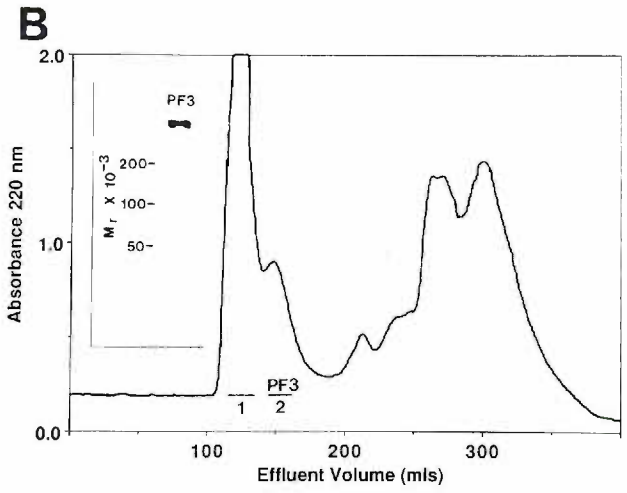

FIG. 2. **Purification of PF1, PF2, and PF3 by molecular sieve chromatography.** *A*, separation of the water supernatant fraction on a TSK3000 column into two major components, PF1 and PF2. Each fraction was pooled as indicated by the *bars* and further purified using reverse-phase chromatography (not shown). The *inset* shows the purified fragments analyzed by SDS-PAGE on a 5 to 10% polyacrylamide gel stained with Coomassie Blue. *B*, the water precipitate, dissolved in column buffer and applied to a TSK4000 column, separates into several peaks. Pools 1 and 2 both contained PF3. The *inset* show an aliquot of peak 2 analyzed by SDS-PAGE on a 3 to 10% polyacrylamide gel and stained with Coomassie Blue. The apparent molecular weight scale was determined by using globular standards (see "Materials and Methods"). *2ME*, 2-mercaptoethanol.

Characterization of PF1 and PF2—Western blot analysis of PF1 and PF2 using mAb201 showed that only PF1 reacted (Fig. 3). Purified antisera pAb7075, made against PF2, demonstrated specific reactivity to fibrillin by immunoblotting (Fig. 4), thus identifying PF2 as a fibrillin fragment. Immunofluorescence labeling of human skin (not shown) demonstrated staining of a network of fibers from immediately below the basement membrane into the deeper dermis which is characteristic of a fibrillin distribution (Sakai *et al.*, 1986). Electron microscopic immunolocalization using pAb7075 as the primary antibody and gold-conjugated secondary antibody (Fig. 5) verified that the structure recognized was the microfibril previously found to contain fibrillin (Sakai *et al.*, 1986). The antisera pAb7075 strongly reacted to PF2 but not PF1 (Fig. 3). The lack of cross-reactivity of the pAb7075 and mAb201 antibodies with PF1 and PF2 indicates that both are fragments of fibrillin, probably from different regions of the parent molecule.

To confirm that the fragments were non-overlapping, peptide maps using trypsin, V8 protease, and CNBr were analyzed using SDS-PAGE (Fig. 6). Fragments with intact disulfide bonds were cleaved and run reduced and unreduced on gels. The fragmentation patterns indicated that there is very little if any overlap of sequences.

Amino-terminal amino acid sequencing shown in Table I indicated that both PF1 and PF2 contain a single polypeptide chain and sequence data bank searches found no homologous

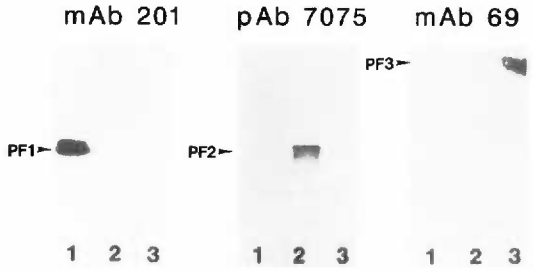

FIG. 3. **Immunoblot analysis of PF1, PF2, and PF3.** Purified fragments were separated on SDS-PAGE on a 3 to 10% polyacrylamide gradient gel, electrotransferred to nitrocellulose, and immunoblotted with mAb201, pAb7075, and mAb69. *Lanes 1* to *3* are PF1, PF2, and PF3, respectively. Each set of three lanes was immunoblotted with the antibody indicated.

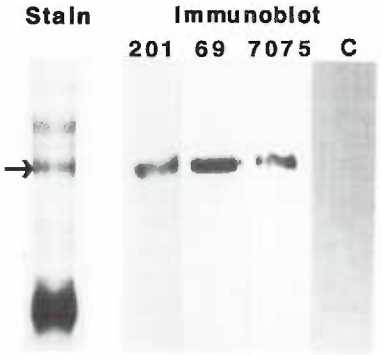

FIG. 4. **Immunoblot analysis of new antibodies mAb69 and pAb7075 using intact fibrillin.** Fibroblast cell culture medium containing fibrillin was separated on a 3 to 5% polyacrylamide gel and stained with Coomassie Blue. The proteins were transferred to nitrocellulose and immunoblotted with the new antibodies, along with mAb201 as a positive control. *Lane C* is blotted with normal serum as a negative control. The *arrow* indicates the position of fibrillin.

could not be analyzed using immunoblotting but did react strongly with mAb69 in enzyme-linked immunosorbent assays (not shown).

The amino acid analysis of PF3 is similar to those of PF1 and PF2 having an unusually high content of cysteine and acidic amino acids. Due to the complexity of this fragment, no sequence data is currently available.

Rotary-shadowed Images of the Pepsin Fragments—Electron micrographs of rotary-shadowed preparations of PF1 and PF2 indicate rod-shaped molecules (Fig. 7, *A* and *B*). PF2 images appeared to be a segmented rod while PF1 was more uniform, thinner, and longer.

Electron microscope pictures of rotary-shadowed PF3 preparations revealed a complex structure (Fig. 7, *C, D,* and *E*). A crab-like unit was observed which consisted of a central dense region surrounded by flexible "arms," giving the impression of several protein chains uniting to form a central core. In pool 1 (Fig. 2*B*) most of the material was in an aggregated form containing from two to several units of PF3 apparently covalently bound since they were chromatographed in the presence of 6 M urea. In contrast, pool 2 consisted mainly of monomeric units and this fragment is referred to as PF3. The number of projecting chains was difficult to determine as they were not always visible or more likely, some had been removed by the action of pepsin during the solubilization of the tissue. However, as many as 8 chains have been observed.

DISCUSSION

The isolation and characterization of fibrillin pepsin fragments PF1, PF2, and PF3 have provided several clues as to the structure of fibrillin and microfibrils. Fibrillin was characterized as a single-chained protein based upon the presence of a single 350-kDa component in an SDS-PAGE gel (Sakai *et al.*, 1986). This conclusion is supported by the isolation of PF1 and PF2 which are native, homogeneous, single-chained fragments, probably protected from pepsin digestion by intramolecular disulfide bonds maintaining a stable secondary structure. The sum of the molecular weights of PF1 and PF2 is 162,000 which is just under half that of intact fibrillin and as both PF1 and PF2 are rod shaped this suggests that at least half of the fibrillin molecule is rod shaped. The relative positions of the fragments along the intact molecule are unknown. The proportion of the fibrillin molecule involved in the formation of PF3 could not be determined because of the heterogeneity of this fragment.

PF3 appears to be a disulfide bonded, cross-linking region that contains fragments of at least 6 and possibly 10 molecules. This corresponds well with biosynthetic studies in tissue culture that show fibrillin molecules are very quickly assimilated into high molecular weight aggregates (Sakai *et al.*, 1989). PF3 is not a homogeneous structure, presumably due to random cleavages made by pepsin during its release from the microfibrillar structure. For this reason no well-defined molecular weight for its constituent chains could be deduced and a clear uniform structure is not discernible in electron micrographs of rotary-shadowed preparations. The high density of metal atoms deposited at the center of PF3 reflects the high profile of this structure and may mask some details. It is also possible that other molecules besides fibrillin could be involved in the formation of PF3. However, only clones producing antibodies to fibrillin were detected when preparing monoclonal antibodies to PF3, providing some evidence, although not conclusive, that this is not the case.

Structures similar to PF3 have been observed in preparations of microfibrils isolated from chick vitreous humor (Wright and Mayne, 1988) without the use of proteolytic enzymes. Two types of microfibrils were described, one being collagen and the second, long beaded chains that appeared to be linear aggregates of PF3-like units. The identity of the protein involved was unknown, but from the results presented here it seems likely that the chains of beads are the macromolecular form of fibrillin. If this is true, then fibrillin is probably the major component of tissue microfibrils as the chains of beads were observed in homogenates of chick vitreous humor which were not treated with proteases. It is not yet known whether other proteins are integral components of these microfibrils but it has been shown that under some circumstances amyloid P, fibronectin, and vitronectin can codistribute with them (Schwartz *et al.*, 1985; Dahlbäck *et al.*, 1989). Antibodies to several low molecular weight components, found in reductive denaturing extracts of tissues, have been prepared and found to label elastin-associated microfibrils in tissues (Jaques and Serafini-Fracassini, 1986; Streeten and Gibson, 1988; Mecham *et al.*, 1988; Gibson *et al.*, 1989). The relationship of these components to fibrillin is not yet clear but it is possible that they are fibrillin fragments produced during extraction of the antigen. It has also been suggested that microfibrils may be attached to elastin via disulfide bonds (Cicila *et al.*, 1985), although there is no protein-chemical data to support this suggestion yet.

Acknowledgments—We gratefully acknowledge Kenine Comstock, Marie Spurgin, Eileen Roux, and Bob Poljak for their excellent technical assistance.

REFERENCES

Bruns, R. R., Press, W., Engvall, E., Timpl, R., and Gross, J. (1986) *J. Cell Biol.* **103,** 393–404
Cicila, G., May, M., Ornstein-Goldstein, N., Indik, Z., Morrow, S., Yeh, H. S., Boyd, C., Rosenbloom, J., Rosenbloom, J., and Yoon, K. (1985) *Biochemistry* **24,** 3075–3080
Cleary, E. G., and Gibson, M. A. (1983) *Int. Rev. Connect. Tissue Res.* **10,** 97–209
Dahlbäck, K., Ljungquist, A., Löfberg, H., Dahlbäck, B., Engvall, E., and Sakai, L. Y. (1989) *J. Invest. Dermatol.*, in press
Friedman, M., Krull, L. H., and Cavins, J. F. (1979) *J. Biol. Chem.* **245,** 3868–3871
Furthmayr, H., Wiedemann, H., Timpl, R., Odermatt, E., and Engel, J. (1983) *Biochem. J.* **211,** 303–311
Gibson, M. A., and Cleary, E. G. (1982) *Biochem. Biophys. Res. Commun.* **105,** 1288–1295
Gibson, M. A., Hughes, J. L., Fanning, J. C., and Cleary, E. G. (1986) *J. Biol. Chem.* **261,** 11429–11436
Gibson, M. A., Kumaratilake, J. S., and Cleary, E. G. (1989) *J. Biol. Chem.* **264,** 4590–4598
Jaques, A., and Serafini-Fracassini, A. (1986) *J. Ultrastruct. Mol. Struct. Res.* **95,** 218–227
Kambe, N., and Hashimoto, K. (1987) *J. Invest. Dermatol.* **88,** 253–258
Keene, D. R., Engvall, E., and Glanville, R. W. (1988) *J. Cell Biol.* **107,** 1995–2006
Low, F. N. (1961) *Anat. Rec.* **139,** 105–122
Mecham, R. P., Hinek, A., Cleary, E. G., Kucich, U., Lee, S. J., and Rosenbloom, J. (1988) *Biochem. Biophys. Res. Commun.* **151,** 822–826
Morris, N. P., Keene, D. R., Glanville, R. W., Bentz, H., and Burgeson, R. E. (1986) *J. Biol. Chem.* **261,** 5638–5644
Prosser, I. W., Gibson, M. A., and Cleary, E. G. (1984) *Aust. J. Exp. Biol. Med. Sci.* **62,** 485–505
Ross, R., and Bornstein, P. (1969) *J. Cell Biol.* **40,** 366–381
Sakai, L. Y. (1989) in *Elastin: Chemical and Biological Aspects* (Tamburro, A., and Davidson, J., eds), Springer-Verlag, Padua, in press
Sakai, L. Y., Engvall, E., Hollister, D. W., and Burgeson, R. E. (1982) *Am. J. Pathol.* **108,** 310–318
Sakai, L. Y., Keene, D. R., and Engvall, E. (1986) *J. Cell Biol.* **103,** 2499–2509
Schwartz, E., Goldfischer, S., Coltoff-Schiller, B., and Blumenfeld, O. O. (1985) *J. Histochem. Cytochem.* **33,** 268–274
Sear, C. H. J., Grant, M. E., and Jackson, D. S. (1981) *Biochem. J.* **194,** 587–598
Streeten, B. W., and Gibson, S. A. (1988) *Curr. Eye Res.* **7,** 139–146
Towbin, H., Staehelin, T., and Gordon, J. (1979) *Proc. Natl. Acad. Sci. U. S. A.* **76,** 4350–4354
Wright, D. W., and Mayne, R. (1988) *J. Ultrastruct. Mol. Struct. Res.* **100,** 224–234